ผลของบาราคอลต่อเซลล์มะเร็งเอ็มบริโอพีสิบเก้า

นายเฉลิมสิน เพิ่มเติมสิน

วิทยานิพนธ์นี้เป็นส่วนหนึ่งของการศึกษาตามหลักสูตรปริญญาวิทยาศาสตรมหาบัณฑิต
สาขาวิชา ชีวเวชเคมี ภาควิชา ชีวเคมี
คณะเภสัชศาสตร์ จุฬาลงกรณ์มหาวิทยาลัย
ปีการศึกษา 2545

ISBN 974-17-3392-5

EFFECTS OF BARAKOL ON P19 EMBRYONAL CARCINOMA CELLS

Mr. Chalermsin Permtermsin

A Thesis Submitted in Partial Fulfillment of the Requirements for
the Degree of Master of Science in Biomedicinal Chemistry

Department of Biochemistry
Faculty of Pharmaceutical Sciences
Chulalongkorn University

Academic Year 2002
ISBN 974-17-3392-5

Thesis Title	Effects of barakol on P19 embryonal carcinoma cells
By	Mr. Chalermsin Permtermsin
Field of Study	Biomedicinal Chemistry
Thesis advisor	Associate Professor Dr. Duangdeun Meksuriyen
Thesis Co-advisor	Associate Professor Dr. Vimolmas Lipipun

Accepted by the Faculty of Pharmaceutical Sciences, Chulalongkorn University in Partial Fulfillment of the Requirements for the Master's Degree

……..……Dean of Faculty of Pharmaceutical Sciences

(Associate Professor Boonyong Tantisira, Ph.D.)

THESIS COMMITTEE

…… Chairman

(Associate Professor Sunanta Pongsamart, Ph.D.)

…….Thesis advisor

(Associate Professor Duangdeun Meksuriyen, Ph.D.)

…… Thesis Co-advisor

(Associate Professor Vimolmas Lipipun, Ph.D.)

…….Member

(Associate Professor Sukanya Jesadanont, Ph.D.)

…… Member

(Assistant Professor Surachai Unchern, Ph.D.)

เฉลิมสิน เพิ่มเติมสิน : ผลของบาราคอลต่อเซลล์มะเร็งเอ็มบริโอพีสิบเก้า (Effects of barakol on P19 embryonal carcinoma cells) อ.ที่ปรึกษา: รศ.ดร.ดวงเดือน เมฆสุริเยนทร์, อ. ที่ปรึกษาร่วม: รศ.ดร.วิมลมาศ ลิปิพันธ์, 96 หน้า. ISBN 974-17-3392-5

การศึกษาความเป็นพิษของบาราคอลที่สกัดมาจากใบอ่อนสดของต้นขี้เหล็กต่อเซลล์มะเร็งเอ็มบริโอพีสิบเก้าด้วยวิธีทางชีวเคมีและสัณฐานวิทยา การทดสอบความเป็นพิษด้วยวิธี XTT assay พบว่าบาราคอลแสดงความเป็นพิษต่อเซลล์แปรผันตรงตามความเข้มข้นและเวลา ในขนาดความเข้มข้นไม่น้อยกว่า 0.8 มิลลิโมลาร์ พบว่าเซลล์ตายประมาณ 95 % ภายในเวลา 72 ชั่วโมง การทดสอบความเป็นพิษต่อเซลล์ด้วยวิธี trypan blue dye exclusion assay พบว่าบาราคอลที่ความเข้มข้น 0.8 และ 1.0 มิลลิโมลาร์ แสดงความเป็นพิษต่อเซลล์มะเร็งเอ็มบริโอพีสิบเก้า โดยมีจำนวนเซลล์ที่มีชีวิตน้อยกว่ากลุ่มควบคุมประมาณ 63-76 % หลังจากเซลล์ได้รับบาราคอลนาน 36-72 ชั่วโมง การเปลี่ยนแปลงทางสัณฐานวิทยาเริ่มสังเกตเห็นหลังจากเซลล์ได้รับบาราคอลที่ความเข้มข้น 0.8 มิลลิโมลาร์ นานเป็นเวลา 48 ชั่วโมง โดยพบว่ารูปร่างเซลล์จะหดลงเป็นรูปทรงกลมแต่ยังเป็นเซลล์ที่มีชีวิตอยู่ ความเป็นพิษต่อเซลล์หลังจากได้รับบาราคอลที่ความเข้มข้นไม่เกิน 0.8 มิลลิโมลาร์ เป็นเวลา 72 ชั่วโมง พบว่าเซลล์สามารถฟื้นตัวได้ หลังจากเลี้ยงในอาหารที่ปราศจากบาราคอล อย่างไรก็ตามพบว่ายังมีการเปลี่ยนแปลงทางสัณฐานวิทยาโดยเซลล์มีขนาดโตและบวมขึ้น การศึกษารูปแบบการตายของเซลล์ด้วยเทคนิค agarose gel electrophoresis พบว่าบาราคอลเหนี่ยวนำให้เซลล์มะเร็งเอ็มบริโอพีสิบเก้าตายแบบ apoptosis การทดสอบความเป็นพิษของบาราคอลต่อเซลล์ประสาทพีสิบเก้าที่ถูกเปลี่ยนสภาพมาจากเซลล์มะเร็งเอ็มบริโอพีสิบเก้าพบว่าหลังจากเซลล์ได้รับบาราคอลที่ความเข้มข้น 0.8 และ 1.0 มิลลิโมลาร์ เป็นเวลานาน 72 ชั่วโมง พบความเป็นพิษต่อเซลล์ประสาทพีสิบเก้าเล็กน้อย โดยมีจำนวนเซลล์ที่มีชีวิตรอดมากกว่า 74% ด้วยวิธี XTT assay การเปลี่ยนแปลงทางสัณฐานวิทยาของเซลล์ที่มีชีวิตจะพบช่องว่างขนาดใหญ่ในไซโทพลาซึม มีจำนวนและความยาวของใยประสาทลดลง การวิเคราะห์ DNA fragmentation ด้วยเทคนิค agarose gel electrophoresis พบ DNA ladders แสดงให้เห็นว่าบาราคอลเหนี่ยวนำให้เซลล์ประสาทพีสิบเก้าตายแบบ apoptosis การศึกษาผลของบาราคอลต่อการทำงานของ intracellular soluble AChE และ membrane-bound AChE ที่ความเข้มข้นในช่วง 0.05-1.0 มิลลิโมลาร์ พบว่าบาราคอลไม่มีผลยับยั้งสมรรถนะของเอนไซม์ทั้ง 2 รูปแบบตลอดช่วงเวลาที่ทำการทดสอบ

ภาควิชา.....ชีวเคมี..... ลายมือชื่อนิสิต.....

สาขาวิชา.....ชีวเวชเคมี..... ลายมือชื่ออาจารย์ที่ปรึกษา.....

ปีการศึกษา.....2545..... ลายมือชื่ออาจารย์ที่ปรึกษาร่วม.....

4376564633 : MAJOR BIOCHEMISTRY

KEY WORDS: P19 CELLS/ P19 NEURONS/ CYTOTOXICITY/ BARAKOL/ ACETYLCHOLINESTERASE/ DNA FRAGMENTATION/ APOPTOSIS
CHALERMSIN PERMTERMSIN: EFFECTS OF BARAKOL ON P19 EMBRYONAL CARCINOMA CELLS: THESIS ADVISOR: ASSOC. PROF. DUANGDEUN MEKSURIYEN, Ph.D., THESIS CO-ADVISOR: ASSOC. PROF. VIMOLMAS LIPIPUN, Ph.D., 96 pp. ISBN 974-17-3392-5

The cytotoxicity of barakol, extracted from fresh young leaves of *Cassia siamea* Lam., was investigated on P19 embryonal carcinoma cells (P19 cells) using biochemical and morphological method. The cytotoxic assay of barakol demonstrated that barakol induced a concentration and time-dependent decrease in the viable cells with 95 % cell death observed at the concentrations of ≥ 0.8 mM following 72 h of exposure, as determined by the XTT assay. Trypan blue dye exclusion assay revealed that barakol at the concentrations of 0.8 and 1.0 mM showed significant cytotoxicity to P19 cells; the viable cell number was lower than the control approximately 63 % - 76 % at 36-72 h of exposure. The alteration of cell morphology was observable after 48 h of exposure with barakol at the concentration of 0.8 mM and appeared to be shrinkage with spherical shape but was still viable. The cytotoxic effect of barakol at the concentrations of ≤ 0.8 mM for 72 h of exposure, was reversible upon replacing culture medium with barakol-free medium. However, most viable cells showed enlarged and swollen morphology. The pattern of cell death in undifferentiated P19 cells demonstrated to be apoptosis, as assessed by agarose gel electrophoresis. After the differentiation of P19 cells to P19 neurons, the cytotoxic assay of barakol on P19 neurons showed that barakol at the concentrations of 0.8 and 1.0 mM exerted slightly cytotoxic effect, which the cell viability was greater than 74 % after 72 h of exposure, as determined by the XTT assay. The viable cell morphology was observable with large cytoplasmic vacuolation, less and short neurites. The analysis of DNA fragmentation on agarose gel electrophoresis showed DNA ladders, which indicated apoptotic cell death. The assay of AChE activity in P19 neurons revealed that barakol at the concentrations ranging from 0.05-1.0 mM did not show significant reduction in the intracellular soluble and membrane-bound AChE activity at any exposure times.

Department……Biochemistry…… Student's signature……..…..…….

Field of study….Biomedicinal Chemistry….. Advisor's signature……...…..

Academic year……..2002……... Co-advisor's signature…….……..…....

ACKNOWLEDGEMENTS

I wish to express my grateful appreciation to Thai Royal Government for granting the scholarship and the Graduate School of Chulalongkorn University for partial financial support.

I would like to thank Office of Atoms for Peace for supplying inverted microscope.

I would like to thank all staff members of the Department of Biochemistry, Faculty of Pharmaceutical Sciences, Chulalongkorn University for providing facilities and valuable suggestion during my study.

I would like to thank Assoc. Prof. Chaiyo Chaichantipyuth, Department of Pharmacognosy, Faculty of Pharmaceutical Sciences, Chulalongkorn University for supplying barakol.

Finally, I wish to express my grateful appreciation to Departments of Microbiology, Pharmacology and Pharmacognosy for supplying of reagents and equipments.

CONTENTS

LIST OF TABLES

LIST OF FIGURES

Figure Page

Figure Page

Figure **Page**

ABBREVIATIONS

%	=	percent
^{0}C	=	degree Celsius
μl	=	microliter
μm	=	micrometer
AChE	=	acetylcholinesterase
AD	=	Alzheimer's disease
Ara-C	=	cytosine arabinoside
ATCC	=	American Type Culture Collection
BBB	=	blood brain barrier
BMPs	=	Bone morphogenetic proteins
BuChE	=	butyrylcholinesterase
BW284C51	=	1,5-bis(4-allyldimethylammonium-phenyl)penten-3-one-dibromide
Cdks	=	Cyclin dependent kinases
conc	=	concentration
DTNB	=	dithiobisnitrobenzoate
EBs	=	embryoid bodies
EC	=	embryonal carcinoma
FBS	=	fetal bovine serum
GABA	=	gamma-aminobutyric acid
GAD	=	glutamic acid decarboxylase
GFAP	=	glial fibrillary acidic protein
h	=	hour
IC_{50}	=	median inhibitory concentration
i.p.	=	intra-peritoneal
iso-OMPA	=	tetraisopropyl pyrophosphoramide
JNK	=	c-Jun amino-terminal kinase
α-MEM	=	α-modified minimal essential medium
min	=	minute
mg	=	milligram

ml	=	milliliter
mM	=	millimolar
nm	=	nanometer
NCS	=	newborn calf serum
NF	=	neurofilament
NMDA	=	N-methyl-D-aspartic acid
PBS	=	phosphate buffered saline
PMS	=	phenazine methosulfate
RA	=	*all-trans* retinoic acid
RAR	=	retinoic acid receptor
RXR	=	retinoid X receptor
sec	=	second
SSEA-1	=	stage specific embryonic antigen-1
V	=	volt
XTT	=	(2,3-bis[2-methoxy-4-nitro-5-sulfophenyl]-2H-tetrazolium-5-carboxanilide

CHAPTER I

INTRODUCTION

Cassia siamea Lam. (Caesalpiniaceae), known as “Khi-lek” in Thai, has been widely used in Thailand and Southeast Asia as food and herbal medicine. Thai traditional healers used the different parts of this plant for various medical purposes. For example, the root is used as an antipyretic, the bark is used to treat skin disease and haemorrhoids, while the leaves and the flowers are used for the treatments of insomnia, hypertension, asthma, constipation and diuresis (Thongsaard, 2001). Chemical constituents of this plant have been reported to contain alkaloids, flavonoids anthraquinones, chromones and terpenoids (Chaichantipyuth, 1979).

Cassia siamea tablet was commercially available since 1998 for treatment of insomnia. A clinical trial on herbal medicine, Khi-lek syrup and Khi-lek tablets, has been reported. The drug with the concentration of anhydrobarakol at 10 mg per dose (400 mg of dried grind-leaves/tablet/5 ml, equivalent to 10 mg of anhydrobarakol) was found to be helpful in 59 and 69 % of the insomniac subjects in the syrup group and tablet group, respectively. The side effects were loose stools (26 %) and abdominal distension (6 %) (Muangman, 2000). Khi-lek tablets produced sleepiness in healthy subjects and also improved quality of sleep in insomniac volunteers (Pooviboonsuk, 2000). At the first time, there was no report of the serious side effect of this product. Until 2000, the hepatotoxicity of barakol was first reported. Up to date, *Cassia siamea* tablet is not available and its hepatotoxicity could not identify any toxic substances.

The physiological and pharmacological properties of barakol, the active constituent extracted from fresh young leaves of *Cassia siamea* Lam., were reported. Administration of ethanolic extract from young leaves of *Cassia siamea* or barakol decreased spontaneous locomotor activity in mice and rats (Arunlakshana, 1949; Jantarayota, 1988). Barakol had anxiolytic property in rats similar to diazepam (Thongsaard, 1996). Barakol did not show protective effect against convulsion induced by picrotoxin, bicucullin and strychnine administrations (Jantarayota, 1988).

These data though conflicting suggest possible action of *Cassia siamea* and barakol on the central nervous system (CNS), in agreement with the CNS depressant effects observed in human receiving foods containing crude forms of *Cassia siamea*.

The toxic effects of barakol at higher doses have been reported. Mice receiving barakol at 150 and 200 mg/kg, i.p., showed the continuous locomotion, hyperreflexia for 60-70 min. Barakol at 225 and 250 mg/kg exerted the hyperactivity, hyperreflexia and hyperventilation. Mice receiving barakol at 270 mg/kg i.p., revealed the spastic contraction, piloerection, hyperreflexia, straub'stail, tremor, hyperpnea and finally death. The median lethal dose in mice (LD_{50}) was 324 mg/kg, i.p. (Jantarayota, 1988). Although animals such as mice or rats have been used for a toxicological evaluation, it is well established that numerous compounds are metabolized quite differently in rodents compared to man. Due to an ethical obstacle to study metabolism and toxicity of barakol in man in *vivo*, the cytotoxic study of barakol on human hepatocyte HepG2 was reported that barakol exhibited a cytotoxic effect at the concentration of $\geq$ 0.75 mM at 24 h of exposure. Median inhibitory concentration (IC_{50}) of barakol on HepG2 cells at 48, 72 and 96 h of exposure were 0.96, 0.77 and 0.68 mM, respectively; whereas the corresponding IC_{50} of acetaminophen were 11.13, 1.39 and 1.30 mM, respectively (Lawanprasert, 2001).

The above information suggested that barakol might pass the blood-brain barrier and might be toxic to the brain. Consequently, the cytotoxicity of barakol at the levels of embryonic and neuronal cells has not been reported. The aim of our experiments is to study the cytotoxic effect of barakol on P19 embryonal carcinoma cells (P19 cells) as a system for studying embryotoxicity, by evaluating biochemical and morphological characteristics. P19 cells are an excellent experimental model of both transform and embryonic cells. The cells are differentiated poorly under normal conditions, extensive differentiation can be induced by RA to differentiate into P19 neurons. P19 neurons, but not P19 cells, are biochemically and morphologically similar to cells of the CNS and express AChE activity (Jones-Villeneuve, 1982; Coleman, 1996). Thus, P19 neurons were also used as a model for the neurotoxicity study and for the investigation of the effect of barakol on AChE activity.

CHAPTER II

LITERATURE REVIEW

Barakol

Barakol, a chromone derivative, was extracted from fresh young leaves of *Cassia siamea* Lam., contains a tricyclic ring structure (Fig. 1). This structure can convert from barakol ($C_{13}H_{12}O_4$) to anhydrobarakol ($C_{13}H_{10}O_3$) by losing a molecule of water.

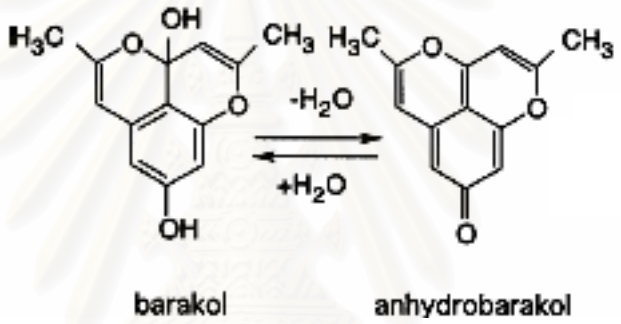

Fig. 1 The structure of barakol (3a, 4-dihydro-3a, 8-dihydroxy-2, 5-dimethyl-1, 4-dioxaphenalene).

The physiological and pharmacological properties of barakol have also been studied in various laboratories. Barakol at 10 mg/kg, i.p., had anxiolytic property in rats similar to diazepam (1 mg/kg, i.p.), rather than showing sedative effects and increase in exploratory and locomotor behaviour. The anxiolytic properties and the increased exploratory behaviour produced by barakol were reduced at higher doses ranging from 25-50 mg/kg, i.p. (Thongsaard, 1996). Barakol at the doses of 50-100 mg/kg, i.p., decreased spontaneous locomotor activity and rearing in mice with a dose-dependent manner during 30 min of observation period, indicating the inhibitory effect of barakol on the basal ganglia in the central nervous system (Sukma, 2002). Barakol at the concentration of 1 μM reduced K^+-stimulated endogenous dopamine release as did the dopamine D_2 receptor agonists without a change in dopamine

uptake, suggesting the capacity of barakol to suppress dopaminergic neuron activity in a way similar to dopamine agonist (Thongsaard, 1996). Barakol at the doses of 25-100 mg/kg, i.p., inhibited methamphetamine-induced hyper-locomotor activity in mice as a dose-dependent manner, suggesting that it had an inhibitory effect on the dopaminergic system in the striatum (Sukma, 2002). In vivo microdialysis study, barakol at 10 and 100 mg/kg, i.p., significantly reduced extracellular level of dopamine in rat striatum with no significant change in other metabolites, indicating that barakol may act at the pre-synaptic D_2 receptor (Thongsaard, 1998). The attenuation of locomotor activity was directly mediated via stimulation of the D_3 postsynaptic receptor (Sukma, 2002).

As mention earlier, barakol has anxiolytic profiles similar to diazepam, which bind at the benzodiazepines sites on the GABA receptor. It remains to be determined whether barakol affects GABAergic mechanisms in a similar manner. However, since barakol has a different behavioural profile from diazepam as it also increased exploration and locomotion and has been shown not to reverse the convulsant effects of bicuculline, strychnine indicating that barakol has no direct action on $GABA_A$ receptor (Sukma, 2002). Barakol can suppress 5-hydroxytryptophan-induced head shakes in rats, which is considered a 5-HT_2 receptor mediated response suggesting barakol may act as 5-HT_2 receptor antagonism. The finding that barakol stimulated dopaminergic system may suggest that the observed serotonergic suppression could be the result of elevated dopaminergic activity (Jantarayota, 1988).

P19 cells and P19 neurons

Embryonic carcinoma (EC) cells have been widely used as a model system for studying early development. These cells resemble those comprising the inner cell mass of preimplantation blastocysts and a number of differentiated cell types, with characteristics of cells of the three germ layers can be obtained reproducibly by different treatments (Newall, 1996; Rossant, 2001).

P19 cells are pluripotent murine embryonal carcinoma cells. This cell line was a normal male karyotype (40:XY) isolated from C3H/He mice (McBurney and Roger, 1982). P19 cells differentiate poorly under normal conditions, extensive

differentiation can be induced by retinoic acid (RA) to differentiate into P19 neurons, glia and fibroblast-like cells in a manner similar that observed *in vivo* (Jones-Villeneuve, 1982). Many of the cells showed a multipolar morphology characteristic for oligodendrocytes. These populations were immunoreactive to O4, an antibody recognizing oligodendrocyte-specific glycolipids. At the same time, the cells expressed the astrocytic marker antigen glial fibrillary acidic protein (GFAP) and exhibited a flat morphology typical of cultured astrocytes (Brustle, 1999). Culture containing up to 90% neurons can be obtained by treating differentiating P19 cells with mitotic inhibitors such as arabinosylcytosine (ara-C, cytosine arabinoside, cytarabine) (Coleman and Taylor, 1996). P19 neurons resemble CNS neurons morphologically and are stably post-mitotic, which could form axons, dendrites and functional synapses. P19 neurons also express a wide variety of neurotransmitters and receptors in mature cultures, including GABA, glutamic acid decarboxylase, GABA-transaminase, neuropeptide Y, serotonin, calcitonin, parathyroid, calcitonin gene related peptide, substance P, and enkephalin (Staines, 1994; Parnas and Linial, 1995; Mansergh, 1996; Eggenberger, 1998; Mansergh, 2000), choline acetyl-transferase, acetylcholinesterase and tetanus toxin receptor (Jones-Villeneuve, 1982; Parnas and Linial, 1995). This would suggest the presence of a wide variety of neuronal subtype in P19 cells when exposure to RA (Mansergh, 1996; Eggenberger, 1998). P19 neurons express NMDA and metabotropic glutamate receptors, but not AMPA/kainite receptors (Ray, 1993; Morley, 1995). In P19 neurons, neurofilaments specific for neurons of peptide subunit of 160,000 molecular weight was staining with indirect immunofluorescence showed that, the staining was located along the processes and cell bodies of every one of the neuronal cells (Jones-Villeneuve, 1982). The physiological studies also showed that EC cells lacked functional glutamate receptors while P19 neurons expressed them at levels near that of CNS neurons in culture (Ray and Gottlieb, 1993). However, the ability of EC cells to differentiate into the whole spectrum of functional neurons and glial cells that characterized the CNS is still lacking.

RA-treated P19 cells differentiate into neurons as indicated by their morphology (soma and neurite) and expression of typical neuronal markers (Jones-Villeneuve, 1982; Parnas and Linial, 1995). Cellular differentiation involves initial commitment of multipotential embryonic cells to a specific cellular lineage and

subsequently differentiation of committed cells. Cellular differentiation is characterized by co-ordinate induction of a repertoire of cell-specific proteins necessary for specialized functions. P19 neurons appear to be powerful tools for studying GABA or glutamate-receptor signaling, functional cholinergic neurons and neurotoxicity because they are genetically manipulable and their differentiation can be controlled. Especially, the process of neurogenesis in P19 cells is similar to that of the mammalian CNS (Jones-Villeneuve, 1982).

P19 cells form embryoid bodies (EBs), when culture with RA, are induced to differentiate into P19 neurons and glia. No AChE activity is present in the undifferentiated P19 cells, and mRNA protection analysis cannot detect AChE mRNA. Commitment to a neuronal differentiation pathway results in increased levels of AChE mRNA, production of tetrameric form of the enzyme and secretion of AChE into the culture medium. Concomitant with subsequent morphological differentiation into neurons, enzyme secretion diminishes and AChE becomes largely tetered to the neuronal cell membranes. The enzyme is attached to the cell surface as a globular tetramer as shown by histochemical and immunohistochemical staining (Coleman and Taylor, 1996).

Mechanism of retinoic acid induction of P19 embryonal carcinoma cells to P19 neurons

Retinoic acid (RA), a vitamin A derivative, was found to have important regulatory functions during embryonic development. Two families of nuclear receptors designated retinoic acid receptors (RARα, RARβ, RARγ, and their isoforms) and retinoid X receptor (RXRα, RXRβ, RXRγ and their isoforms) transduce the RA signal. These receptors are members of the steroid/thyroid superfamily of ligand-activated transcription factors and known to be expressed in the early embryo. RARs bind to, and are activated by, both all-*trans* retinoic acid and its 9-*cis* isomer, whereas RXRs bind and are activated by 9-*cis* RA only. RAR and RXR heterodimers efficiently activate transcription of target genes by binding to retinoic acid response elements (RAREs) and are believed to transduce the retinoid signal to the transcription machinery and the chromatin template through transcriptional

intermediary factors that directly interact with the ligand receptors. RA regulates the growth and differentiation of many cell types, such as the P19 cells depending on the concentration of RA and the culture conditions (Slack, 1995).

Acetylcholinesterase

Vertebrates possess two cholinesterase genes, producing the enzyme AChE and butyrylcholinesterase (BuChE) (Massoulie, 1998). BuChE hydrolyzes butyrylcholine, in addition to acetylcholine, while AChE specifically hydrolyzed acetylcholine to choline and acetic acid. AChE has been found in neuronal cells, red blood cells (Krupka, 1964), and muscle cells (Wilson, 1973). It is distinguished from the BuChE of serum chiefly by differences in substrate specificity. This difference is now perfectly explained by the size of an acyl pocket in the active site of these enzymes, that accommodates a butyryl moiety in the case of BuChE, but not in AChE because it is limited by two bulky phenylalanine side chain (Massoulie, 1998). Subsequently, BW284C51 is relatively specific inhibitors, for AChE and ethopropazine and iso-OMPA for BuChE (Vellom, 1993). The mechanism of action of AChE is considered primarily in relation to two steps in the hydrolytic process: (1) the acetylation reaction, in which an acetyl enzyme is formed from the enzyme-substrate complex and (2) the deacetylation reaction, in which the acetyl enzyme is hydrolyzed to reform the free enzyme. Acetylcholine contains a trimethylammonium group and an ester linkage. The active center of AChE contain two corresponding parts, (1) a negatively charged “anionic” site, which binds the trimethylammonium group and (2) “esteratic” site, which catalyzed the hydrolysis of the ester bond. The charged forms of such substances are more strongly bound to AChE than the uncharged form as in the case of physostigmine, which contains an ionizable amino group, dimethylaminoethanol is bound more firmly than its uncharged analog (Krupka, 1964).

AChE has also been hypothesized to play developmental roles in the nervous system, aids outgrowth of neurites, promote proliferation and cell-cell interactions (Grisaru et al., 1999). On the other hand, inhibitors of AChE are therapeutically useful to patients with diseases of inadequate neurotransmission in which levels of acetylcholine receptors decrease such as acquired autoimmune myasthenia gravis.

Although the function of AChE is apparently simple, its patterns of structure and distribution are remarkably complex. First, the transcript of the AChE gene is subjected to alternative splicing and its protein products can associate covalently with each other and with noncatalytic subunits. Second, the oligomers can occur in cytoplasmic, membrane-bound and extracellular matrix-associated forms. Third, AChE is found not only at neuromuscular junctions, but also at cholinergic interneuronal synapses, in some non-cholinergic neurons, and in some nonneural cells such as erythrocytes. Fourth, a related enzyme, BuChE can capable of hydrolyzing ACh. BuChE is expressed in some of the same sites as AChE, including the neuromuscular junction (Feng, 1999).

The role of AChE in termination of cholinergic neurotransmission is well recognized, but less well appreciated is the considerable complexity of AChE molecular forms and their biological roles and interrelationships. A single gene encodes AChE forms in nerve cells and muscle cells (Rotundo, 1989). The catalytic subunits exist corresponding to membrane-bound and secretable soluble form, which arise from alternative splicing events (Rotundo, 1989; Legay, 1999). All newly synthesized AChE are transported from the rough endoplasmic reticulum to the Golgi apparatus where they acquire N-acetylglucosamine and are transported to the plasma membrane where they become associated with the cell surface or are secreted into the culture medium. Newly synthesized AChE is degraded intracellular with a half-life of about 1.5 h by a mechanism, which is insensitive to lysosomtropic agents (Rotundo, 1989). In the CNS three globular forms of the enzyme predominate: a monomer (G1; 4-5S), dimer (G2; 6-7S) and tetramer (G4; 10-11S) (Schegg, 1992), with trace amounts of asymmetric isoforms, which are anchored to membranes by collagen-like subunits (Valero, 1999). Each of these forms may be freely soluble or tightly bound within membranes, in contrast to BuChE, which is not bound in any significant way to cellular membranes of the CNS tissue (Meisami, 1984). Freely soluble forms exist within the cell and are secreted from it. Membrane-bound AChE, which requires detergent for solubilization, may be attached to membrane within the cell or be integral to the exterior plasma membrane. Additionally, in the peripheral nervous system and to a small extent in the CNS, there exist asymmetric forms of AChE characterized by attachment to collagen-like tails; these forms require high salt concentrations in order to be solubilized (Schegg, 1992). It is noteworthy that, to

date, the various molecular forms of AChE have experimentally identical catalytic properties, however, their biological roles are not necessarily the same (Grisaru, 1999).

Alzheimer's disease

Alzheimer's disease (AD) is a neurodegenerative disorder that represents the most common cause of adult-onset dementia, represents 40-60 % of all dementia disorders. AD is characterized by an insidious onset and a slowly deteriorating cognitive function (Hakansson, 1993). From a neuropathological point of view, AD is characterized by brain atrophy accompanied by neuronal loss primarily in temporal cortex and in limbic areas such as hippocampus and characteristic hallmarks such as neurofibrillary tangles, β-amyloid plaques and amyloid angiopathy (Felician, 1999; Amenta, 2001). Numerous attempts have been made to restore the activity in the cholinergic system with transmitter-oriented therapy.

Therapeutic strategies of AD should be directed to achieve the three main goals detailed below: (1) improvement of cognitive function, (2) control of troublesome behaviors, and (3) showing down the progression of disease. These goals for being achieved require as much as possible early and correct diagnosis and to establish appropriate strategies that include pharmacological and non-pharmacological treatment. In the late 1970s it was discovered that the brains of AD patients were deficient in acetylcholine, one of the main neurotransmitters of the CNS that serves to increase attention and facilitate learning. This discovery led to the development of the cholinergic hypothesis, which states that cognitive, functional and behavioural dysfunction associated with AD may be caused by an inability to transmit neurologic impulses across cholinergic synapses. Today, the symptomatic treatment of AD is based on cholinergic pharmacologic enhancement. Clinical trials with precursor agents such as choline or lecithin (Maltby, 1994), or some cholinergic receptor agonists, have been uniformly disappointing with virtually all investigators reporting negative results and have had unacceptable adverse effects (Mayeux and Sano, 1999). The most promising results in clinical trials of AD patients have been obtained with cholinesterase inhibitors, which indirectly increase the content of

acetylcholine in the cholinergic synapse (Sunderland, 1998; Benzi, 1998; Holmes, 2000; Bullock, 2002).

The only class of drugs that have been effective so far for the symptomatic treatment of AD are the cholinesterase inhibitor. These drugs act by slowing the biochemical breakdown of acetylcholine by inhibiting AChE in the synaptic cleft, thereby decreasing the hydrolysis of ACh released from presynaptic neurons. Thus, at least theoretically, prolonging cholinergic neurotransmission. Of interest is that humans have 2 types of cholinesterase: AChE and BuChE. The physiological role of BuChE is unknown, but levels of this enzyme have been shown to increase as AD progresses, whereas levels of AChE decrease (Gauthier, 2002). AChE inhibitors have widely been studied for the cognitive-enhancing treatment for AD. These drugs have been shown to provide temporarily the modest improvement in symptoms of AD and to stabilize or slow for some time the decline of cognitive function and functional ability. Furthermore, a variety of neuropsychiatric symptoms occur in AD, such as agitation, psychosis, depression, apathy, disinhibition, anxiety, purposeless behavior, and disorders of sleep and appetite, have been related to cholinergic deficiency and improve after treatment with cholinomimetic agents (Cummings, 1998). Up to now, research has continued on the cholinergic deficiency of AD, and cholinomimetic therapies have been developed to partially relieve the memory and cognitive abnormalities and also neuropsychiatric symptoms.

Two distinct forms of cell death

The two distinct forms of cell death, necrosis and apoptosis, have been defined in terms of mechanism, sequence of events, biochemistry and morphology. Necrosis refers to a range of morphological changes resulting from the enzymatic digestion, the disruption of cellular membranes and the denaturing of proteins that accompanies cell death. Necrosis does not involve any regular DNA and protein degradation pattern and is companied by swelling of the entire cytoplasm and of the mitochondrial matrix, which occur shortly before the cell membrane ruptures (Kroemer, 1998). Apoptosis, in contrast, is an active process under genetic control, highly selective mechanism of cell death allowing for the removal of cells that are redundant or excessively damaged (Patricia, 1998). The comparison between necrosis

and apoptosis are summarized in table 1. It is now become clear that many diseases are characterized by dysregulation of apoptotic programs such as liver failure, leukemia, autoimmune disease and cancer. Many of these programs involve a family of receptors and their ligands, the death receptor/ligand family (Peter, 1997). The hope now is to interfere with apoptosis regulation in these systems and to develop a new therapeutic concept.

Table 1 Comparative features of necrosis and apoptosis (Kroemer, 1998)

Apoptosis	**Primary necrosis**
Physiological or pathological (subnecrotic damage)	Accidental
Susceptibility tightly regulated	Always pathological
Plasma membranes near-to-intact until late	Unregulated or poorly regulated
Heterophagic elimination	Plasma membrane destroyed early
No leakage of cell content; no inflammation	Leakage of cell content
Cellular enzymes participate, causing characteristic biochemical or morphological features including chromatin condensation (pyknosis) nuclear fragmentation (karyorrhexis) regular DNA fragmentation pattern selective protein degradation by specific protease (caspase) subtle changes in plasma membranes cell shrinkage no mitochondrial swelling	Biochemical and morphological features include swelling of the entire cytoplasm mitochondrial swelling inflammation
	Secondary necrosis
	Cytolysis secondary to apoptosis when dying cells fail to be removed by heterophagy

Apoptosis

Apoptosis is a process in which cells activate an intrinsic suicide mechanism that systematically destroys themselves. The dominant stage of apoptosis occurs through the activation and function of caspases, a highly conserved family of cysteine proteases with specificity for aspartic acid residues in their substrates. It is the cleavage of certain key substrates that orchestrates the death and packaging of the cell for clearance. It has reported that neuronal cells are eliminated by apoptosis process estimate 50 % or more during development but leaves neurons, which are indispensable for the function of the nervous system (Raff, 1993). This process seems essential because unnecessary neurons might disturb the development of neural networks. Apoptosis has been postulated as a model for neuronal death in human neurodegenerative disease because of morphological similarities at the cellular levels (Okazawa, 1996).

Cells undergoing apoptosis display certain biochemical and morphological characteristics, which differ from those shown by necrotic cells. During apoptosis, fusion of endoplasmic reticulum with the plasma membrane causes contraction of the cytoplasm with visible membrane blebbing. The chromatin consensus becomes convoluted and is deposited along the inner surface of the nuclear membrane. Protein and RNA levels decrease in both apoptosis and necrosis. One hallmark of apoptotic cell death is the internucleosomal cleavage of cellular DNA, in contrast to necrosis (Batistatou and Greene, 1993; Saraste and Pulkki, 2000). Ultimately, the cell fragments into membrane bound vesicles containing organelles and fragmented chromatin also call apoptotic bodies and rapid phagocytosis by neighboring cells, macrophages and parenchymal cells (Tran and Miller, 1999; Saraste and Pulkki, 2000). Apoptotic bodies can be recognized inside these cells, but eventually they become degraded. If the fragmented cell is not phagocytosed it will undergo degradation which resembles necrosis in a process called secondary necrosis (Saraste and Pulkki, 2000).

The detection methods of apoptosis were evaluated by morphological and biochemical hallmarks, such as internucleosomal DNA fragmentation, caspase

activation assay. However, many previous studies reported that the internucleosomal DNA fragmentation has been a major advance in the detection of apoptosis (Saraste and Pulkki, 2000). The DNA cleavage is observed in cells undergoing apoptosis after separated in agarose gel electrophoresis, in contrast to necrosis only smear band occurs (Dragunow and Preston, 1995). Apoptosis is the degradation of DNA by endogenous DNases, which cut the internucleosomal regions into double stranded DNA fragments of 180-200 base pairs (Saraste and Pulkki, 2000; Sastry and Rao, 2000). Internucleosomal fragmentation has been demonstrated with well-characterized apoptotic process in a wide variety of situation and cell types (Batistatou and Greene, 1993; Slack, 1995; Glozak and Rogers, 1996,1998; Ninomiya, 1997; Saraste and Pulkki, 2000).

Cell viability assays

Cell viability assays are used to measure the proportion of viable cells following a potentially traumatic procedure. Most viability assays rely on breakdown in membrane integrity that is determined by the uptake of a dye to which the cell is normally impermeable such as trypan blue, or the release of a dye normally taken up and retained by viable cells such as neutral red.

1. Tetrazolium salt XTT assay

The use of tetrazolium salts, such as MTT, commenced in the 1950s and is based on the fact that live cells reduce tetrazolium salts into colored formazan compounds. The biochemical procedure is based on the activity of mitochondria enzymes which are inactivated shortly after cell death. This method was found to be very efficient in assessing the viability of cells. A colorimetric method based on the tetrazolium salt, XTT, was first described by P.A. Scudiero in 1988. Whilst the use of MTT produced a non-soluble formazan compound, which necessitated dissolving the dye in order to measure it (Borenfreund, 1988), the use of XTT produces a soluble dye. The use of XTT greatly simplifies the procedure of measuring proliferation, and is, therefore, an excellent solution to quantify the cells and their viability without using radioactive isotopes. This assay can perform in a microtiterplate format and

miniaturization allows many samples to be analyzed rapidly and simultaneously. The assay also reduces the amount of culture medium and cells required as well as cost of plastic ware. Colorimetric assays allow samples to be measured directly in the microtiterplate with microplate reader. These colorimetric assays are very rapid and convenient because this technique needs no washing or harvesting of the cells (Mosmann, 1983).

The assay with XTT is based on the cleavage of the yellow tetrazolium salt XTT to form an orange formazan dye by mitochondrial dehydrogenase in metabolic active cells, which are inactivated shortly after cell death. Therefore, this conversion only occurs in viable cells. The formazan dye formed is soluble in aqueous solutions and is directly quantified using a microtiter plate reader. Cells, grown in tissue culture plate, are incubated with the yellow XTT solution (final concentration 1 mg/ml) for 6-12 h. During this incubation period, orange formazan solution is formed, which is spectrophotometrically quantified using a microtiter plate reader. An increase in number of living cells results in an increase in the overall activity of mitochondrial dehydrogenases in the sample. This increase directly correlates to the amount of orange formazan formed. The dye formed is water-soluble and the dye intensity can be read at 450-500 nm (Rochm, 1991).

2. Trypan blue dye exclusion assay

The assay with trypan blue relies on a breakdown in membrane integrity that is determined by the uptake of a trypan blue dye to which the cell is normally impermeable. Cells are incubated for 1-2 min with 0.4 % trypan blue at room temperature before counting or take a photograph (Slater, 2001).

3. Neutral red dye uptake assay

The assay with neutral red dye uptake method use neutral red dye, which is preferentially absorbed into lysosomes. Only viable uninjured cells are, therefore, capable of maintaining the process intact. Cells are incubated with 50 μg/ml for 20-

30 min in growth medium, the cells were examined under the microscope (Riddell, 1986; Borenfreund, 1988; Barile, 1994).

DNA fragmentation assay

Cell death is an important part of the cell cycle. The cell lives, consumes energy, and divides itself repeatedly until a moment when these activities are no longer sustained and the cell dies. Upon this death, it is possible to detect different morphological, biochemical, and molecular features that allow us to distinguish the two basic types of cell death: apoptosis and necrosis. While necrosis and various mechanisms inducing it have long been known and understood, it is the intricate mechanism of apoptosis that remains unresolved and has led scientists to focus on it during the last decades. In addition, the different pathways and mechanisms of this program are still being identified and every year new facts appear (Rudolf, 2000).

Determination of AChE activity

1. Intracellular soluble AChE activity assay

Soluble AChE activity was determined by a photometric method of Ellman et. al. (Ellman, 1961). The enzyme activity is measured by following the hydrolysis of acetylthiocholine to thiocholine and acetate by AChE. Thiocholine reacts with dithiobisnitrobenzoate ion to produce yellow color of 5-thio-2-nitrobenzoic acid. The rate of color production is measured at 412 nm. The reaction with the thiol has been shown to be sufficiently rapid so as not to be rate limiting in the measurement of the enzyme and in the concentrations used does not inhibit the enzymatic hydrolysis.

2. Membrane-bound AChE activity assay

Membrane-bound AChE activity was detected by a direct-coloring thiocholine method of Karnovsky and Roots (Karnovsky and Roots, 1964). The basis of the method is that thiocholine is believed to reduce ferricyanide to ferrocyanide preferentially. The latter combines with Cu^{++} ions to form the insoluble copper

ferrocyanide (Hatchett's brown). The Cu^{++} ions in the medium are complexed with citrate to prevent formation of copper ferricyanide. The advantages of the presently described method are: color is produced directly at the site of enzymatic activity, facilitating estimation of the optimum incubation time; the precipitate is finely granular, so that, even with prolong incubation, needle-like deposits are not observed; intense color and contrast can consequently be produced, and sites of low activity more easily detected.

Rationale of the study

These physiological and pharmacological properties of *Cassia siamea* and barakol together with the traditional medicine encouraged further studies whether this plant has effects on the CNS function apart from the reported sedation and decreased locomotor activity in mice. However, the cytotoxic study of barakol on embryo and CNS cells was not available. It was the purpose of this experiment to evaluate the cytotoxicity of barakol, using P19 cells and P19 neurons as a cellular model.

In our experimental designs, the investigation of the toxic effects of barakol in P19 cells and P19 neuron, were evaluated in both concentration-dependent and time-course manner. Cytotoxicity was assessed by the method of XTT assay, trypan blue dye exclusion assay and neutral red dye uptake assay. The method of XTT assay is based on the cleavage of the yellow tetrazolium salt XTT to form an orange formazan dye by mitochondrial dehydrogenase in metabolic active cells, which are inactivated shortly after cell death. Therefore, this conversion only occurs in viable cells (Rochm, 1991). The trypan blue dye exclusion assay, is rely on a breakdown in membrane integrity that is determined by the uptake of a trypan blue dye to which the cell is normally impermeable (Slater, 2001). The neutral red dye uptake assay is preferentially absorbed into lysosomes. Only viable cells, therefore, are capable of maintaining the process intact (Barile, 1994). The pattern of cell death induced by barakol was detected by DNA agarose gel electrophoresis, which showed the internucleosomal cleavage of cellular DNA, one hallmark of apoptotic cell death (Chen, 1997; Saraste and Pulkki, 2000). Internucleosomal DNA cleavage is observed only in cells undergoing apoptosis contrast to necrosis. Finally, the effect of barakol

on AChE activity in P19 neurons was also determined. The soluble form of intracellular AChE was analyzed with the spectrophotometric method of Ellman et. al. The basis of this method is the hydrolysis of acetylthiocholine to thiocholine and acetate by AChE. Thiocholine reacts with dithiobisnitrobenzoate ion to produce yellow color of 5-thio-2-nitrobenzoic acid. The rate of color production is measured at 412 nm (Ellman, 1961). The membrane-bound AChE was carried out with direct coloring method of Karnovsky and Roots. The basis of the method is that thiocholine is believed to reduce ferricyanide to ferrocyanide preferentially. The latter combines with Cu^{++} ions to form the insoluble copper ferrocyanide (brown color) (Karnovsky and Roots, 1964).

Objectives

1. To study the cytotoxic effect of barakol on P19 embryonal carcinoma cells and P19 neurons.
2. To investigate the DNA degradation to evaluate the pattern of cell death.
3. To explore the effect of barakol on acetylcholinesterase.

CHAPTER III

MATERIALS AND METHODS

Materials

P19 embryonal carcinoma cells (ATCC, # CRL 1825); *all-trans* RA (Sigma); poly-L-lysine (Sigma); cytosine arabinoside (Ara-C, Sigma); tetrazolium salt XTT (Sigma); PMS (Sigma); α-MEM (Gibco); newborn calf serum (Gibco); fetal bovine serum (Seromed); ethidium bromide (Fluka); acetylthiocholine iodide (Flukaiso-OMPA (Sigma); RNase A (USB Corporation); proteinase K (USB Corporation); 100 base pair DNA ladder (Amersham Pharmacia Biotech); BW284C51 (Sigma); sodium dodecyl sulfate (Fluka);); neutral red (General Chemical and Pharmaceutical); potassium ferricyanide (Merck); dithiobisnitrobenzoic acid (DTNB, Sigma); 0.4 % trypan blue (Gibco); 0.25 % trypsin (Sigma); agarose (Gibco)

Culture vessels and Equipments

15 ml and 50 ml polypropylene conical tube; single channel and eight-channel micropipette; 25 cm^3 and 75 cm^3 tissue culture flask; 6, 24, 96-well plates; sterilization filters; pipette aid; peristaltic pump; hot air oven; autoclave; laminar flow hood; CO_2 incubator; freezer (-20 ^{0}C and –80 ^{0}C); sonicator; hemocytometer; inverted microscope; microplate reader (Anthos); barakol (was a gift of Associate Professor Chaiyo Chaichantipyuth, Department of Pharmacognosy, Faculty of Pharmaceutical Sciences, Chulalongkorn University).

Methods

1. Cell culture techniques

1.1 P19 cell culture

P19 cells were propagated in α-modified minimal essential medium (α-MEM) supplemented with 7.5% newborn calf serum and 2.5% fetal bovine serum (FBS) at 37 °C and 5% CO_2 in a humidified atmosphere. Cells were routinely passaged every 3-4 days (Jones-Villeneuve, 1982; Yao, 1995).

1.2 P19 neuron culture

Differentiation of P19 cells into P19 neurons was carried out as follow: cells in exponential growth were washed with Ca^{2+} and Mg^{2+} free phosphate buffer saline (PBS) then, incubated 1-2 min with 0.25 % trypsin, to remove them from the tissue surface. They were plated at a density of 10^5 cells/ml into a bacteriological grade petri dish in α-MEM supplemented with 5 % FBS and 0.5 μM RA where they aggregated spontaneously. On 2 day, the culture medium was changed by transferring the suspension of EBs into a 15 ml conical centrifuge tube, allowing the aggregates to settle for 20-30 minutes then aspirating the medium and replacing it with new medium of the same composition including 0.5 μM RA. To allow neuronal differentiation, the EBs (on day 4) were pooled to a 50 ml conical centrifuge tube, allowing the EBs to settle for 20-30 minutes, after that the medium was removed and the EBs were re-suspended in 5 ml of fresh α-MEM supplemented with 10 % FBS. Cells were triturated through a 5 ml pipette for 30-40 times firmly against the bottom of the tube to yield a single cell suspension, staining with 0.4 % trypan blue and counted in a hemocytometer. Optimal neuronal differentiation was obtained by plating dissociated cells at a density of 10^6 cells/ml and replated in the absence of RA into a multi-well plates (coated with 50 μg/ml poly-L-lysine in PBS and sterilized under ultraviolet light for 30-60 min). The cells were then allowed to adhere and grow. On day 2, the medium was renewed, supplemented with 10 μM Ara-C to

inhibit non-neuronal cells proliferation. The medium was half feed every 2-3 day. At day 7 after plating, P19 neurons were mature for experimental assays (Jones-Villeneuve, 1982; Sberna, 1997; Yokote, 2000). Histochemical staining of cholinergic neuron was carried out using Karnovsky and Roots method (Karnovsky and Roots, 1961).

2. Determination of cytotoxic effect of barakol on P19 cells

2.1 Chemical preparation

All chemicals in these studies were of the analytical or purest grade available. They were dissolved in ultra-purified water and sterilized before use, except RA was dissolved in 95 % ethanol. Barakol was freshly prepared, filtration-sterilized and diluted with ultra-pure water to appropriate concentrations immediately before used. Range-finding studies of barakol were performed at final concentrations of 0, 0.05, 0.1, 0.2, 0.4, 0.8 and 1.0 mM.

2.2 Concentration-dependent study

P19 cells were seeded at a density of 10^5 cells/ml into sterile 96-well plates and allowed to settle and adhere for 24 h. The medium was discarded and replaced with fresh α-MEM medium supplemented with barakol at various concentrations ranging from 0.05-1.0 mM. Following 24 h of exposure, cell viability of P19 cells was assessed using tetrazolium salt XTT assay and trypan blue dye exclusion assay.

2.3 Time-course study

To assess the expression of barakol toxicity with time, P19 cells were seeded at a density of 4×10^4 cells/ml into sterile 96-well plates for 24 h. The medium was discarded and replaced with α-MEM medium containing barakol at various concentrations ranging from 0.05-1.0 mM. Incubation with barakol was continued for 24-72 h. At the end of each time study, cell viability of P19 cells was

assessed by tetrazolium salt XTT assay, trypan blue dye exclusion assay and neutral red dye uptake assay.

2.4 Recovery study

P19 cells were seeded at a density of 4 x 10^4 cells/ml into sterile 96-well plates for 24 h. The medium was discarded and replaced with α-MEM containing barakol at various concentrations of 0.4, 0.8 and 1.0 mM. Incubation with barakol was continued for 72 h. At the end of incubation, the medium was replaced to barakol-free medium. The viable cell number of P19 cells was determined following a 48 and 96 h recovery period using trypan blue dye exclusion assay and neutral red dye uptake assay.

2.5 DNA fragmentation assay

P19 cells were seeded at 5x10^5 cells/ml in 6-well plates at a final volume of 2 ml. Following 24 h of incubation, the medium was discarded and changed to fresh medium containing barakol at the concentrations of 0.5 and 1.0 mM. After 72 h of exposure, cells were scraped (combined with floating cells), collected and centrifuged at 1,200 rpm for 10 min. The supernatant was discarded and washed the pellet with ice-cold PBS. The cell suspension was centrifuged at 1,200 rpm for 5 min and wash once again with PBS. Then discarded the aqueous solution and added lysis buffer (10 mM Tris-HCl, pH 7.5, 10 mM NaCl, 10 mM EDTA, 100 μg /ml proteinase K, and 0.5% SDS). After 1 h of incubation at 50 ^{0}C, DNA was extracted with 2 ml of phenol (neutralized with TE buffer, pH 7.5) and 1 ml of chloroform:isoamyl alcohol (24:1). Aqueous layer was extracted with 2.5 volume of ice-cold ethanol and 10 % of volume of 3 M sodium acetate pH 5.2. After incubated overnight at -20 ^{0}C, the solution was centrifuged at 13,000 g for 10 min. Then, discarded the supernatant and re-suspended the pellets in 50 μl of TE buffer, pH 7.5 and added 0.1 μg/ml of RNase A. RA-treated P19 cells at 0.5 μM for 4 days and culture of P19 cells for 4 days (until the spontaneous cell death was occurred) were used as a positive control. DNA (20 μg) was separated with 1.5 % agarose gel with 0.5 x TBE buffer at 100 V for 1 h compared with non-treated group (control) using

100 base pair DNA ladder as a standard. The gel was stained with ethidium bromide (1 μg/ml), washed with water and photographed under UV transilluminator (Chen, 1997).

3. Determination of cytotoxic effect of barakol on P19 neurons

3.1 Concentration-dependent study

P19 cells were induced to differentiate into P19 neurons as mentioned above. The EBs were triturated and seeded at a density of 10^6 cells/ml into 96-well plates. On day 7 after plating, the medium was renewed with fresh medium and incubated with barakol at various concentrations ranging from 0.05-1.0 mM for 24 h. At the end of incubation, cell viability of P19 neurons was assessed using tetrazolium salt XTT assay and trypan blue dye exclusion assay.

3.2 Time-course study

The EBs were triturated and seeded at a density of 10^6 cells/ml into 96-well plates. On day 7 after plating, the medium was discarded and replaced with fresh medium supplemented with barakol at various concentrations ranging from 0.05-1.0 mM for 24-72 h. At the end of each time study, cell viability of P19 neurons was assessed using tetrazolium salt XTT assay, trypan blue dye exclusion assay and neutral red dye uptake assay.

3.3 DNA fragmentation assay

The EBs were triturated and seeded at a density of 10^6 cells/ml in 6-well plates at a final volume of 2 ml. On day 7, the medium was discarded and replaced with fresh medium supplemented with barakol at concentrations of 0.5 and 1.0 mM. After 72 h of exposure, DNA of P19 neurons were extracted and analyzed on agarose gel electrophoresis as previously described.

4. Techniques for the assessment of cell viability

4.1 Tetrazolium salt XTT assay

At the end of incubation, the medium was aspirated from the cells and replaced with 100 μl fresh α-MEM and 25 μl of tetrazolium salt XTT mixture solution (1mg/ml in hot media plus 25 μM PMS). The cultures were incubated at 37 ^{0}C for 4-6 h. The medium was then removed into a new 96-well plates and measured absorbance at 450 nm on a microplate reader. The absorbance of the vehicle control was assigned a value of 100 % viability and any decrease/increase was calculated as a percentage of this value.

$$\% \text{ Cell viability} = \frac{\text{Absorbance (sample)}}{\text{Absorbance (control)}} \times 100$$

4.2 Trypan blue dye exclusion assay

At the end of exposure period, cells in each well were triturated for 30-40 times to detach cells. Then, mixed a single-cell suspension (10-20 μl) with 0.4 % trypan blue at a ratio of 1:1. After incubated a few minute (less than 5 min), cell suspension was filled in the chamber of hemocytometer using a microscope with 10X ocular and 10X objective. The numbers of viable cells (bright cells) were counted in each of squares (Cookson, 1994; Egan, 1997; Cereser, 2001). If over 10 % of the cells represent clumps, repeat triturated again. Calculate the number of viable cells per ml as follow:

Cell number (cells/ml) = average viable cell count per square x 10^4 x dilution factor.

4.3 Neutral red dye uptake assay

At the end of exposure period, cells were stained with 50 μg/ml of neutral red (diluted in culture medium). After incubated at 37 ^{0}C for 20-30 min, cell morphology of viable cells, appeared in red spot in intracellular of the cells, was observed under microscope (Riddell, 1986; Barile, 1994).

.

5. Effect of barakol on AChE activity

5.1 Effect of barakol on intracellular soluble AChE

On day 7 after plating, P19 neurons were exposed with barakol at various concentrations ranging from 0.05-1.0 mM. After 24, 48 and 72 h of exposure time, the medium was aspirated and washed twice with ice-cold PBS. After added 200 μl of fresh ice-cold PBS, cells were triturated for 30-40 times to detach cells and transferred to a microcentrifuge tube. Cells were centrifuged at 12,000g at 4 ^{0}C for 10 min and washed twice with ice-cold PBS and centrifuged again. The supernatant was discarded, added 200 μl of phosphate buffer pH 8.0 and sonicated briefly at 10 sec intervals for 30 sec. AChE activity assay was performed by Ellman's method in a reaction mixture containing 0.75 mM acetylthiocholine iodide, 0.3 mM dithiobisnitrobenzoic (DTNB 39.6 mg were dissolved in 10 ml of 0.1 M phosphate buffer pH 7 and 15 mg of sodium bicarbonate) and 20 μM iso-OMPA (at the final volume of 300 μl). Absorbance was read at 415 nm at 30 sec intervals for 15-30 min after adding of AChE. Protein determination was evaluated according to the method of Lowry and bovine serum albumin was used as a standard protein. The extinction coefficient of the yellow color of 5-thio-2-nitrobenzoic acid can be converted to absolute unit:

$$\text{Rate (moles/l.per min)} = (\Delta \text{absobance/min})/1.36 \times 10^4$$

5.2 Effect of barakol on membrane-bound AChE

On day 7 after plating, P19 neurons were incubated with barakol at various concentrations ranging from 0.05-1.0 mM. After 24, 48 and 72 h of exposure time periods, the medium was aspirated and washed with ice-cold PBS. The cells were fixed in 0.4 % formaldehyde for 10 min. After that, the solution was discarded and incubated with 20 μM iso-OMPA for 10 min (specific inhibitor for butyrylcholinesterase). AChE activity was stained using Karnovsky and Roots method. The reaction mixtures were consisted of 5 mg of acetylthiocholine iodide, 6.5 ml of 0.1 M phosphate buffer pH 8.0, 0.5 ml of 0.1 M sodium citrate, 1 ml of 30 mM copper sulfate, 1 ml of H_2O and 1 ml of 5 mM potassium ferricyanide (in the presence of iso-OMPA). The stock solutions were kept at 4 ^{0}C for several weeks. The final solution was clear, greenish in color and stable for hours. After incubation overnight, the brown color was developed and a photograph was taken.

6. Statistical analysis

All experiments were performed at least in triplicate for each concentration. Cells treated only with ultra-purified water were included as vehicle controls. Statistical analysis was carried out with a statistical SPSS program. These studies used one-way analysis of variance (ANOVA) followed by Tukey multiple comparison test to evaluate significant difference. Results are presented as mean ± S.D. and are considered significant if $P<0.01$ or $P<0.05$.

CHAPTER IV

RESULTS

1. Differentiation of P19 cells

1.1 Morphological features of P19 cells

P19 cells are easy to grow in monolayer and can be maintained if certain pitfalls are avoided. These cells do not stop replicating in a density-dependent manner and thus readily over grow and finally death if the subculture is not on schedule. Cultures used for differentiation should be relatively free of debris and should not have acid medium. P19 cells showed fibroblast-like morphology, which were poorly differentiated under normal condition (Fig. 2A)

1.2 Morphological features of embryoid bodies (EBs)

Undifferentiated P19 cells growing in the absence of RA tended to grow in monolayers and appear fibroblast-like morphology, which adhered directly to plastic well or flask without having recourse to the use of the attachment factors. One day after seeding P19 cells in bacteriological-grade petri dishes and treated with 0.5 μm RA, cells spontaneously aggregated into spherical shape, also called EBs, of various sizes (Fig. 2B). The EBs observed under phase contrast microscope were frequently aggregates and may show stalk-like structures protruding from the body. On day 2, the number of cells in aggregates and the size were increased. On day 4, the size of EBs became increasing and some EBs were aggregated together. In the process of differentiation, there were a few cells or aggregates adhere to the petri dish.

1.3 Morphological features of P19 neurons

Neuronal differentiation was stimulated by allowing P19 cells to aggregate in bacterial grade petri dishes for 4 days in α-MEM medium supplemented with 0.5 μM RA. Cells were replated in medium lacking RA in tissue culture wells

coated with poly-L-lysine to promote neuronal phenotype. One day after plating, cells were aggregated together. On day 2, most of the cells were small and some cells exerted short neuritic processes, which showing the characteristic morphology of neuronal cells: soma and neurites (Fig. 2C). These cells with a neuron-like morphology will hence be referred to as P19 neurons. They were observed either as isolated cells or as aggregates of various sizes. After 3 days of culturing, more cell bodies were trapped within these clusters to form islets. The size as well as compactness of the islets varied. The islets were cross-linked by bundles of neurites or extremely long single neurites and bundles of neurites diverged out in several directions from the islet. On day 4, long interwoven neurite extensions emanated from the cell aggregates. The clusters of neurons now gave off multiple neurites. On day 7 of culturing, P19 neurons were highly enriched, which were estimated by visual examination that at least 90 % of the cells exhibited this neuronal phenotype. The neurites made contact with each other and complicate patterns evolved because of their branching. These cells, which were usually small and round shape, showed the characteristic morphology of neuronal cells (Fig. 2D).

P19 neurons were distinguished as phase-bright rounded cells with extended processes. Glia and other non-neuronal cells were often seen beneath neuron-like cells and appeared as flattened, non-phase bright cells (Fig. 2D). Although non-neuronal cells were abundant in cultures on day 2 after plating, their cell number steadily declined upon treatment of 10 μM ara-C. This treatment was selective for retaining post-mitotic neurons and resulted in highly enriched neuronal population. At this time, virtually all the cells appeared morphologically very similar to mature primary neurons; however, exact quantification of the proportion of precursor P19 cells that became P19 neurons were not determined except the AChE activity.

1.4 Histochemical staining of AChE positive neurons.

P19 cells were cultured as EBs for 4 days in the presence of RA and then allowed to differentiate morphologically to P19 neurons after day 7 of culturing. Membrane-bound AChE activity of P19 neurons was stained by the method of Karnovsky and Roots (Karnovsky and Roots, 1961) as described in the Methods.

Histochemical staining for AChE activity showed a brown color indicated that P19 cells differentiated to P19 neurons exhibited cholinergic positive neurons (Fig. 3).

2. Determination of cytotoxic effect of barakol on P19 cells

2.1 Concentration-dependent study

Initial cytotoxicity assessments of barakol on undifferentiated P19 cells with XTT assay revealed that significant cytotoxicity occurred after incubated with barakol at the concentrations of ≥ 0.8 mM, following 24 h of exposure. Percentages of cell viability significantly decreased to 87 and 78 after exposed with barakol at the concentrations of 0.8 and 1.0 mM, respectively (Fig. 4). Trypan blue dye exclusion assay was used to evaluate the viable cell numbers. At all experimental concentrations ranging from 0.05-1.0 mM, barakol did not reveal significantly cytotoxic to P19 cells following 24 h of exposure (Fig. 5). Phase contrast photomicrographs of barakol-treated and non-treated of P19 cells after stained with trypan blue revealed that there were a few number of floating cell death after exposure with barakol at the concentrations of 0.8-1.0 mM. Cell morphology showed no observable difference in the presence and absence of barakol (Fig. 6).

2.2 Time-course study

To further testify the cytotoxic effect of barakol at longer time period, the time-course study of barakol was evaluated using the XTT assay. The results showed that barakol at the concentration of 0.4 mM exerted slightly cytotoxic effect to P19 cells after 36 h of exposure, cell viability approximately 87 % of the control. Following 72 h of incubation period, cell viability was significantly declined to 67 % of the control. Barakol at the concentration of 0.8 mM showed more cytotoxic effect to P19 cells, cell viability was approximately decreased to 25 % of the control after 36 h of exposure. The results indicated that barakol was exerting a cytotoxic effect to P19 cells in a time dependent manner (Fig. 7).

Trypan blue dye exclusion assay was used to investigate the viable cell numbers. Barakol at the concentration of 0.8 mM exhibited significant cytotoxicity to P19 cells after 36 h of exposure. The viable cell number was

approximately 52 % of the control (Fig. 8). Barakol at the concentration of 0.4 mM at 48 h of treatment showed less cytotoxicity to P19 cells, with the viable cell number approximately 85 % of the control.

Morphological observation of P19 cells was determined by trypan blue staining and observed under microscope. After 48 h of exposure, barakol-treated group at the concentration of 0.4 mM also exerted morphology indifferently (Fig. 9B) compared with control group (Fig. 9A). Barakol at the concentration of 0.8 mM showed slightly observable difference in the morphology of P19 cells. Their morphology revealed smaller than un-treated cells and exhibited a round shape. There were a few number of cell death (showing in a blue cells) after staining with trypan blue (Fig. 9C). At the concentration of 1.0 mM of treatment, most of cells were shrinkage and exhibited in round shape. There were a few number of cell death after they were stained with trypan blue (Fig 9D). At 72 h of exposure, barakol-treated groups at the concentration of 0.4 mM also exerted morphological indifferently. Barakol-treated groups at the concentrations of 0.8 and 1.0 mM were found to exhibit smaller and spherical shape and fewer cell density than untreated group but still viable. There were a few number of cell death, which stained with trypan blue (Fig. 10). To confirm the cell viability, the neutral red dye was used to stain the viable cells (Fig. 11).

2.3 Recovery study

To study the recovery of P19 cells after treated with barakol at the concentrations of 0.4, 0.8 and 1.0 mM for 72 h. At the end of incubation time, the medium was discarded and followed by substitution with fresh barakol-free medium. After allowing the cells to recover for 48 and 96 h, the cells were stained with trypan blue and counted in hemocytometer. The results showed that the cell numbers of P19 cells were significantly increased after incubated with barakol at the concentrations of 0.4 and 0.8 mM (Fig. 12). However, barakol at the concentration of 1.0 mM showed indifferently increase in the cell number following 96 h of incubation with barakol-free medium. After the barakol-treated P19 cells at the concentrations of 0.4 mM (Fig. 13A and 13B), 0.8 mM (Fig. 14A and 14B) and 1.0 mM (Fig. 15A and 15B) for 72 h and following by 96 h of incubation with barakol-free medium, cell morphology was observed. The results exhibited that barakol-treated P19 cells at 0.4 mM showed

the increase in cell density and the alteration of cell morphology into small shape and packed cells. There were a few number of cell death in the trypan blue stain (Fig. 13C) and most cells were still viable as shown in neutral red stain (Fig. 13D). At 0.8 mM of barakol-treated P19 cells, morphology was altered in a swollen and spherical shape (Fig. 14C and 14D). At 1.0 mM of barakol-treated P19 cells, morphology was enlarged, swollen and spherical shape. There were a few number of cell death, some cells exerted fibroblast morphology (Fig. 15C and 15D).

2.4 DNA fragmentation assay

The pattern of cell death was investigated with agarose gel electrophoresis technique. The result showed that barakol-treated cells exhibited a pattern of internucleosomal DNA fragmentation characteristics of a type of cell death designated as apoptosis (Fig. 16). Barakol at the concentrations of 0.5 mM (lane 2) and 1.0 mM (lane 3) showed a pale DNA ladder compared with RA-treated P19 cells for 4 day (lane 4) and spontaneous cell death (aging culture)(lane 5) used as a positive control, which showed a clear pattern of internucleosomal DNA cleavage (discrete fragments differing in size from one another) and was different from a negative control (lane1).

3. Determination of cytotoxic effect of barakol on P19 neurons

3.1 Concentration-dependent study

Cytotoxicity effect of barakol on P19 neurons showed that barakol at various concentrations ranging from 0.05-1.0 mM did not exert cytotoxic effect to P19 neurons following 24 h of exposure, assessed by both XTT assay (Fig. 17) and trypan blue dye exclusion assay (Fig. 18). The morphological observation under inverted microscope revealed that there was no difference in the presence of barakol at the indicated concentration range. There was slightly observable different in the length of neurites at the concentration of $\geq$ 0.8 mM.

3.2 Time-course study

Time-course study with XTT assay showed that barakol at the concentrations of ≤ 0.4 mM did not exert cytotoxic to P19 neurons at 24-72 h of exposure. Barakol exhibited significant cytotoxicity to P19 neurons at the concentrations of 0.8 mM at 36 h of exposure (Fig. 19). Barakol at the concentration of 1.0 mM for 72 h showed a low cytotoxicity to P19 neurons. The percentage of cell viability was greater than 74 % of the control at all exposure concentrations.

Time-course study with trypan blue dye exclusion assay was used to investigate the viable cell number (Fig. 20). At 24-72 h of exposure, barakol at the concentration of 1.0 mM did not show significantly cytotoxic to P19 neurons. The cell number of P19 neurons, in the absence or in the presence of barakol at all exposure concentrations for 72 h, was slightly decreased.

Morphological observation of P19 neurons was determined by trypan blue staining and observed under microscope. The results showed that there was no morphological difference between un-treated and barakol-treated groups at the concentrations of 0.4-1.0 mM for 24 h (Fig. 21). After 48 h of exposure, barakol-treated cells at the concentration of 0.4 mM exerted morphology indifferently compared with the control group. Barakol at the concentration of 0.8 mM showed observable difference in the morphology of P19 neurons. Their morphology revealed the appearance of vacuolation in P19 neurons. There were a few number of cell death (showing in a blue cells) after staining with trypan blue. At the concentration of 1.0 mM, neurite did not appear and there was a lot of vacuolation intracellularly (Fig. 22). After 72 h of exposure, barakol-treated groups at the concentration of 0.4 mM also exerted morphology indifferently. Barakol at the concentration of 0.8 mM exhibited shorter neurite than the control group. Their morphology revealed vacuolation in P19 neurons. Barakol-treated P19 neurons at 1.0 mM, did not exhibit neurite outgrowth and there was a large vacuolation in the soma (Fig. 23).

Neutral red staining of P19 neurons revealed that there were a lot of viable cells after exposure to barakol at the concentrations ranging from 0.4-1.0 mM for 24 h (Fig. 24). At 48-72 h of exposure, barakol at the concentration of 0.4 mM did not exert cytotoxic to P19 neurons. However, barakol-treated P19 neurons, at the

concentrations of 0.8-1.0 mM for 48 h (Fig. 25) and for 72 h (Fig. 26), exhibited vacuolation in the soma but still revealed viable cells.

3.3 DNA fragmentation assay of P19 neurons

P19 neurons were exposed to barakol at the concentrations of 0.5 and 1.0 mM for 72 h, then the DNA extraction and DNA fragmentation assay was prepared. The result showed that barakol exhibited a pattern of pale internucleosomal DNA fragmentation after P19 neurons were incubated with barakol at the concentrations of 0.5 mM (lane 2) and 1.0 mM (lane 3) compared to 100 base pair DNA ladder (lane 1) and a negative control group (lane 4). This characteristic of a type of cell death was designated as apoptosis (Fig. 27).

4. Effect of barakol on AChE activity in P19 neurons

4.1 Effect of barakol on intracellular soluble AChE

P19 neurons were incubated with barakol at the concentrations ranging from 0.05-1.0 mM for 24-72 h. Intracellular soluble AChE was extracted and AChE assay was performed with Ellman's method. These results revealed that there was no significant AChE activity in barakol-treated group compared with vehicle control group (Fig. 28).

4.2 Effect of barakol on membrane-bound AChE

The inhibitory effect of barakol on membrane-bound AChE was studied. The results showed that barakol at the concentrations ranging from 0.4-1.0 mM for 24-72 h of exposure, revealed no discernible different in membrane-bound AChE inhibitory activity. Barakol-treated groups at all concentrations for 24 h (Fig. 29), 48 h (Fig. 30) and 72 h (Fig. 31) also exhibited brown color, which were not different from the control group.

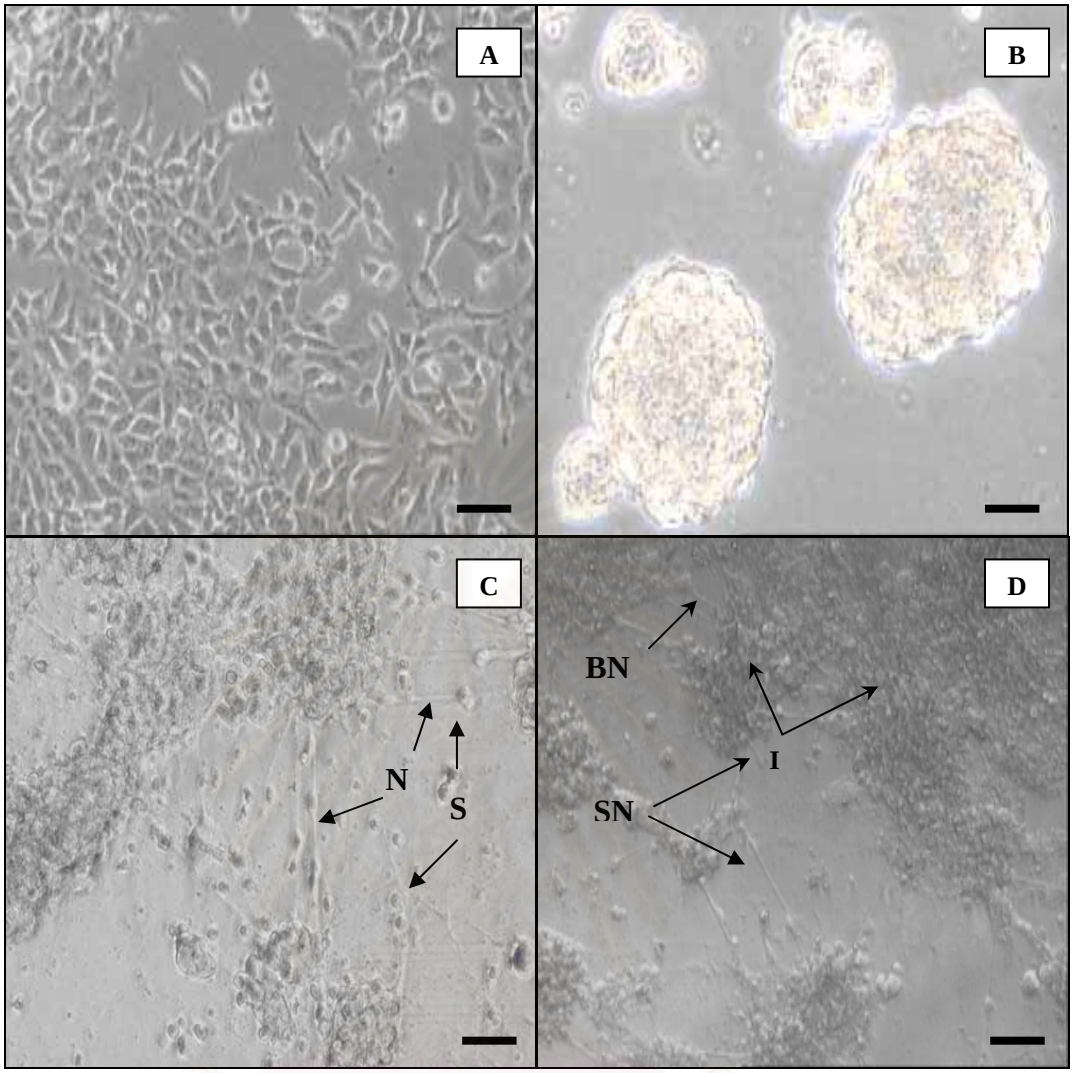

Fig. 2 Morphology of P19 cells, EBs and P19 neurons. P19 cells were growing in monolayer as fibroblast morphology (A). EBs were obtained after seeding P19 cells in petri dish in the presence of 0.5 μM RA for 4 days. EBs were observed under phase contrast microscope showing multicellular aggregates and roughly spherical morphology (B). Aggregates of P19 cells were dissociated and plated onto tissue culture wells. On day 2, P19 neurons appeared whose processes grew rapidly from the aggregate (C). Cultures obtained from day 7 after plating, cells were highly enriched in neurons (D). More cell bodies were trapped within these clusters to form "islets". The size as well as compactness of the islets varied. The islets were cross-linked by bundle of neurites or extremely long single of neurites diverged out in several directions from the islet and non-neuronal cells. N = neurite, S = soma, I = islet, SN = single of neurite, BN = bundle of neurites. Bar = 10 μm.

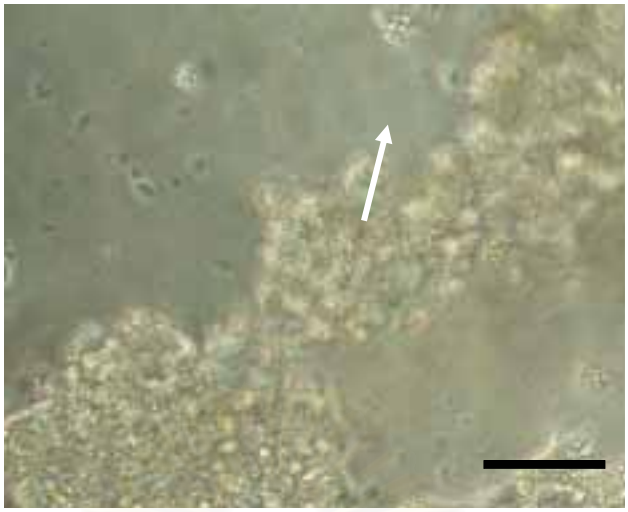

Fig. 3 Histochemical detection of AChE activity. After plating for neuronal differentiation for 7 days in tissue culture plates, membrane-bound AChE activity of P19 neurons was stained by the method of Karnovsky and Roots as described in the Methods. Histochemical stain for AChE activity showed a brown color, which indicated that P19 cells differentiated to P19 neurons exhibited cholinergic positive neuron (white arrow). Bar = 10 μm.

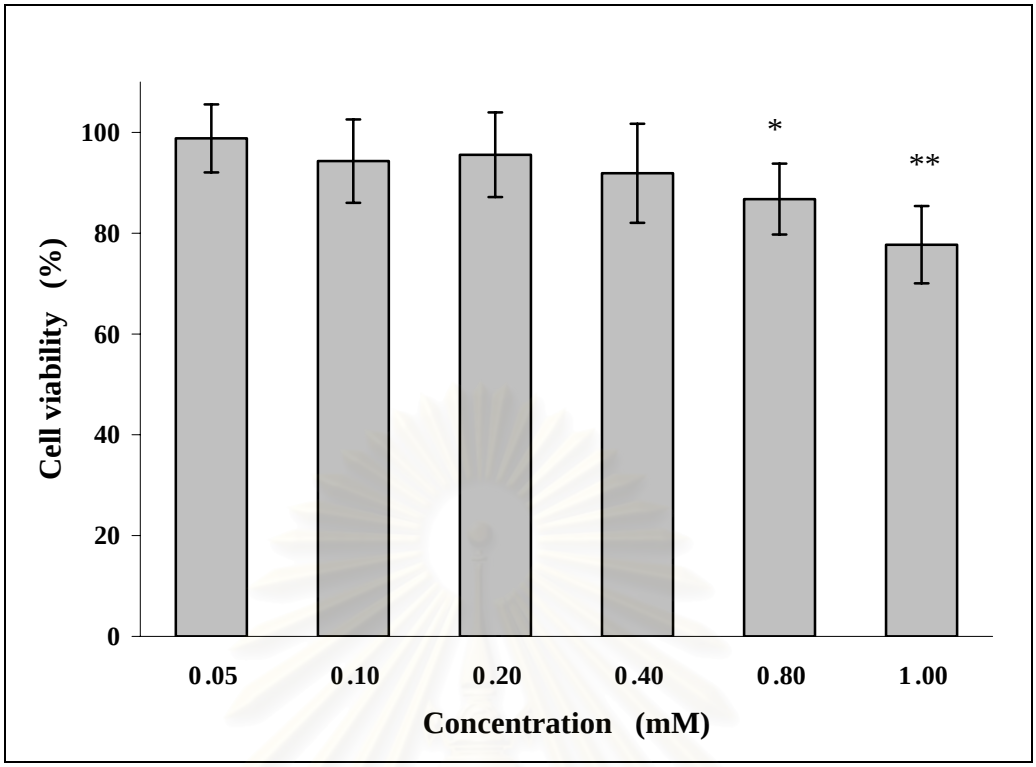

Fig. 4 Concentration-dependent study of barakol on P19 cells assessed by XTT assay. P19 cells were seeded at 10^5 cells/ml into 96 well plates. After 24 h of incubation, P19 cells were exposed to various barakol concentrations ranging from 0.05-1.0 mM for 24 h. At the end of exposure time, cell viability was determined by tetrazolium salt XTT assay. Data are presented as mean ± S.D compared with control group. Each data was investigated at least triplicate. Statistical significance was evaluated by one-way analysis of variance. In the Tukey multiple comparison test determined the concentration of barakol at which the percentage of cell viability was significantly different. * denote $P<0.05$, ** denote $P<0.01$ versus vehicle control group. n = 11.

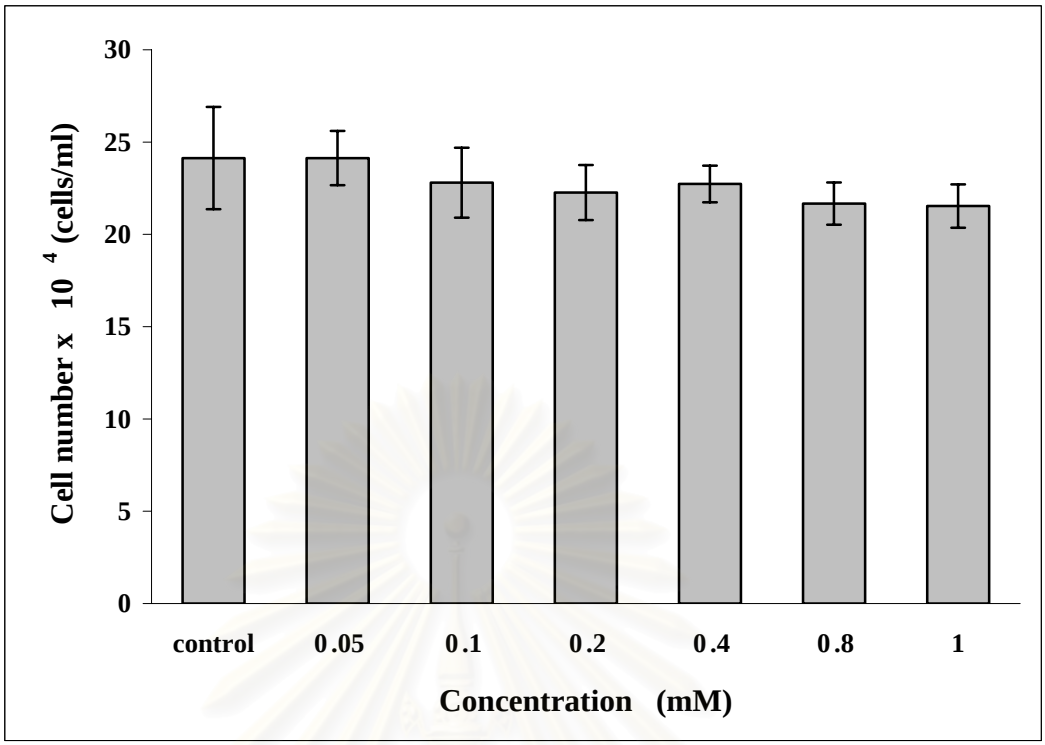

Fig. 5 Concentration-dependent study of barakol on P19 cells assessed by trypan blue dye exclusion assay. P19 cells were seeded at 10^5 cells/ml into 96 well plates. After 24 h of incubation, P19 cells were treated with barakol at the indicated concentrations. Following 24 h of exposure, cells were triturated to detach cells and stained with 0.4 % trypan blue. After staining, P19 cells were counted under microscope using hemocytometer. Data are investigated at least triplicate and presented as mean ± S.D. n = 6.

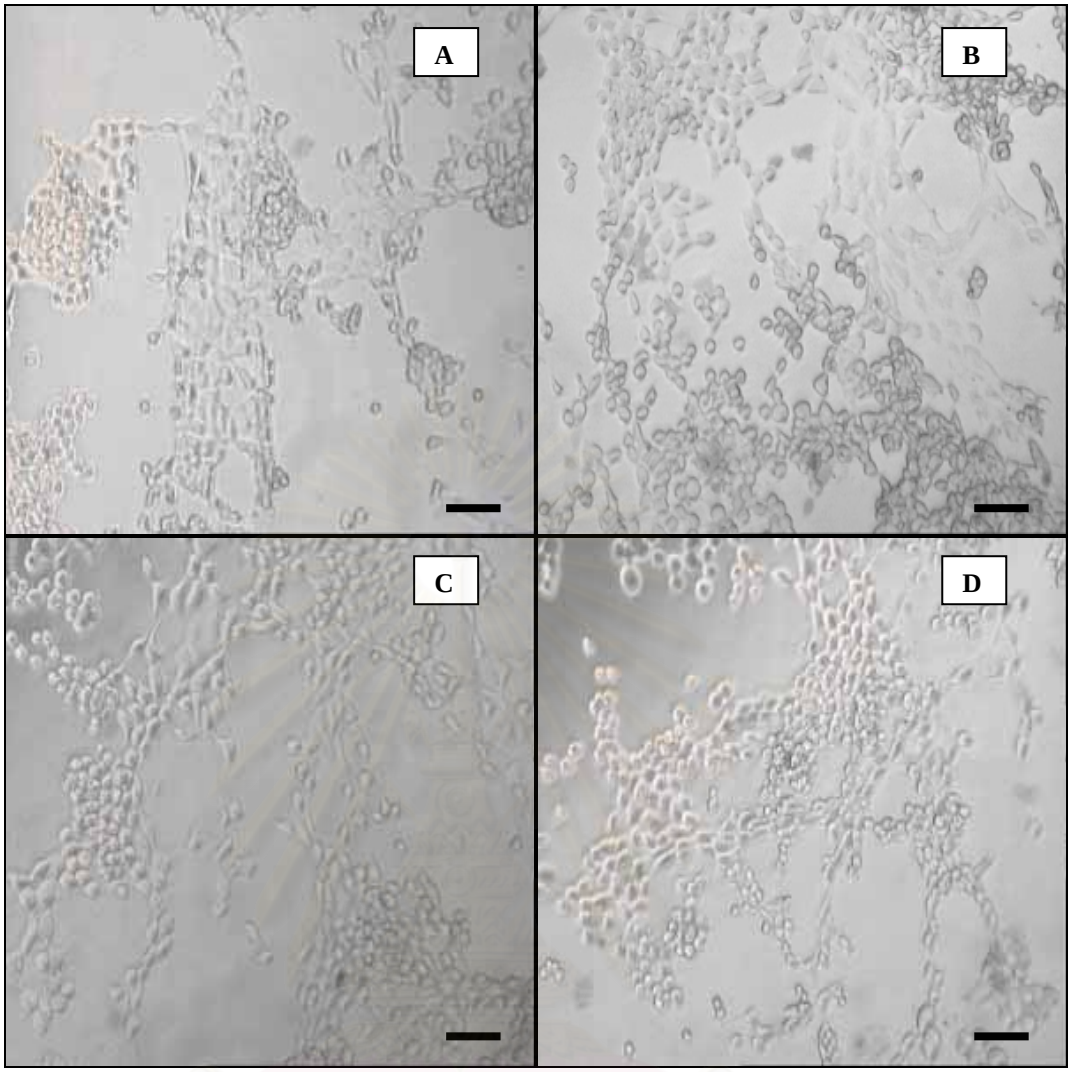

Fig. 6 Phase contrast photographs of barakol-treated P19 cells for 24 h and stained with trypan blue. P19 cells were seeded at 10^5 cells/ml into 96 well plates. After 24 h of incubation, P19 cells were treated with barakol as indicated concentrations of 0 mM (A), 0.4 mM (B), 0.8 mM (C), and 1.0 mM (D). Following 24 h of exposure, P19 cells were stained with 0.4 % trypan blue and photographs were taken under microscope. Bar = 10 μm.

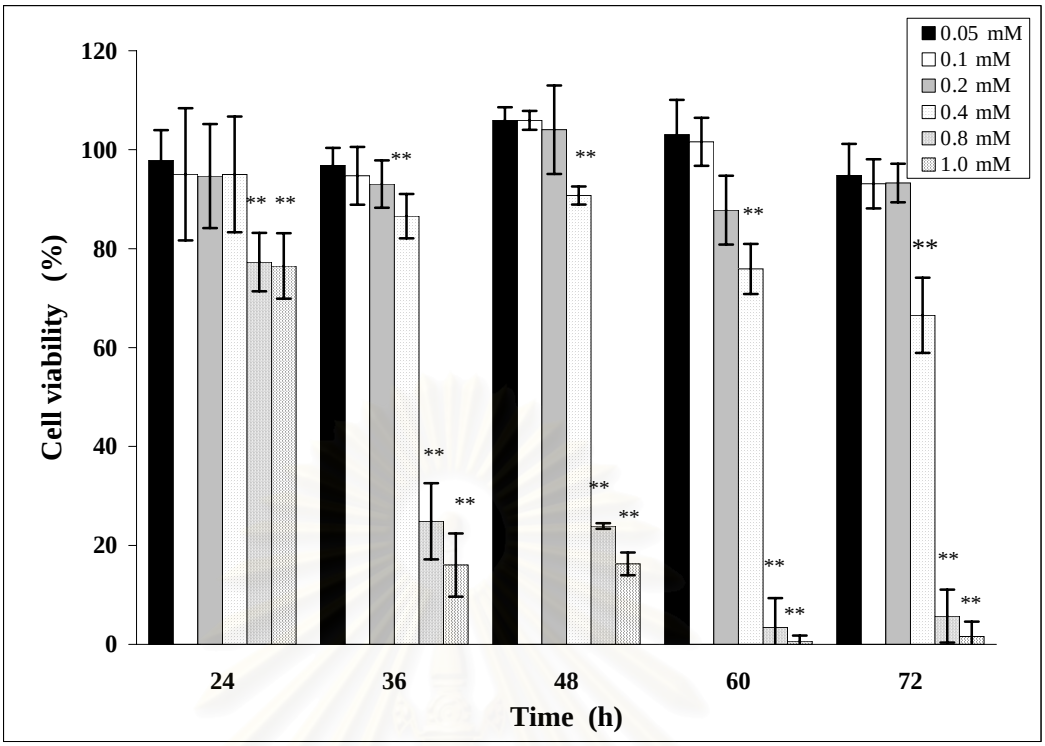

Fig. 7 Time-course study of barakol on P19 cells assessed by XTT assay. P19 cells were treated with barakol at the concentrations ranging from 0.05-1.0 mM for 24, 36 48, 60 and 72 h. Barakol-treated cells in each well were compared to untreated control group. Each barakol concentration was tested in triplicate in a randomized manner. Statistical analysis was performed by ANOVA. In the Tukey multiple comparison test determined the concentration of barakol at which the percentage of cell viability was significantly different. Data are presented as mean ± S.D. n = 9.
** denote $P<0.01$ versus control.

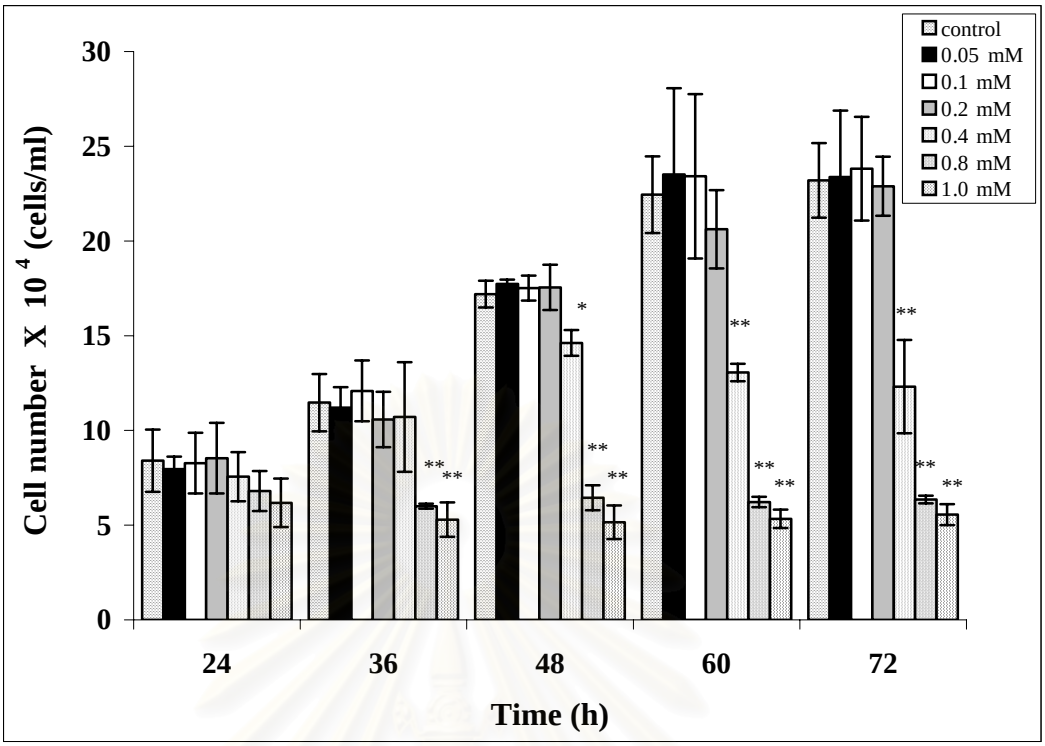

Fig. 8 Time-course study of barakol on P19 cells assessed by trypan blue dye exclusion assay. P19 cells were treated with varying barakol concentrations from 0.05-1.0 mM for 24, 36 48, 60 and 72 h. Barakol-treated cells in each well were compared to untreated control groups. Each barakol concentration was tested in triplicate in a randomized manner. Each barakol concentration was tested in triplicate in a randomized manner. Statistical analysis was performed by ANOVA. In the Tukey multiple comparison test determined the concentration of barakol at which the percentage of cell viability was significantly different. Data are presented as mean ± S.D. n = 3. * denote $P<0.05$, ** denote $P<0.01$ versus control.

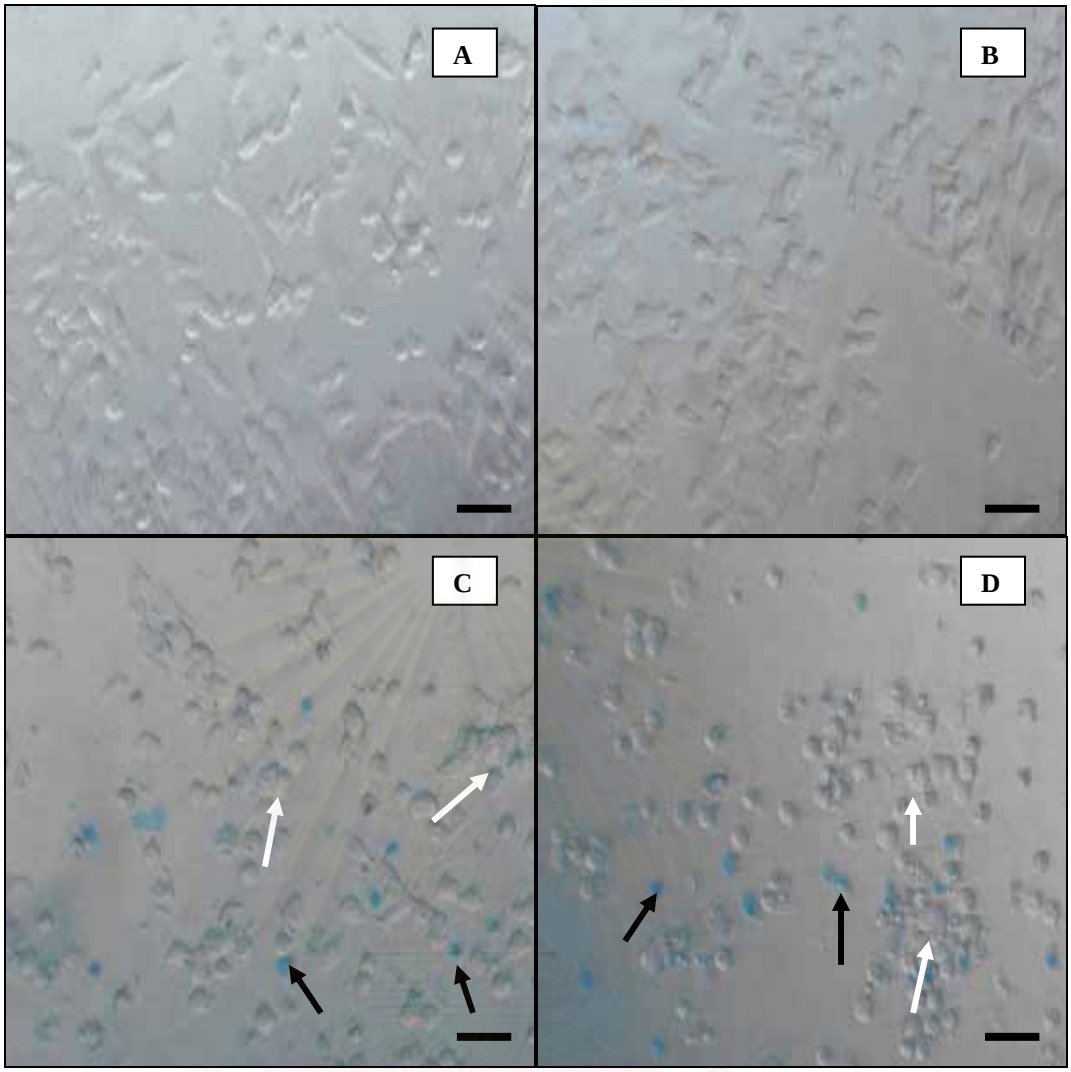

Fig. 9 Phase contrast photographs of barakol-treated P19 cells for 48 h and stained with trypan blue. Cell morphology after staining with trypan blue was observed. There were no discernible morphological difference between treated with barakol at a concentration of 0.4 mM (B) and control group (A). After exposure to 0.8 mM of barakol (C), there were a few number of cells observable difference; cells were shrinkage and appeared in spherical shape (white arrow). After exposure to 1.0 mM of barakol (D), there were observable morphological difference; most cells assumed spherical shape. There were a few number of cells stained with trypan blue indicated as dead cells (black arrow) and un-stained indicated as viable cells (white arrow). Bar = 10 μm.

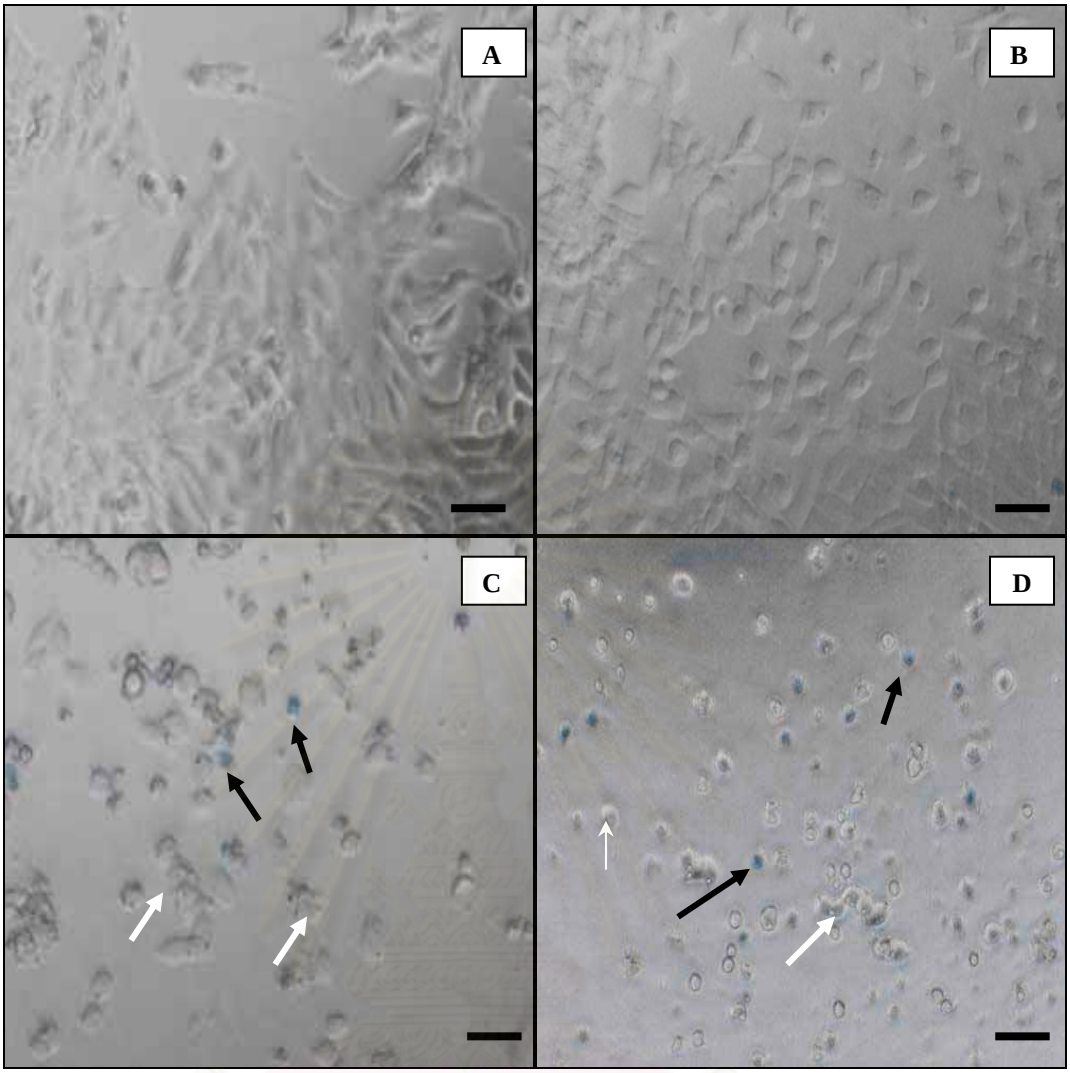

Fig. 10 Phase contrast photographs of barakol-treated P19 cells for 72 h and stained with trypan blue. There were no discernible morphologically difference between barakol-treated at 0.4 mM (B) compared with control group (A) after staining with trypan blue was observed. After exposure to 0.8 mM of barakol, there were a few number of cells observable difference; cells morphology assumed spherical shape (white arrows). After exposure to 1.0 mM of barakol (D), there were observable morphological difference; most cells were shrinkage and appeared in spherical shape. There were a few number of cells stained with trypan blue indicated as dead cells (black arrow) and un-stained indicated as viable cells (white arrow). Bar = 10 μm.

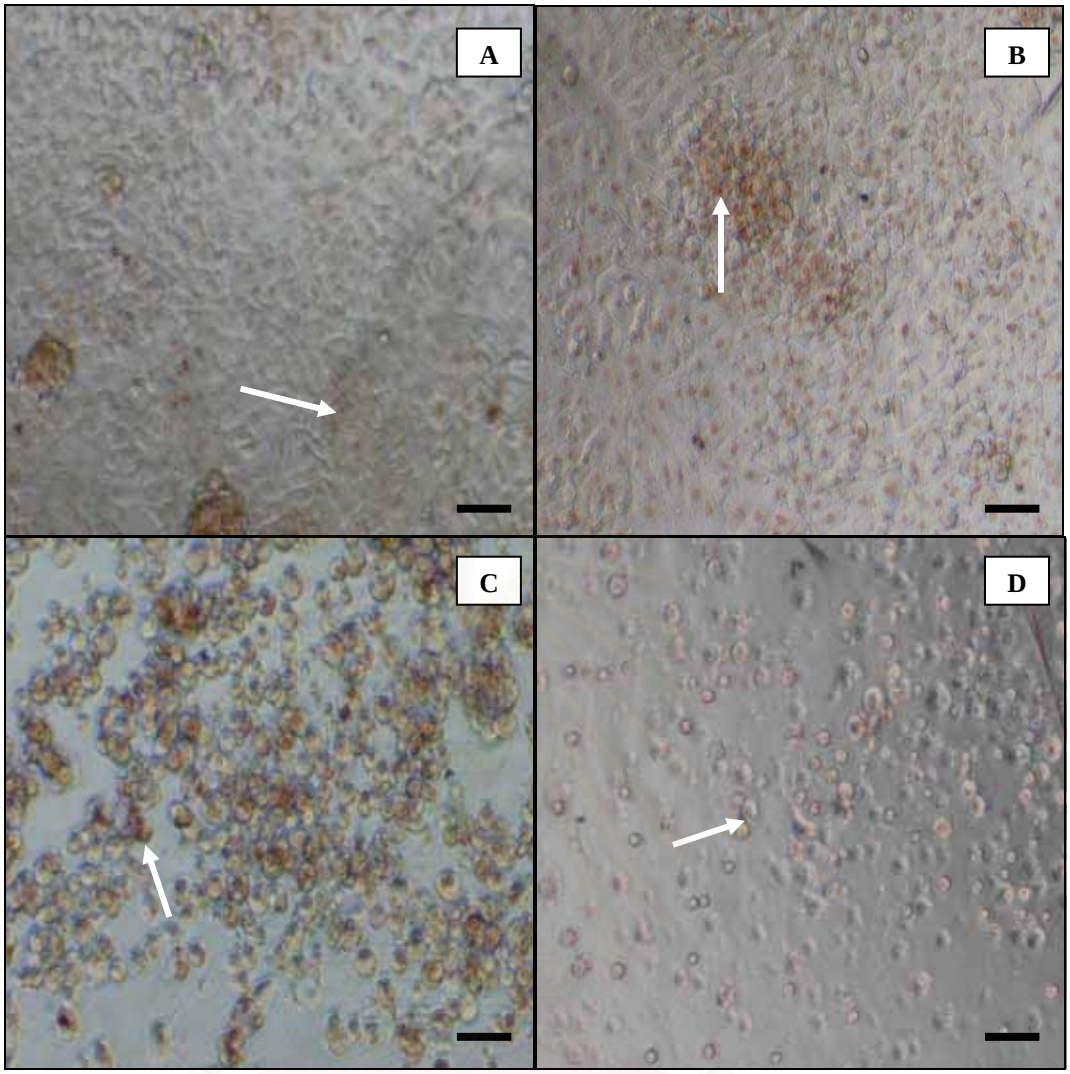

Fig. 11 Phase contrast photographs of barakol-treated P19 cells for 72 h and stained with neutral red. After exposure to barakol at 0 mM (A), 0.4 mM (B), 0.8 mM (C), and 1.0 mM (D), at the end of incubation the medium was discarded and the cells were stained with neutral red for 20-30 min. Cell viability was observed and a photograph was taken under microscope. White arrow indicated an accumulation of the dye in lysosomes, which indicated as viable cell. Bar = 10 μm.

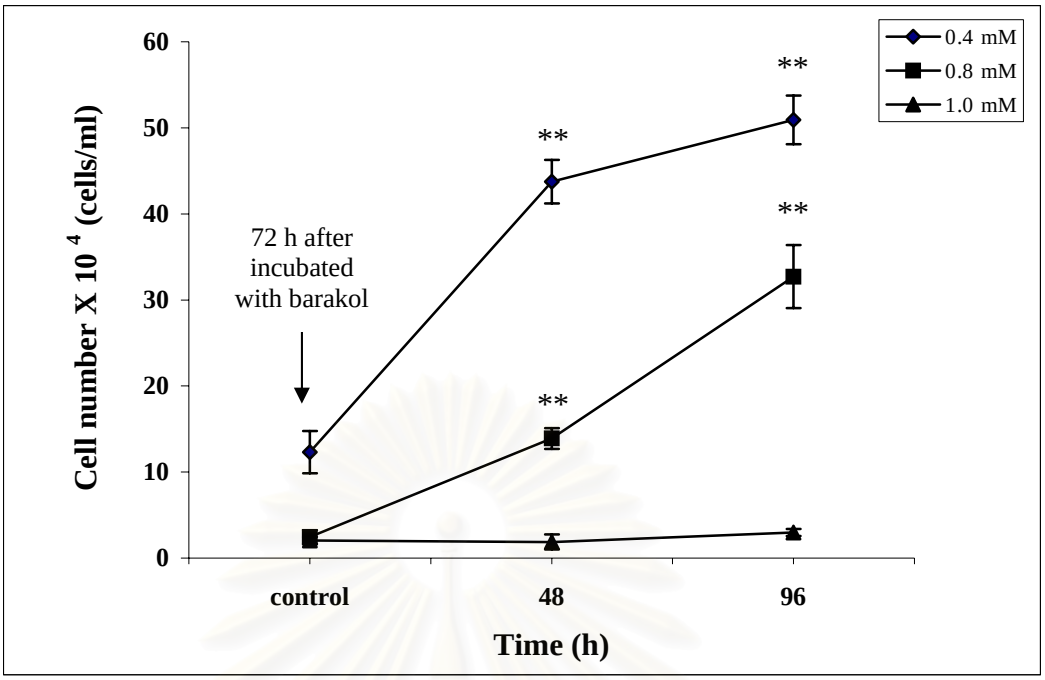

Fig. 12 Recovery study of P19 cells after exposure with barakol for 72 h. P19 cells were incubated with barakol at the concentrations of 0.4, 0.8 and 1.0 mM for 72 h. Then the medium was replaced with barakol-free medium. After the following 48 and 96 h, cells were stained with trypan blue and counted under microscope. Each barakol concentration was tested in triplicate in a randomized manner. Statistical analysis was performed by ANOVA. In the Tukey multiple comparison test determined the concentration of barakol at which the percentage of cell viability was significantly different. Data are presented as mean ± S.D. n = 3. ** denotes $P<0.01$ versus control.

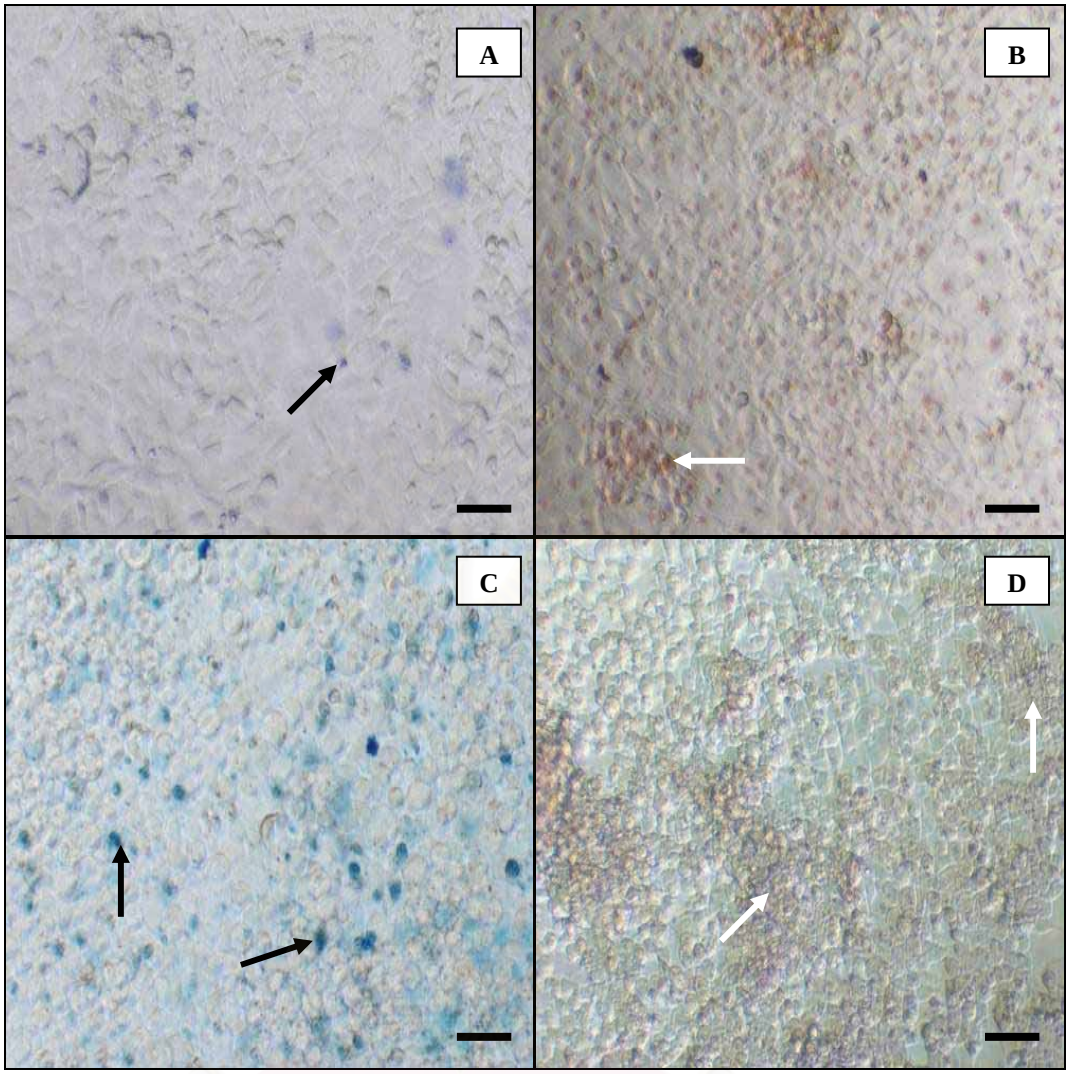

Fig. 13 Recovery study of barakol-treated P19 cells at 0.4 mM and stained with trypan blue and neutral red. At the end of exposure with barakol for 72 h, the cells were stained with trypan blue (A) and neutral red (B). Following by 96 h of incubation with barakol-free medium, the cells were stained with trypan blue (C) and neutral red (D). Black arrow indicated dead cell and white arrow indicated viable cell. Bar = 10 μm.

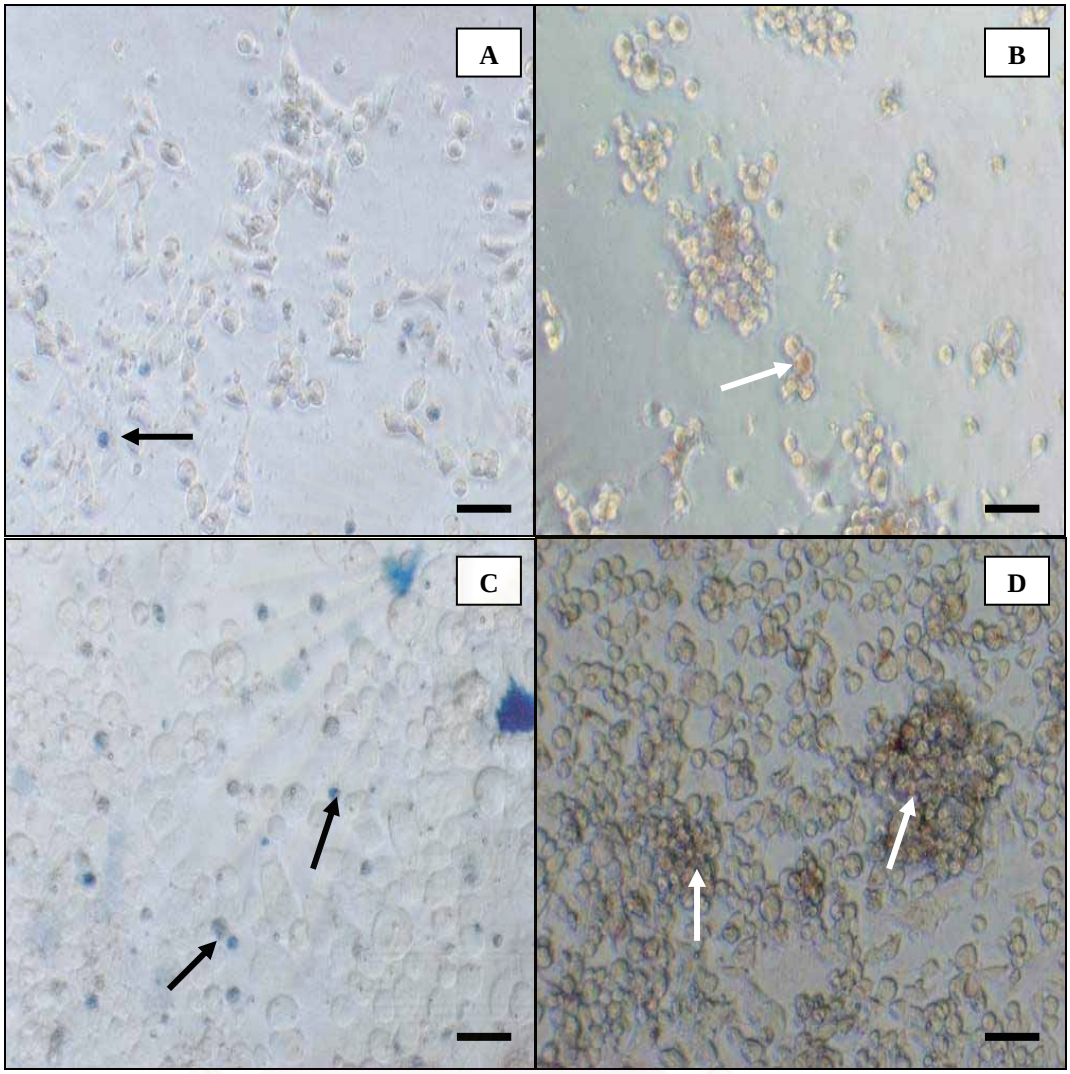

Fig. 14 Recovery study of barakol-treated P19 cells at 0.8 mM and stained with trypan blue and neutral red. At the end of exposure with barakol for 72 h, the cells were stained with trypan blue (A) and neutral red (B). Following by 96 h of incubation with barakol-free medium, the cells were stained with trypan blue (C) and neutral red (D). Black arrow indicated dead cell and white arrow indicated viable cell. Bar = 10 μm.

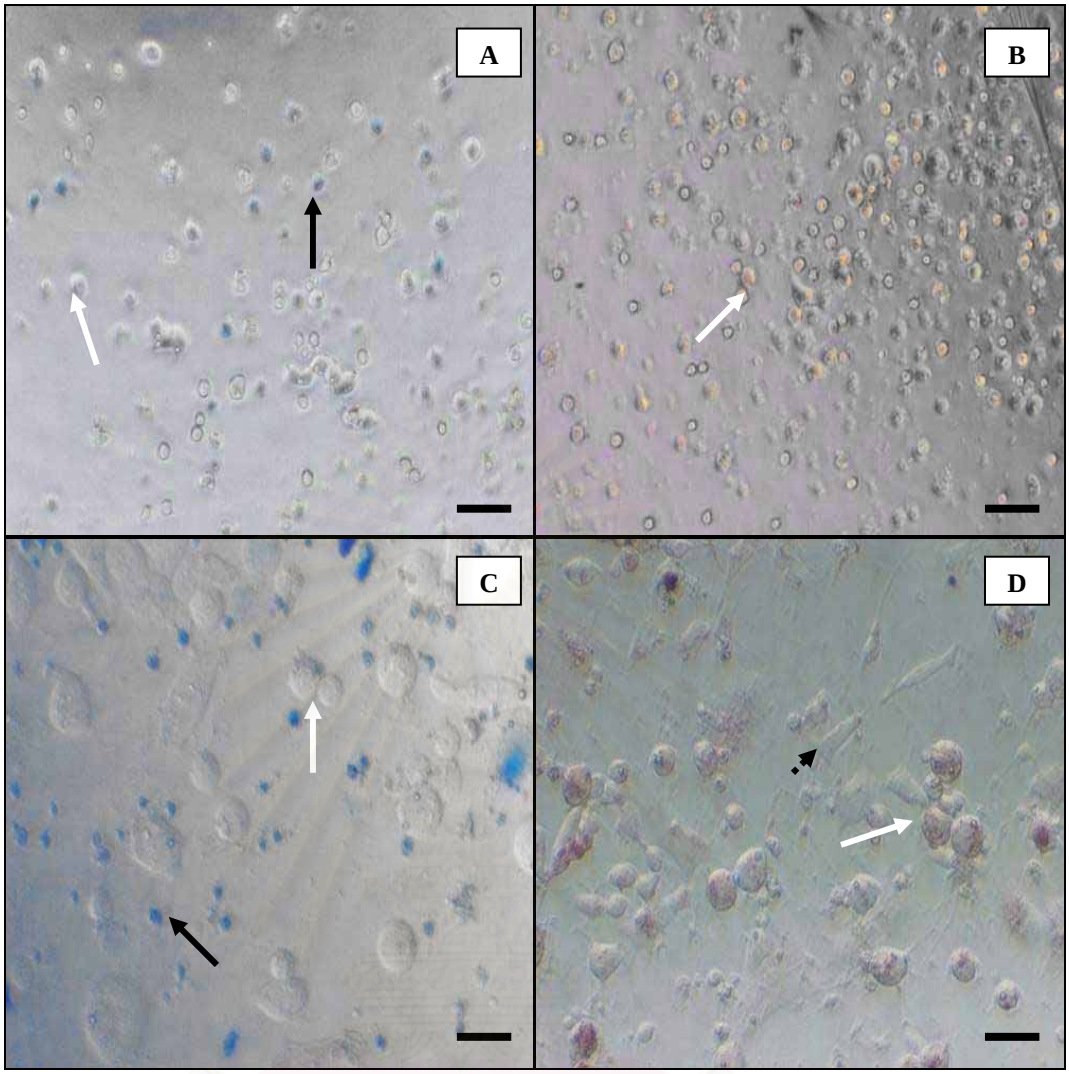

Fig. 15 Recovery study of barakol-treated P19 cells at 1.0 mM and stained with trypan blue and neutral red. At the end of exposure with barakol for 72 h, the cells were stained with trypan blue (A) and neutral red (B). Following by 96 h of incubation with barakol-free medium, the cells were stained with trypan blue (C) and neutral red (D). Black arrow indicated dead cell, white arrow indicated viable cell and head arrow indicated fibroblast morphology. Bar = 10 μm.

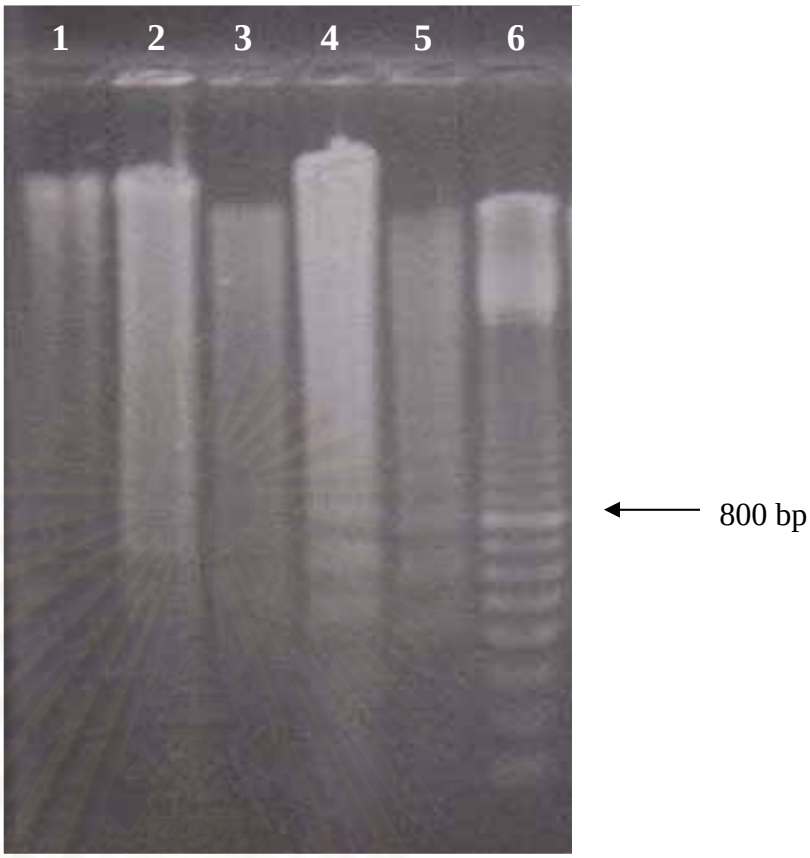

Fig. 16 Internucleosomal DNA fragmentation of barakol-treated P19 cells. P19 cells were cultured in α-MEM with no barakol addition (lane 1), 0.5 mM (lane 2) and 1.0 mM barakol (lane 3) for 72 h of exposure, 0.5 μM RA-treated P19 cells for 4 days (lane 4), spontaneous cell death (lane 5) and 100 base pair DNA ladder as a marker (lane 6). The DNA (20 μg) was separated with 1.5 % agarose gel electrophoresis at 100 V for 1 h and stained with ethidium bromide.

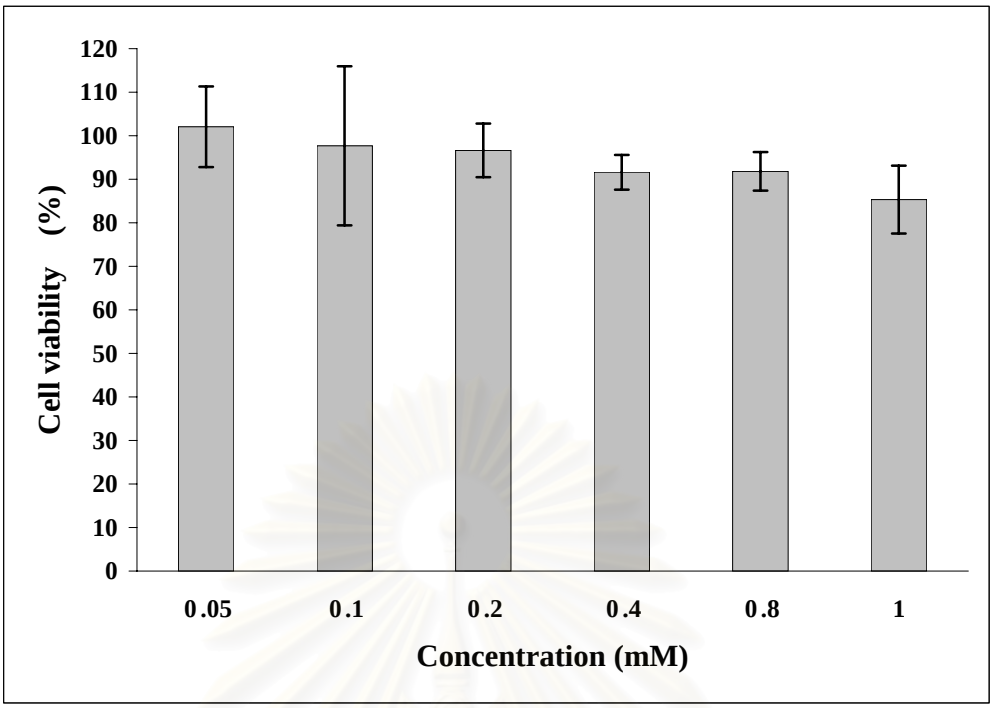

Fig. 17 Concentration-dependent study of barakol on P19 neurons assessed by XTT assay. P19 cells were differentiated in α-MEM supplemented with 5 % FBS containing 0.5 μM retinoic acid. After 4 days of culture in petri dishes with RA, EBs were triturated and plating on poly-L-lysine-coated 96-well plates. Two days after plating, 10 μM Ara-C was added to inhibit non-neuronal proliferation. On day 7 after plating, P19 neurons were incubated with barakol at the concentrations ranging from 0.05-1.0 mM. Following 24 h, cell viability was determined by XTT assay. Results were given as a percentage of the cell viability of treated compared with untreated groups. Each barakol concentration was tested in triplicate in a randomized manner. Data are represented as mean ± S.D. n = 3.

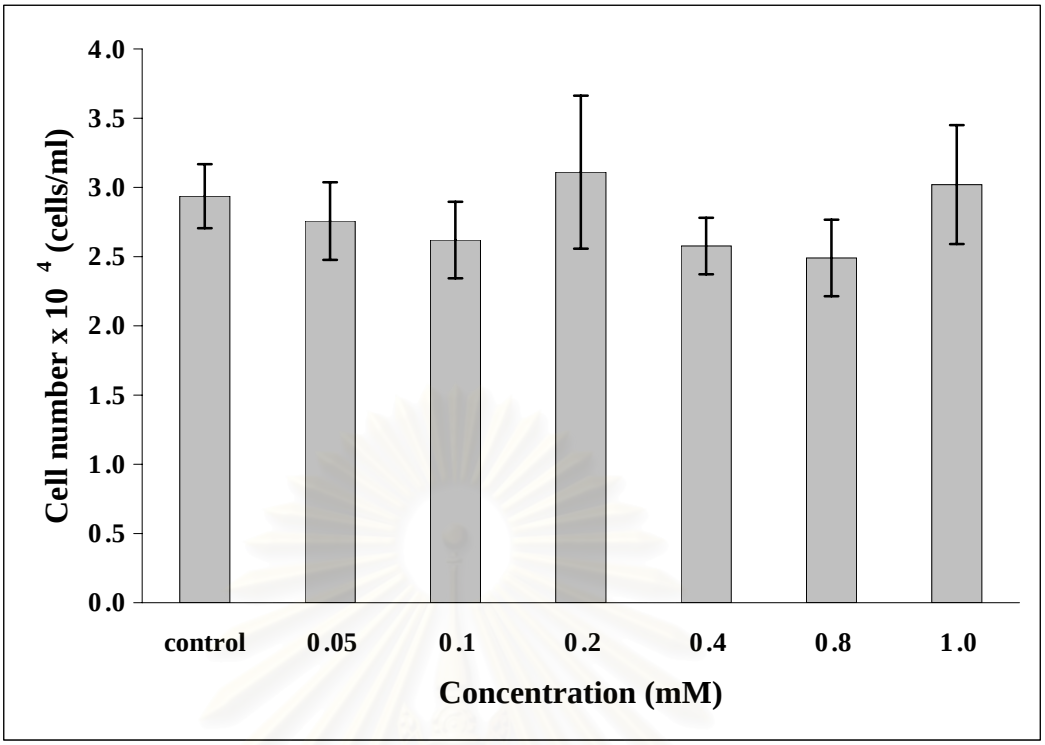

Fig. 18 Concentration-dependent study of barakol on P19 neurons assessed by trypan blue dye exclusion assay. P19 neurons were exposed to barakol at the concentrations ranging from 0.05-1.0 mM for 24 h. At the end of incubation, cells were detached from surface by triturated 20-30 times and incubated for 1-2 min with 0.4 % trypan blue at room temperature and counted under microscope. Each barakol concentration was tested in triplicate in a randomized manner. Each value is represented as mean ± S.D. of triplicate determinations. n = 3.

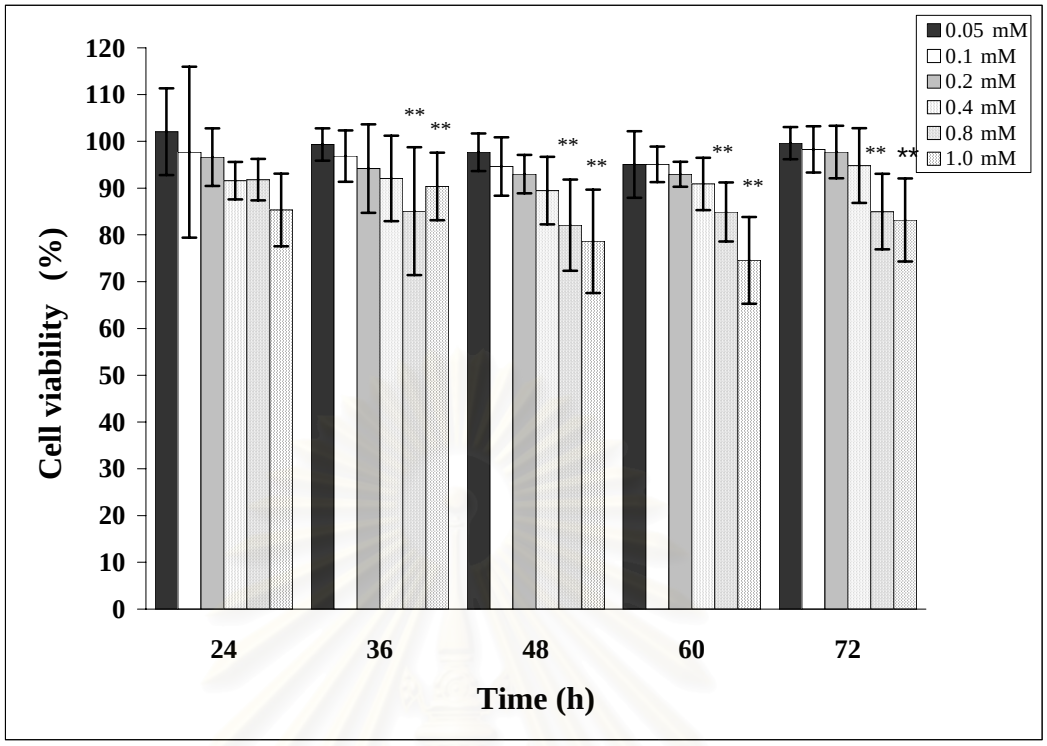

Fig. 19 Time-course study of barakol on P19 neurons assessed by XTT assay. Barakol-treated groups in each well were compared to untreated control groups. Each barakol concentration was tested in triplicate in a randomized manner. Statistical analysis was performed by ANOVA. In the Tukey multiple comparison test determined the concentration of barakol at which the percentage of cell viability was significantly different. Data are presented as mean ± S.D. ** denote $P<0.01$. n = 4.

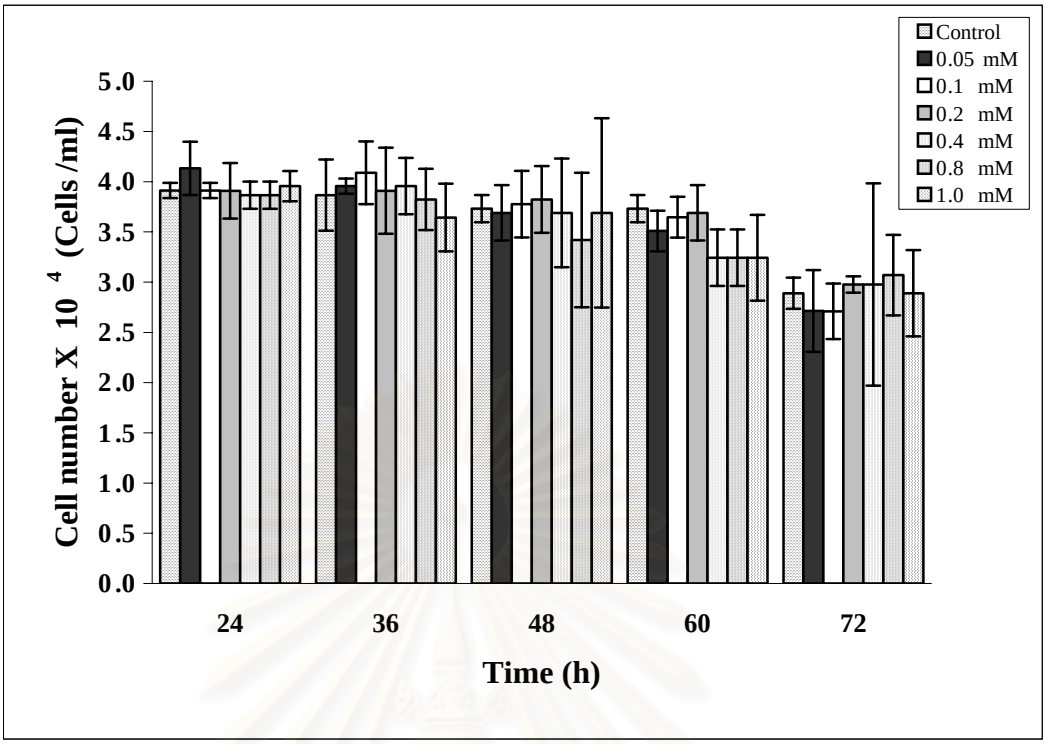

Fig. 20 Time-course study of barakol on P19 neurons assessed by trypan blue dye exclusion assay. After P19 neurons were treated with barakol at the concentrations ranging from 0.05-1.0 mM for 24-72 h, the cells were stained with trypan blue and counted under microscope. Each barakol concentration was tested in triplicate in a randomized manner. Data are presented as mean ± S.D. n = 3.

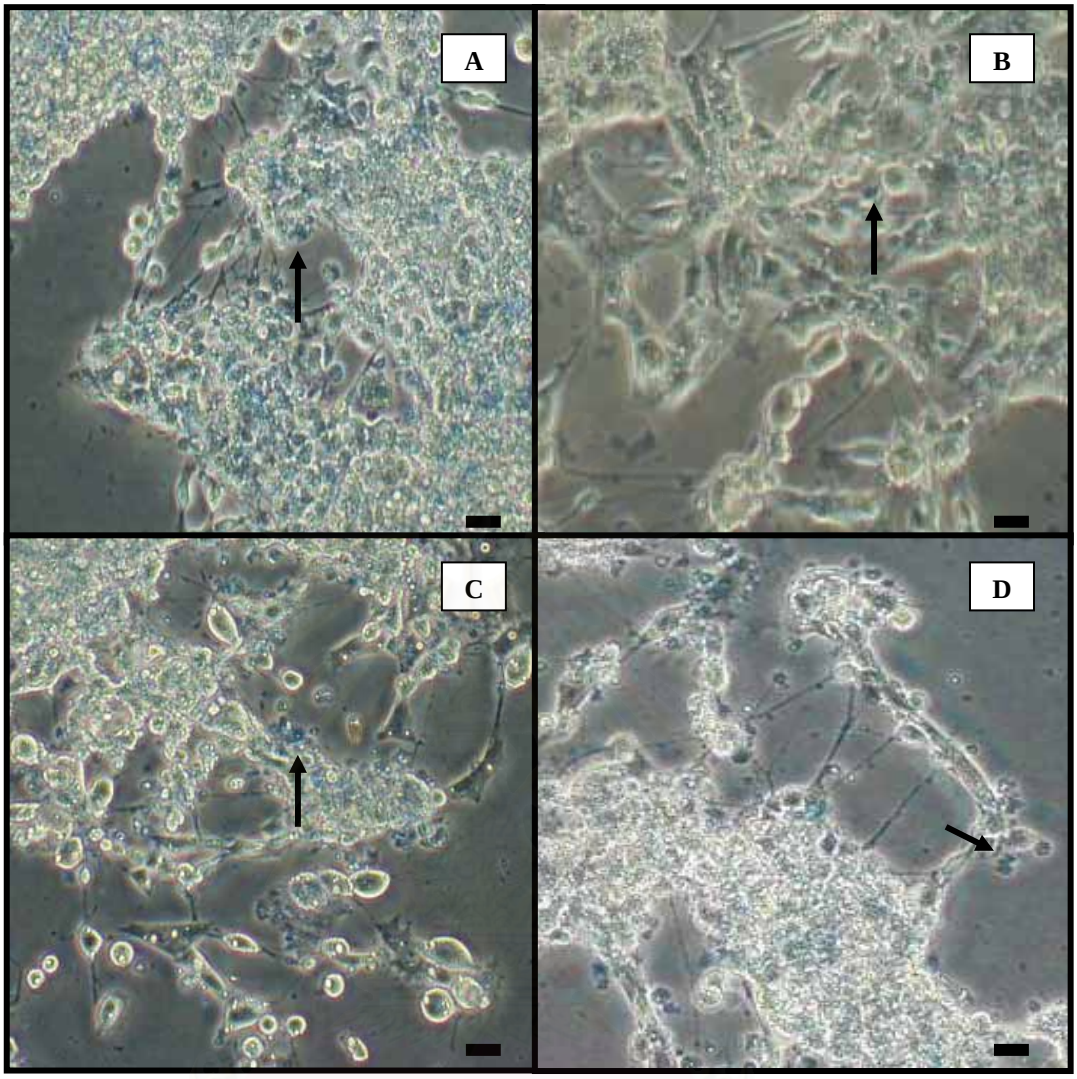

Fig. 21 Phase contrast photographs of barakol-treated P19 neurons for 24 h and stained with trypan blue. At the end of incubation period, P19 neurons were stained with 0.4 % trypan blue and photographs were taken. Cell viability was observed on un-treated P19 neuron (A), 0.4 mM (B), 0.8 mM (C), and 1.0 mM (D) of barakol-treated P19 neurons. Black arrow indicated as dead cell. Bar = 10 μm.

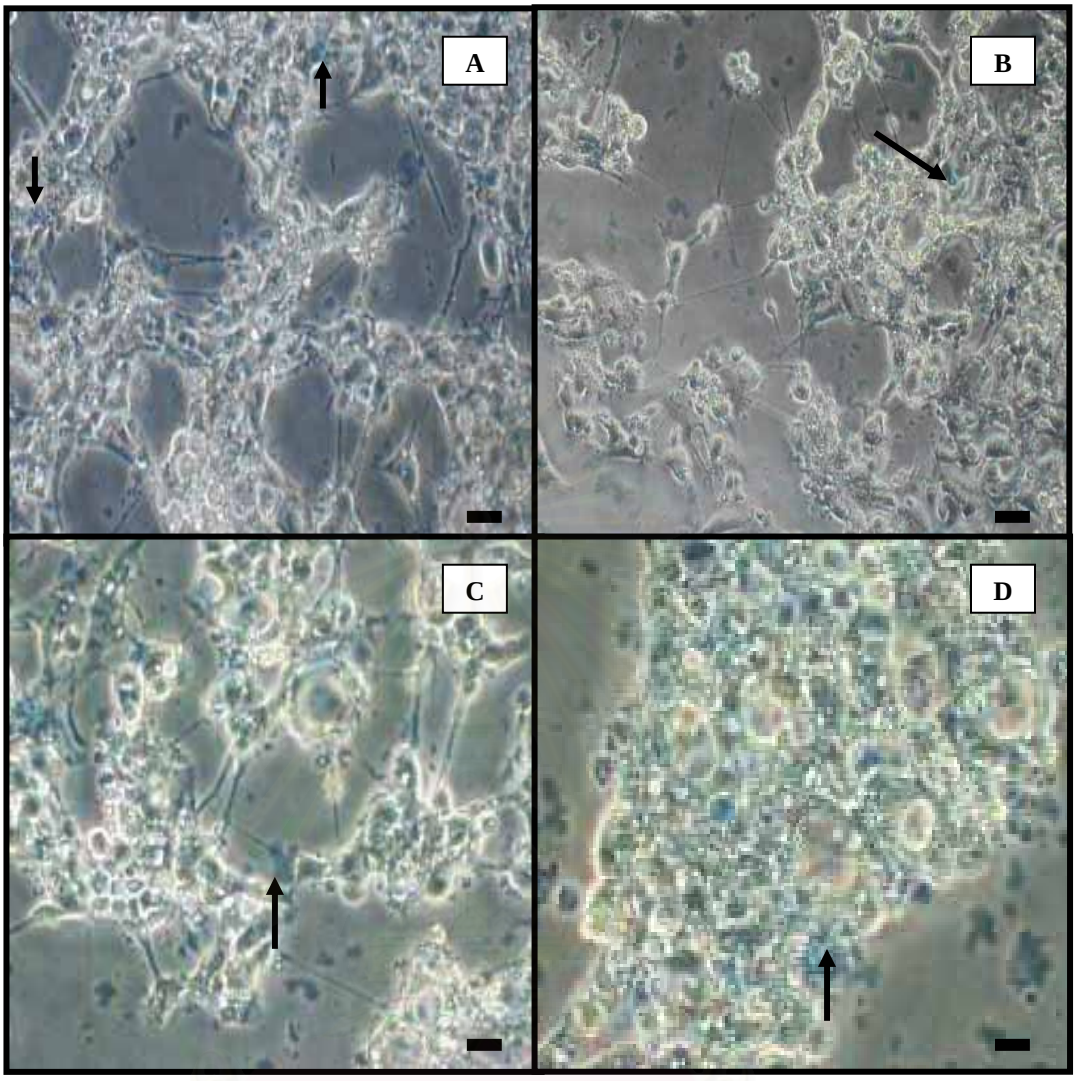

Fig. 22 Phase contrast photographs of barakol-treated P19 neurons for 48 h and stained with trypan blue. At the end of incubation period, P19 neurons were stained with 0.4 % trypan blue and photographs were taken. Cell viability was observed on un-treated P19 neuron (A), 0.4 mM (B), 0.8 mM (C), and 1.0 mM (D) of barakol-treated P19 neurons. Black arrow indicated as dead cell. Bar = 10 μm.

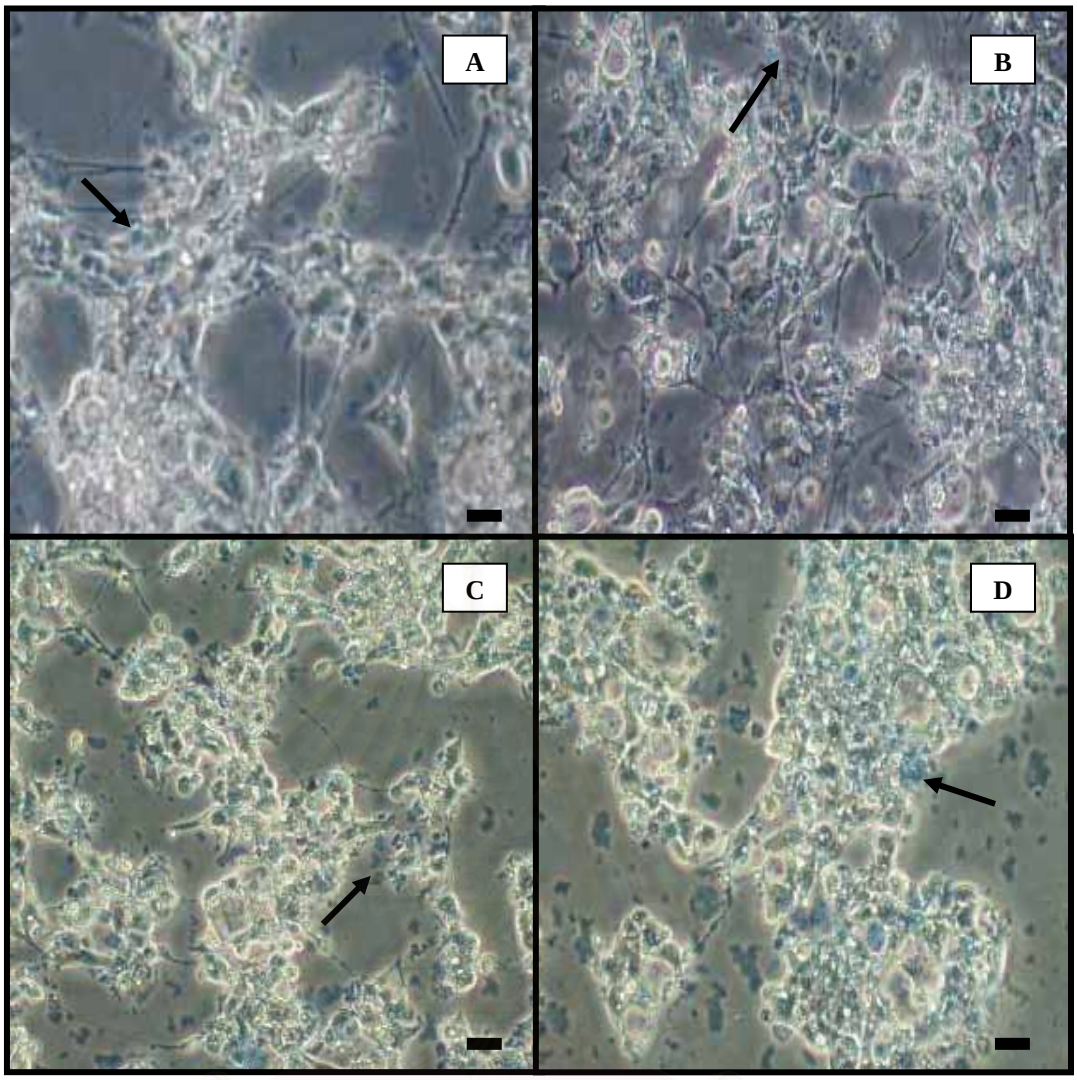

Fig. 23 Phase contrast photographs of barakol-treated P19 neurons for 72 h and stained with trypan blue. At the end of incubation period, P19 neurons were stained with 0.4 % trypan blue and photographs were taken. Cell viability was observed on un-treated P19 neuron (A), 0.4 mM (B), 0.8 mM (C), and 1.0 mM (D) of barakol-treated P19 neurons. Black arrow indicated as dead cell. Bar = 10 μm.

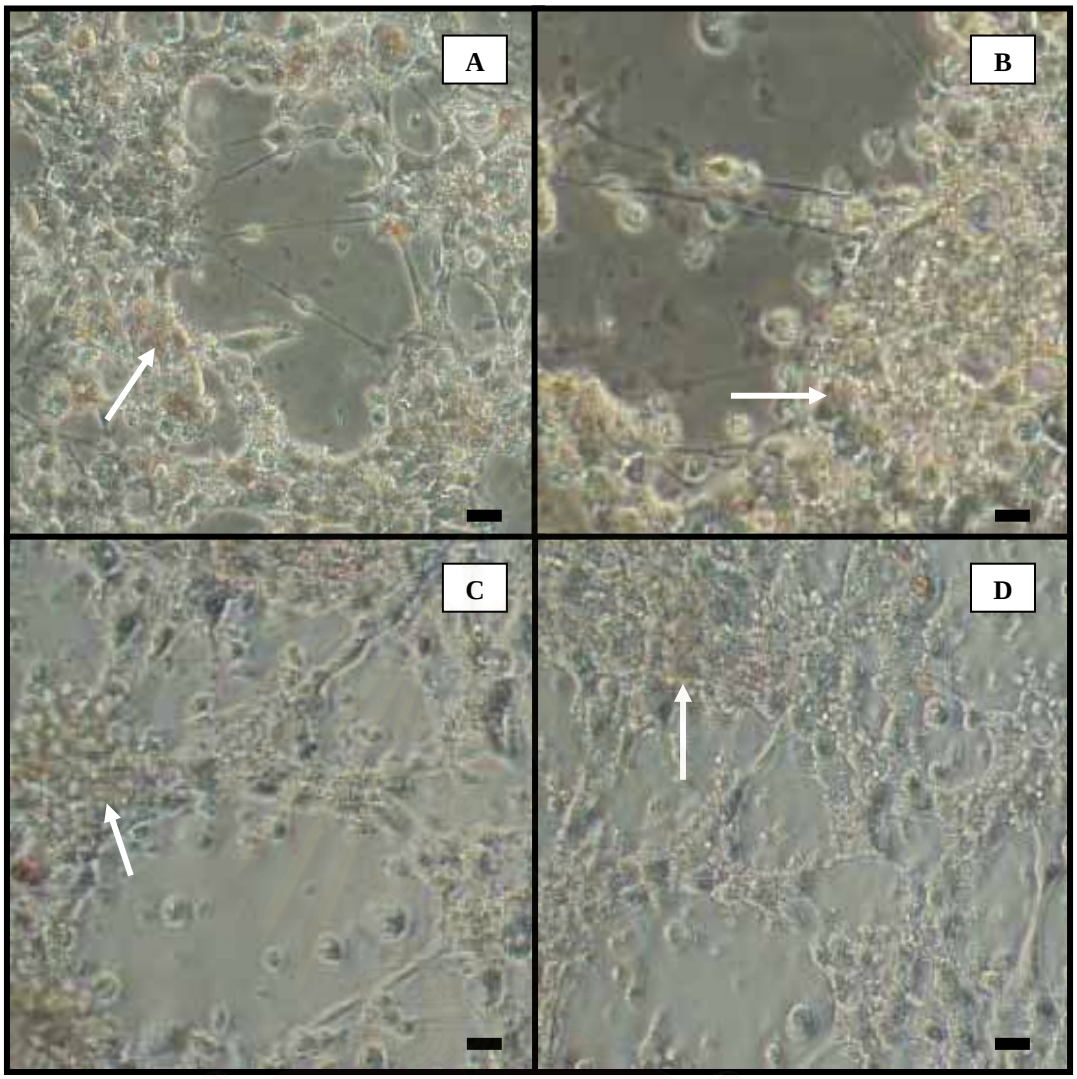

Fig. 24 Phase contrast photographs of barakol-treated P19 neurons for 24 h and stained with neutral red. At the end of exposure time, the medium was discarded and stained with neutral red for 30 min. Cell viability was observed on un-treated P19 neurons (A), 0.4 mM (B), 0.8 mM (C), and 1.0 mM (D) of barakol-treated P19 neurons. White arrow indicated as viable cell. Bar = 10 μm.

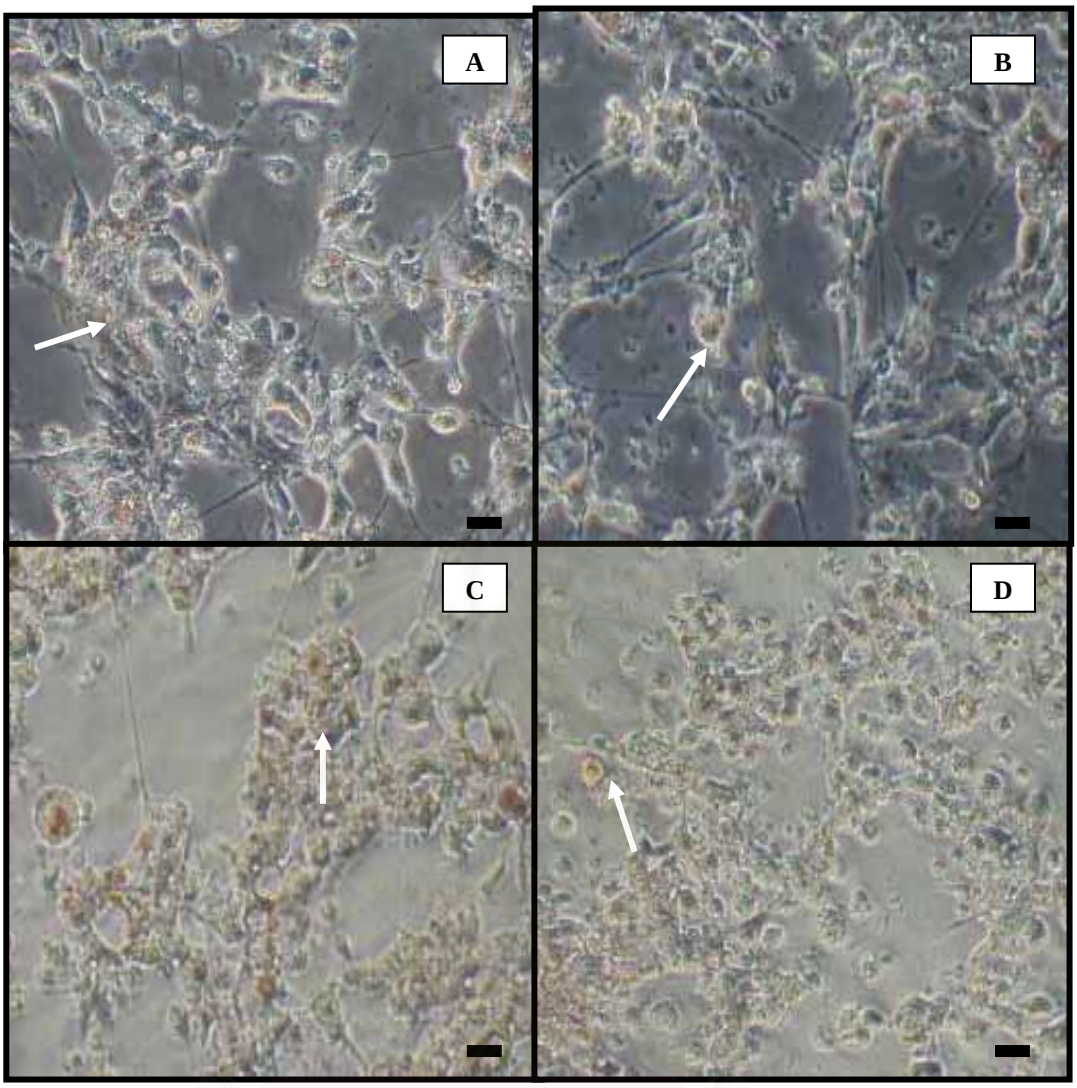

Fig. 25 Phase contrast photographs of barakol-treated P19 neurons for 48 h and stained with neutral red. At the end of exposure time, the medium was discarded and stained with neutral red for 30 min. Cell viability was observed on un-treated P19 neurons (A), 0.4 mM (B), 0.8 mM (C), and 1.0 mM (D) of barakol-treated P19 neurons. White arrow indicated as viable cell. Bar = 10 μm.

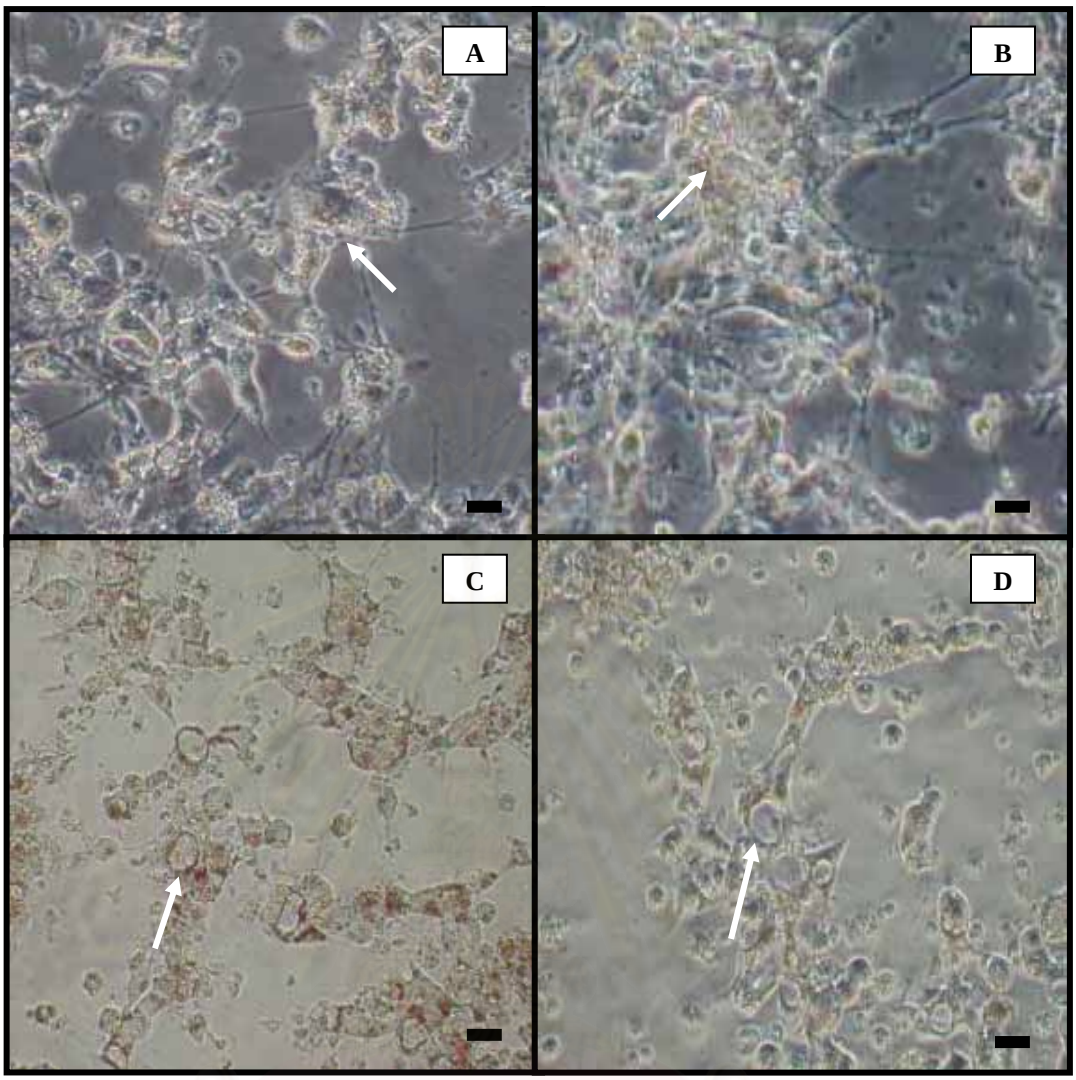

Fig. 26 Phase contrast photographs of barakol-treated P19 neurons for 72 h and stained with neutral red. At the end of exposure time, the medium was discarded and stained with neutral red for 30 min. Cell viability was observed on un-treated P19 neurons (A), 0.4 mM (B), 0.8 mM (C), and 1.0 mM (D) of barakol-treated P19 neurons. White arrow indicated as viable cell. Bar = 10 μm.

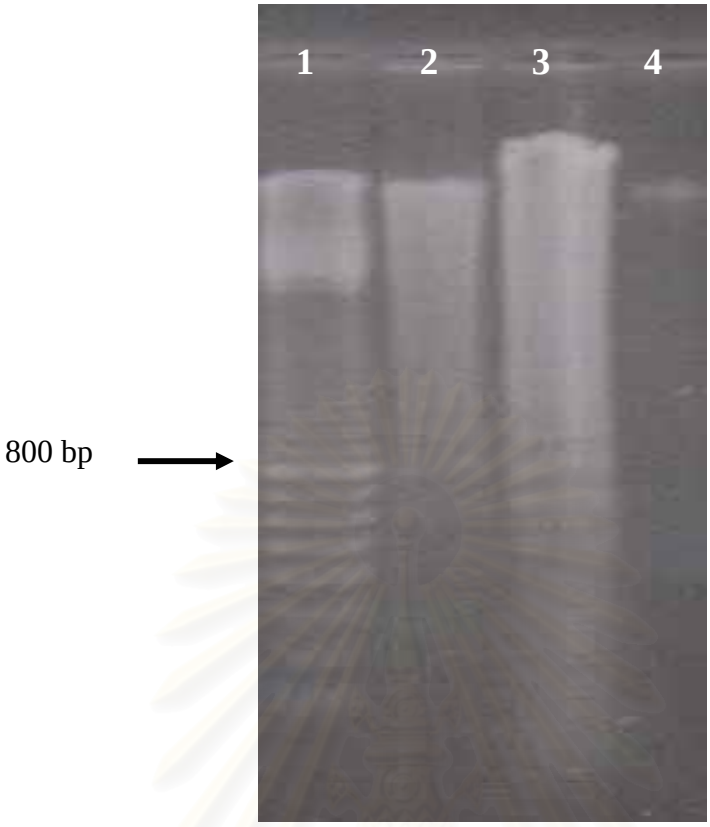

Fig. 27 Internucleosomal DNA fragmentation of barakol-treated P19 neurons. After P19 neurons were incubated with barakol at the concentrations of 0.5 and 1.0 mM for 72 h. The DNA (20μg/lane) was analyzed by 1.5 % agarose gel electrophoresis at 100 V for 1 h followed by ethidium bromide staining. The 100 base pair DNA ladder as a marker (lane1), 0.5 mM (lane 2) and 1.0 mM (lane 3) barakol and un-treated control group (lane 4) were demonstrated.

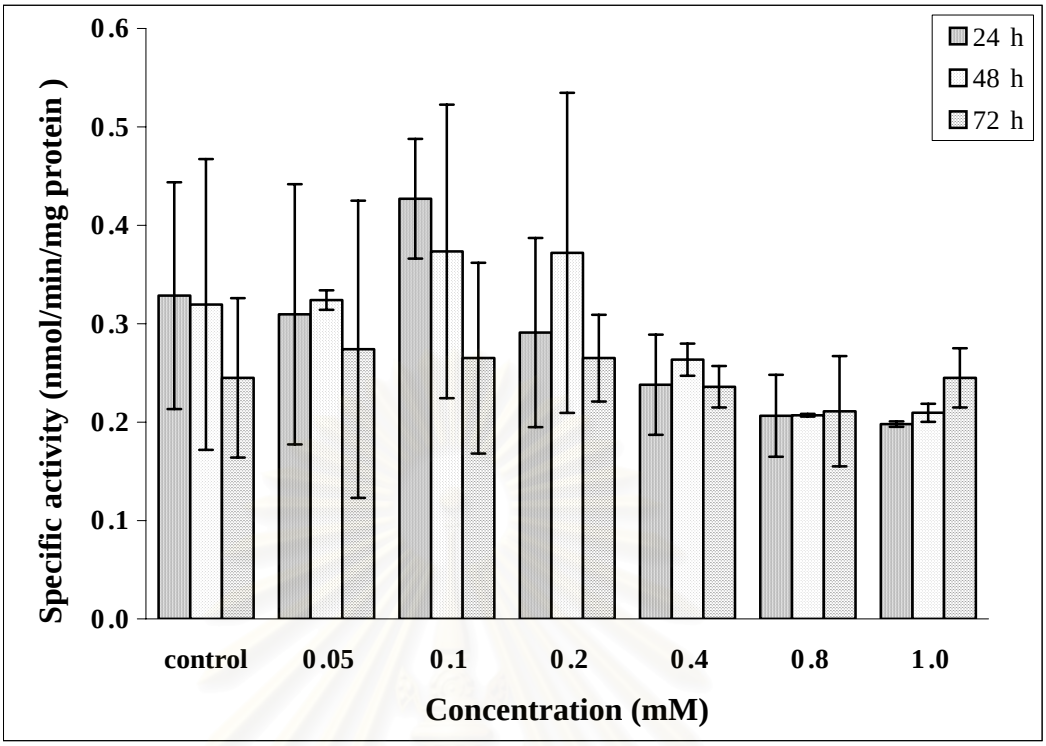

Fig. 28 The effect of barakol on intracellular soluble AChE in P19 neurons. On day 7 after plating, P19 neurons were incubated with barakol at the concentrations ranging from 0.05-1.0 mM. The intracellular soluble AChE was extracted by briefly sonicated at 10 sec interval for 30 sec. The AChE activity was performed by Ellman's method in a reaction mixture containing; 0.75 mM acetylthiocholine iodide, 0.3 mM DTNB and 20 μM iso-OMPA. Absorbance was read at 415 nm at 30 sec intervals for 30 min. Protein was determined by Lowry method. Each barakol concentration was tested in triplicate in a randomized manner. Data are represented as mean ± S.D. n = 3.

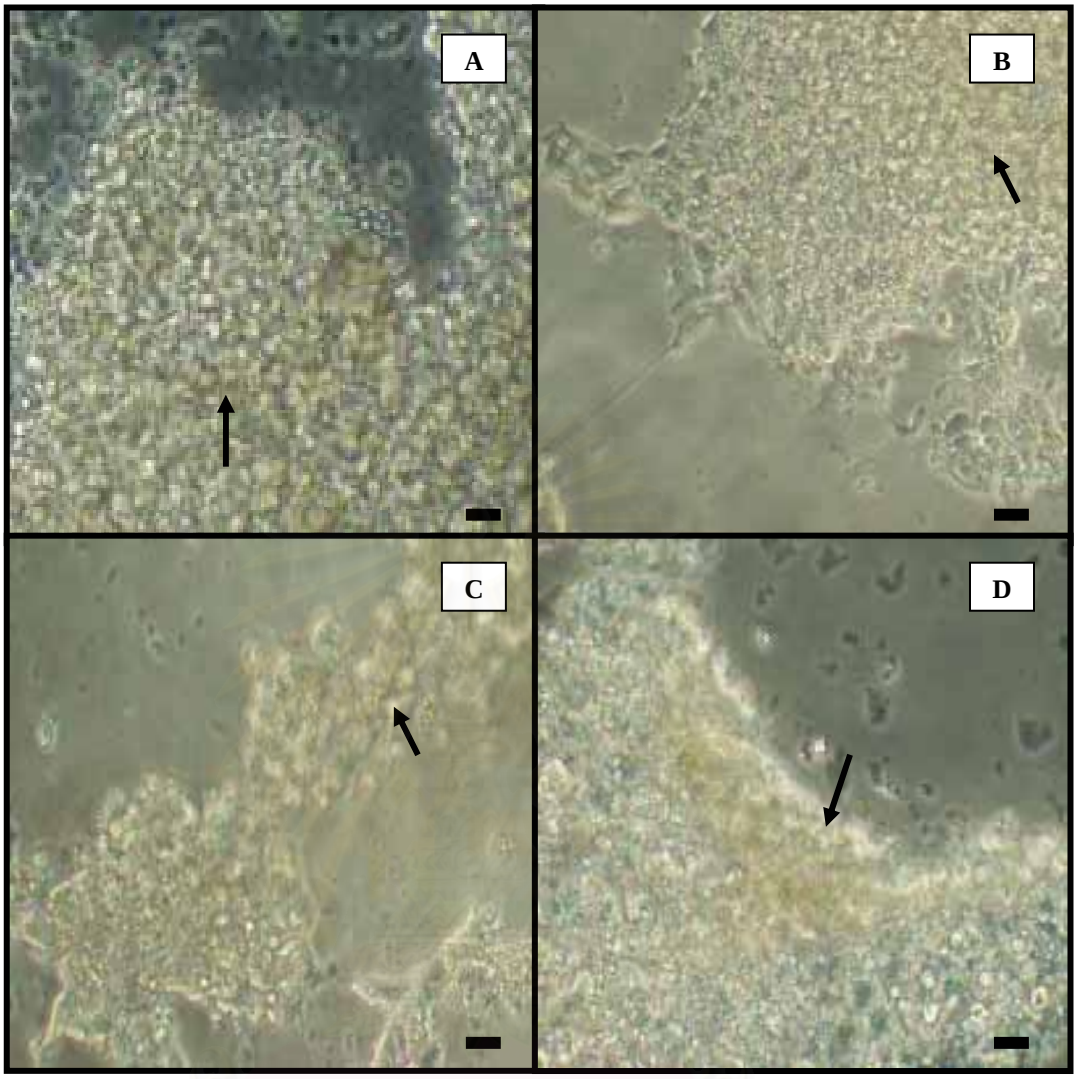

Fig. 29 Membrane-bound AChE activity in barakol-treated P19 neurons for 24 h. At the end of exposure, the medium was discarded and membrane-bound AChE activity was stained with Karnovsky and Roots as described in Methods. Photographs showed in un-treated P19 neurons (A), 0.4 mM (B) 0.8 mM (C), and 1.0 mM (D) of barakol-treated P19 neurons. Bar = 10 μm.

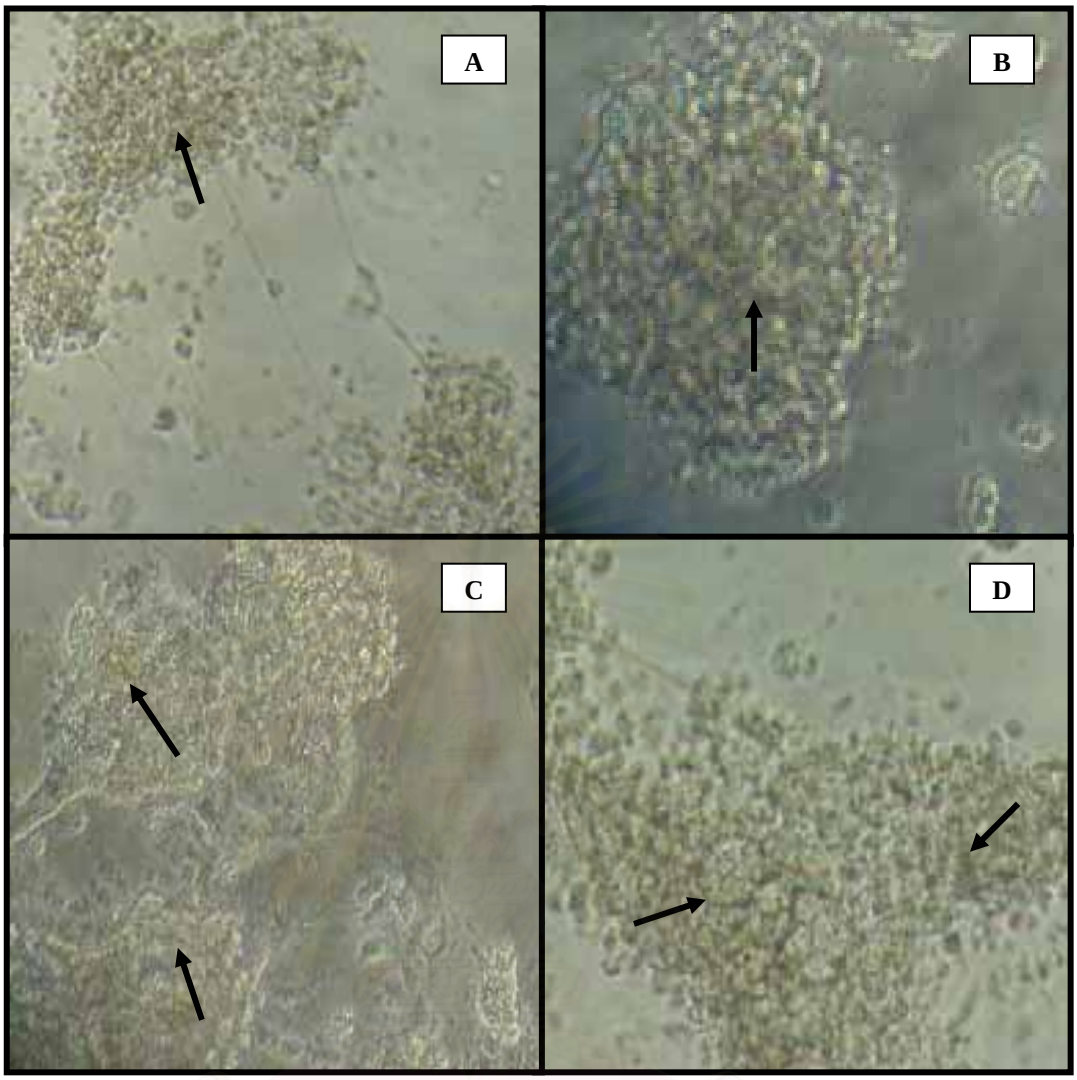

Fig. 30 Membrane-bound AChE activity in barakol-treated P19 neurons for 48 h. At the end of exposure, the medium was discarded and AChE activity was stained with Karnovsky and Roots. Photographs showed in un-treated P19 neurons (A), 0.4 mM (B), 0.8 mM (C), and 1.0 mM (D) of barakol-treated P19 neurons. Black arrow indicated as cholinergic neurons. Bar = 10 μm.

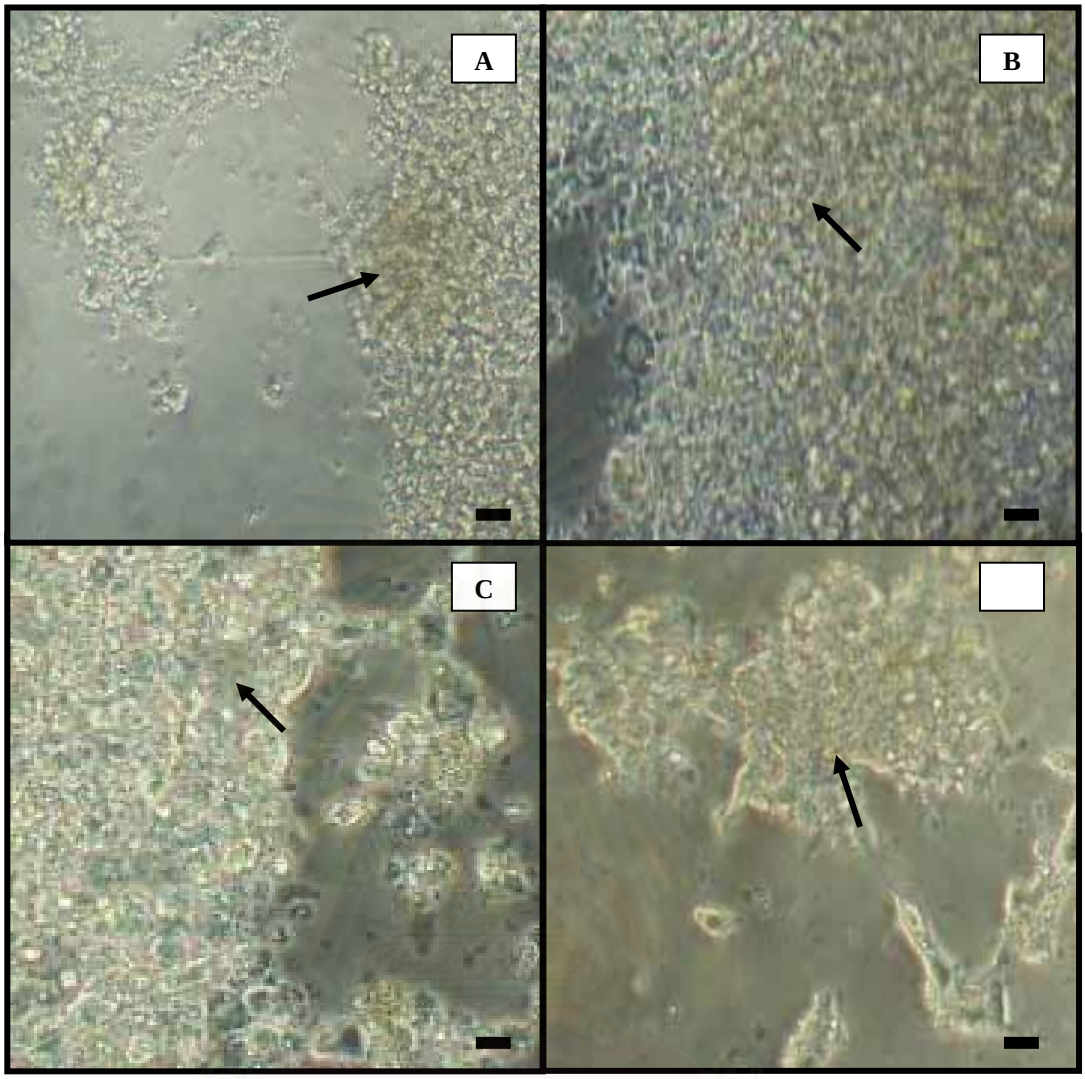

Fig. 31 Membrane-bound AChE activity in barakol-treated P19 neurons for 72 h. At the end of exposure, the medium was discarded and membrane-bound AChE activity was stained with Karnovsky and Roots. Photographs showed in un-treated P19 neurons (A), 0.4 mM (B), 8 mM (C), and 1.0 mM (D) of barakol-treated P19 neurons. Black arrow indicated as cholinergic neurons. Bar = 10 μm.

CHAPTER V

DISCUSSION AND CONCLUSION

Testing of pharmaceutical and industrial chemicals for developmental toxicity currently employs studies using live animals. Recent initiatives have developed protocols, which refine these studies and reduce the numbers of animal used. However, given the many complex interacting processes that are involved in embryonic development, replacement of these studies with alternative *in vitro* tests is considered unlikely to occur in the foreseeable future, and there has been a tendency to neglect or even move away from the development of screens for risk assessment. Thus, to date, the use of *in vitro* tests in developmental toxicology has largely been confined to mechanistic studies and analogue screening where *in vivo* or *in vitro* comparison has shown close agreement (Newall, 1996).

Although animal model are valuable for studying effects of developmental toxicants, use of cell culture can facilitate studying mechanism by which developmental toxicants elicit their effects at the cellular and sub-cellular level. For the purposes of studying developmental toxicity, optimal cell culture systems are those which undergo differentiation with patterns similar to those occurring in vivo, and which respond to exogenous stimuli in a manner similar to in vivo response. Thus, cellular morphology and expression of tissue-specific markers in cell culture systems should reflect in vivo morphology and gene expression (Seeley and Faustman, 1998). The discovery of the cells isolated from the inner cell mass of mouse blastocysts can be maintained in an undifferentiated state forming a totipotent EC cell line, is therefore a timely advance in the development of *in vitro* screens for teratogenic potential (Newall, 1996). EC cells form the inner cell mass of the mammalian blastocysts can be cultured and manipulated in vitro, then returned to the embryonic environment where they develop normally, and contribute to all somatic and germ cell lineages. These cells resemble those comprising the inner cell mass of preimplantation blastocysts and a number of differentiated cell types in endodermal, mesodermal and neuroectodermal, which characteristics of cells of the three germ layers can be obtained reproducibly by different treatments (Jonk, 1992). An obvious

advantage of using EC cell lines over primary cell cultures is that they reduce the number of animals required for toxicity testing. Another advantage of using cell lines is the relative ease with which they can be transfected for studying mechanism of development the effects of gene expression or repression on differentiation (Seeley and Faustman, 1998). Thus, embryonic cells are an attractive *in vitro* model for cytotoxicity, factor that regulate neuronal differentiation and embryotoxicity studies (Rohwedel, 2001; Yao, 1995).

P19 cells are pluripotent murine embryonal carcinoma cells that can be induced by RA to differentiate into P19 neurons that are biochemically and morphologically similar to cells of the CNS (Jones-Villeneuve, 1982; Ray and Gottlieb, 1993; Seeley and Faustman, 1998). Previous investigations have indicated that the commitment to differentiation by RA in P19 cells is cell cycle dependent. A 4 h pulse treatment with RA of cells in the G1 phase of the cell cycle, but not in S or asynchronously growing, is sufficient to induce their differentiation as determined by a reduction of their ability to grow in soft agar and expression of SSEA-1 antigen (Mummery, 1987). P 19 neurons developed many neuronal markers (Jones-Villeneuve, 1982; Staines, 1994; Slack, 1995, Mansergh, 1996; Eggenberger, 1998 and Mansergh, 2000). Electron micrographs of 21-day-old cultures revealed that synaptic contacts were indeed formed and that some axons and presynaptic boutons contained, large, dense-core vesicles (Staines, 1994; Finley, 1996). In addition, cultures containing up to 90% neurons can be obtained by treating differentiating P19 cells with ara-C to inhibit proliferation of non-neuronal cells (Coleman, 1996). P19 neurons matured in culture (> 5 days after plating), detectable GAD and GABA staining intensified and extended from the cell bodies into the processes (Lin, 1996). Thus, P19 cells of embryonic origin and P19 neurons, which express several neuronal-specific proteins commonly found in the CNS and display distinct neuronal morphology, can be used to analyse *in vitro* the cytotoxicity. Therefore, these systems represent *in vitro* alternatives to animal tests for mutagenicity, embryotoxicity and also neurotoxicity (Seely and Faustman, 1998; Rohwedel, 2001).

Cytotoxicity is considered primarily as the potential of a compound to induce cell death. Most in vitro cytotoxicity tests measure necrosis. However, an equally

important mechanism of cell death is apoptosis, which requires different methods for its evaluation. Furthermore, detailed studies on dose and time dependence of toxic effects to cells, together with the observation of effects on the cell cycle and their reversibility, can provide valuable information about mechanisms and type of toxicity, including necrosis, apoptosis or other events (Eisenbrand, 2002). Until now, several in vitro systems using embryonic cells have been established for testing on the basis of cytotoxicity and differentiation analyses. Most of these studies included parameter such as protein content, colony size, enzyme activity, plating efficiency, morphological analysis, membrane permeability, immunological analysis and cell surface receptor expression (Sehlmeyer, 1996; Rohwedel, 2001). A convenient way to estimate the number of viable cells growing in multi-well plates is to use a colorimetric assay and an automatic microplate reader. A tetrazolium salt has been used to develop a quantitative colorimetric assay for mammalian cell survival and proliferation. The assay detects living, but not dead cells and the signal generated is dependent on the degree of activation of the cells (Mosmann, 1983). To study the cell viability in our experiments, a colorimetric method of XTT were used. In addition, membrane integrity were measured by dye exclusion (trypan blue)(Cookson, 1994; Egan, 1997; Cereser, 2001), vital dye uptake (neutral red) (Riddell, 1986; Barile, 1994; Cereser, 2001). Morphological analysis on P19 cells and P19 neurons was used to analyse the cytotoxicity of barakol as well (Borenfreund and Puerner, 1985; Seeley and Faustman, 1998). Incubation of P19 cells with barakol resulted in a significantly dramatic decrease in cellular survival. By comparing the toxic effects of barakol in P19 cells and P19 neurons, a higher sensitivity was detected in P19 cells than in P19 neurons. Resulting in decreased cell survival in P19 cells was higher than in P19 neurons. Although at present it is quite impossible to draw any correlation between the effects of barakol in P19 cells and P19 neurons, it has been reported that cytotoxic effect of toxicants in different cell types may showed the same or an even higher or less sensitivity (Rohwedel, 2001; Cereser, 2001). In addition, at this point it is not clear how many distinct types of neurons and glia can be derived from P19 cells (Jones-Villeneuve, 1982). Lineage studies *in vivo* showed that neurons and glia can be sister cells even at the final rounds of cell division during neurogenesis (Rohwedel, 2001). Finally, possibly, the level and/or activity of enzymes or protein important to barakol toxicity becomes more fully developed in mature neurons. Several enzymes of importance to brain metabolism have been shown to increase in activity with time

in culture (Sawyer, 1999; Cereser, 2001). Thus it seems to be difficult to draw a correlation between cytotoxic effects on undifferentiated P19 cells and P19 neurons. In addition, it is difficult to extrapolate the correlation of embryotoxicity and neurotoxicity between *in vitro* and *in vivo* (Rohwedel, 2001).

These studies were also noticeable that cell viability assessed by the XTT assay could be detectable cytotoxicity faster than by the trypan blue dye exclusion assay. This result may depend on the sensitivity and limitation of each technique. The colorimetric cytotoxicity assay based on the tetrazolium dye, demonstrated a higher sensitivity of embryonic stem cells to teratogens than of differentiated fibroblast (Rohwedel, 2001). In addition, the XTT assay determines cell survival indirectly via the alteration of metabolic activity in live cells, in contrast, the trypan blue dye stains dead cells only. The disadvantages of trypan blue dye exclusion assay such as (1) the cells must be separated into a single cells suspension, the clumps or aggregates of cells may be difficult for counting which could count more or less than the exactly cell number; (2) the number of counted cells should be more than 200 cells for the valuable statistical analysis; and (3) this technique to be excessively time consuming and giving poor reproducibility. Thus, cytotoxicity assays measure xenobiotic induced alterations in metabolic pathways or structure integrity of the cells which may or may not be related to direct of cell death.

Time-course study also revealed that, after 72 h of treatment, the cell number of un-treated and barakol-treated P19 neurons decreased about 25 % compared with 24 h of treatment (Fig**.** 20). These results might be due to the spontaneous cell death, which has been reported that during the development of the vertebrate nervous system, up to 50 % of many cell types of neurons normally dies soon after they form synaptic connections with their target cells. This massive cell death is thought to reflect the failure of these neurons to obtain adequate amounts of specific neurotrophic factors that are produced by the target cells and that are required for the neurons to survive (Raff, 1993).

Although there is no single method or model that can extrapolate the toxicity from animals to humans, the species differences in toxicity often can be explained by pharmacokinetic or pharmacodynamic of drugs. To make an accurate interpretation

and a reasonable prediction of potential toxicity in humans, it is important to elucidate the underlying mechanism responsible for the species differences in metabolism and pharmacokinetics (Lin and Lu, 1997). Furthermore, for differentiation between cytotoxicity and reversible cell damage, recovery of the cell needs to be appropriately considered and this might help interpret results of studies *in vivo* (Eisenbrand, 2002). Barakol-treated P19 cells at the concentrations of ≤ 0.8 mM showed the recovery of cell number, while at a higher concentration of 1.0 mM, P19 cells could not be recovered. However, the recovery study of barakol on P19 neurons could not be evaluated because of the lacking of proliferation of post-mitotic P19 neurons.

Apoptosis can be evaluated by the observation of cell morphology, membrane rearrangements, DNA fragmentation, caspase activation and cytochrome c release from mitochondria (Batistatou, 1993; Dragunow and Preston, 1995; Eisenbrand, 2002). In our experiment, agarose gel electrophoresis was used to characterized the pattern of cell death, which previously reported that chromatin fragmentation into oligonucleosomal length fragments by a non-lysosomal Ca^{2+} and Mg^{2+} dependent endonuclease has long been considered to be the hallmark, and potentially even the initiating mechanism of apoptosis (Fesus, 1993; Batistatou, 1993; Eisenbrand, 2002). Studies of DNA fragmentation of barakol-treated P19 cells and barakol-treated P19 neurons showed a similar pattern of DNA ladder on agarose gel electrophoresis. The results suggested that barakol could induce cell death via the apoptotic mechanism. Demonstration of the internucleosomal DNA fragmentation has been a major advance in the detection of apoptosis, however, it is now also clear that fragmentation of DNA into oligonucleosmoes is usually a late event and it does not occur in all forms of apoptosis and may be more or less significant in different cell types or in response to different apoptotic stiumli (Fesus, 1993; Dickson, 1998; Sastry and Rao, 2000). Thus, to confirm apoptotic cell death, it should further investigate the induction of apoptosis by barakol in P19 cells and P19 neurons with another appropriate techniques such as terminal deoxynucleotidyl transferase-mediated dUTP nick end labeling (TUNEL) assay, cells containing DNA strand breaks become visible in light microscope (Saraste and Pulkki, 2000) and a novel approach to study the presence of apoptosis, which demonstrates the activation of downstream caspases. This can be detected by western blotting of target proteins that have been cleaved by

caspases or by demonstration of caspase activity by enzyme assay (Saraste and Pulkki, 2000).

The distinction between the cytotoxicity of barakol on P19 cells and P19 neurons or other different cell types may be complicated by specific effects of physiological variables (Lin and Lu, 1997). Additionally, it has previously reported that the toxic effect of barakol in human hepatoma cell line HepG2 is mediated by oxidative stress (Lawanprasert, 2001). However, there is no reason to expect that they will be identical in P19 cells or P19 neurons or HepG2 cells. Barakol also induced apoptosis in P19 cells and P19 neurons indicated by DNA ladder at a similar manner to the cells when treated with RA. It was reported that RA induced the p27 protein, which in turn inhibited the Cdk4-dependent kinase, leading to the activation of retinoblastoma, which ultimately promoted cell cycle arrest and apoptosis in P19 cells (Glozak, 1996; Glozak and Roger, 2001). However, the mechanism whereby barakol exerts their toxicity on P19 cells and P19 neurons at intracellular targets have not been investigated and it is not known whether apoptotic pathways in P19 cells or P19 neurons are identical to RA demonstrate here.

P19 cells exhibited no AChE activity. However, after aggregation with RA and plating for morphological differentiation, neuronally induced cells showed increasing levels of AChE activity in cell homogenates (Coleman and Taylor, 1996). AChE exists distinct molecular forms, due to alternative splicing at the 3′ end of the gene. The carboxy-terminal sequences encoded by the alternative spliced exons direct the cellular localization of the enzyme but do not affect its catalytic properties (Coleman and Taylor, 1996; Grisaru, 1999). AChE was found as soluble or membrane-bound AChE (Rotundo, 1989; Schegg, 1992; Coleman and Taylor; 1996; Legay, 1999). The appearance of cholinergic activity on nerve cells often precedes synaptogenesis. It has been hypothesized that cholinesterase is important in development of the mammalian nervous system (Meisami, 1984; Schegg, 1992; Coleman, 1996). Altlhough AChE has often been used as a marker for terminal differentiation of neurons, developmentally regulated expression of AChE in neuronal cells is not well understood (Coleman and Taylor, 1996). According to the cholinergic hypothesis of AD, which was discovered that the brains of AD patients

were deficient in acetylcholine, one of the main neurotransmitters of the CNS that serves to increase attention and facilitate learning (Maltby, 1994; Francis, 1999). To day, the symptomatic treatment of AD is based on cholinergic enhancement. The only class of drugs that have been effective so far for the symptomatic treatment of AD are the cholinesterase inhibitor which indirectly increase the content of acetylcholine in the cholinergic synapse (Sunderland, 1998; Benzi, 1998; Holmes, 2000; Bullock, 2002). Our preliminary studies on AChE inhibitory effect of barakol exerted that barakol could inhibit AChE from both sources of rat brain and electric eel in a dose-dependent manner and demonstrated IC_{50} values of 0.40 and 0.21 mM, respectively (Table. 12). Lineweaver-Burk plots for the AChE activity demonstrated that barakol was a reversible, competitive AChE inhibitor with an inhibition constant (K_i) of 0.084 mM (Fig. 32). It was noticeable that barakol at the concentrations of ≤ 0.2 mM did not exhibit the cytotoxic effect to both P19 cells and P19 neurons. Furthermore, the aqueous extract of *C. siamea* could inhibit AChE from both sources indifferently (IC_{50} = 1.31 mg/ml). The inhibitory effect of barakol on AChE activity and the ability to cross the BBB could support that barakol might enhance the central cholinergic neurotransmission by decreasing the rate of acetylcholine hydrolysis. Thus, barakol, as well as the crude extract of *C. siamea*, might show a considerable promise to slow the progression of AD. The effect of barakol on membrane-bound AChE in P19 neurons showed that barakol exerted ineffectiveness to directly inhibit membrane-bound AChE activity, contrast to the direct AChE inhibition of barakol in rat brain and electric eel AChE. The result might be discussed that Karnovsky and Roots developed this method to detect AChE activity especially in tissues, which have shown potent AChE activity and the brown color of product was rapidly occurred in a short time (approximately ≤ 2 h). In contrast, membrane-bound AChE activity in P19 neurons was less potent than in tissue, leading to longer incubation period for un-treated P19 neurons to produce an insoluble product. In addition, barakol showed a weak competitive AChE inhibitor. Thus, the method of Karnovsky and Roots might not be appropriate to demonstrate a direct inhibitory effect of barakol on membrane-bound AChE in P19 neurons. The effect of barakol on intracellular soluble AChE activity in P19 neurons revealed that barakol did not exert an inhibitory effect on intracellular AChE activity. This result might suggest that barakol could not pass the plasma membrane of P19 neurons to inhibit intracellular soluble AChE directly. On

the other hand, if barakol could pass the BBB as well as the plasma membrane of P19 neurons, barakol might be metabolised by the enzyme in P19 neurons and become inactive to inhibit intracellular AChE. The metabolic enzymes have been shown to increase in activity with time in neuronal culture (Sawyer, 1999). The concrete reason for this evidence must be further clarified.

The brain is different from other organs in several aspects, one of the most important features is that the brain is completely separated from the blood by the BBB. All organs are perfused by capillaries lined with endothelial cells that have small pores to allow for the rapid movements of drugs into the organ interstitial fluid from the circulation. However, the capillary endothelium of the brain lacks these pores and, therefore, drugs must cross the BBB and enter the brain by simple diffusion. In contrast, many synthetic AChE inhibitors or other drugs showed high potency only *in vitro* but *in vivo,* they lost the ability to inhibit the enzyme activity or exert another activity in the target site in CNS. Many studies conclude that they did not pass the BBB, in contrast to barakol. Our *in vitro* cytotoxic studies suggest that barakol is a promising candidate for further study in animal model, which has been reported the LD_{50} was 324 mg/kg, i.p. (Jantarayota,1988). The interesting topics for further investigation are the effect of barakol on memory impairment and toxicological studies before the potential assessment of barakol in clinical trial.

In summary, barakol was toxic to P19 cells as well as P19 neurons. The reason for this apparent discrepancy has not been elucidated but could be due either to the differences in cell type although P19 neurons was originated from P19 cells, or possibly expression of endogenous scavenging molecules such as glutathione (Sawyer, 1999). The lowest concentrations of barakol tested at 0.4 mM and 0.8 mM were toxic to P19 cells and P19 neurons, respectively. Furthermore, after exposed with barakol at the concentrations of $\leq$ 0.8 mM, P19 cells could be recovered by which exhibited the increase in cell number with slightly change in cell morphology. Finally, the inhibitory effects of barakol on both intracellular soluble AChE and membrane-bound AChE in P19 neurons showed ineffectiveness.

REFERENCES

Abney, E. R., Bartlett, P. P., and Raff, M. C. (1981). Astrocytes, ependymal cells, and oligodendrocytes develop on schedule in dissociated cell cultures of embryonic rat brain. **Dev. Biol**. 83, 301-310.

Amenta, F., Parnetti, L., Gallai, V., and Wallin, A. (2001). Treatment of cognitive dysfunction associated with Alzheimer's disease with cholinergic precursors. Ineffective treatments or inappropriate approaches? **Mech. Ageing Dev**. 122, 2025-2040.

Arunlakshana, O. (1949). Studies of indigenous drugs:1. Pharmacological actions of the leaves of *Cassia siamea*. **Siriraj Hosp. Gaz**. 1, 434-443.

Barile, F. A. (1994). **Introduction to in vitro cytotoxicology: Mechanism and methods**. CRC Press, U.S.A. p 53.

Batistatou, A. and Greene, L. A. (1993). Internucleosomal DNA cleavage and neuronal cell survival/death. **J. Cell. Biol**. 122, 523-532.

Benzi, G. And Moretti, A. (1998). Is there a rationale for the use of acetylcholinesterase inhibitors in the therapy of Alzheimer's disease? **Eur. J. Pharmacol**. 346, 1-13.

Borenfreund, E. and Puerner, J. A. (1985). Toxicity determined in vitro by morphological alterations and neutral red absorption. **Toxicol. Lett**. 24, 119-124

Borenfreund, E., Babich, H., and Alguacil, N. M. (1988). Comparisons of two in vitro cytotoxicity assays-the neutral red and tetrazolium MTT tests. **Toxicol. in Vitro** 2, 1-6.

Boudjelal, M., Taneja, R., Matsubara, S., Dolle, P., and Chambon, P. (1997). Overexpression of Stra13, a novel retinoic acid-inducible gene of the basic helix-loop-helix family, inhibits mesodermal and promotes neuronal differentiation of P19 cells. **Genes & Development** 11, 2052-2065.

Brustle, O., Jones, k., Learish, R. et. al. (1999). Embryonic stem cell-derived glial precursors: a source of myelinating transplants. **Science** 285, 754-756.

Bullock, R. (2002). New drugs for Alzheimer's disease and other dementias. **Brit. J. Psychiat.** 180, 135-139.

Cereser, C., Boget, S., Parvaz, R., and Revol, A. (2001). An evaluation of thiram toxicity on cultured human skin fibroblasts. **Toxicology** 162, 89-101.

Chaichantipyuth, C. (1979). A phytochemical study of the leaves of *Cassia siamea* and *Cassia spectabilis*, **A thesis submitted for the degree of Master of Science in Pharmacy**, Chulalongkorn University, Bangkok.

Coleman, B. A. and Taylor, P. (1996). Regulation of acetylcholinesterase expression during neuronal differentiation. **J. Biol. Chem**. 271, 4410-4416.

Cookson, M. R., McClean, R., Williams, S. P. et. al. (1994). Use of astrocytes for *in vitro* neurotoxicity testing. **Toxicol. in Vitro** 8, 817-819.

Cummings, J. L. (2000). Cholinesterase inhibitors: A new class of psychotropic compounds. **Am. J. Psychiat.** 157, 4-15.

Cummings, J. L., Back, C. (1998). The cholinergic hypothesis of neuropsychiatric symptoms in Alzheimer's disease. **Am. J. Geriat. Psychiat.** 6:S64-S78.

Dickson, A. J. (1998). Apoptosis regulation and its applications to biotechnology. **Trends Biotechnol.** 16, 339-342.

Dragunow, M. and Preston, K. (1995). The role of inducible transcription factors in apoptotic nerve cell death. **Brain Res. Rev**. 21, 1-28.

Egan, D., James, P., Cooke, D., and O'Kennedy, R. (1997). Studies on the cytostatic and cytotoxic effects and mode of action of 8-nitro-7-hydroxycoumarin. **Cancer Lett.** 118, 201-211.

Eggenberger, M. McKinney, R. A., Fischer, J. A. and Muff, R. (1998). Differential expression of calcitonin and parathyroid hormone/parathyroid hormone-related protein receptor in P19 embryonic carcinoma cells treated with retinoic acid. **Endocrinology** 139, 1023-1030.

Eisenbrand, G., Zobel, B. P., Baker, V. et. al. (2002). Methods of in vitro toxicology. **Food. Chem. Toxicol**. 40, 193-236.

Ellman, G. L., Lourtney, D. K., Andres, V., Featherstone, R. M. (1961). A new and rapid colorimetric determination of acetylcholinesterase activity. **Biochem. Pharmacol**. 7, 88-95.

Felician, O. and Sandson, T. S. (1999). The neurobiology and pharmacotherapy of Alzheimer's disease. **J. Neuropsych. Clin. N.** 11, 19-31.

Feng, G., Krejci, E., Molgo, J. et. al. (1999). Genetic analysis of collagen Q: Roles in acetylcholinesterase and butyrylcholinesterase assembly and in synaptic structure and function. **J. Cell Biol**. 144, 1349-1360.

Fesus, F. (1993). Biochemical events in naturally occurring forms of cell death. **FEBS**. 328, 1-5.

Finley, M. F. A., Kulkarni, N. and Huettner, J. E. (1996). Synapse formation and establishment of neuronal polarity by P19 embryonic carcinoma cells and embryonic stem cells. **J. Neurosci**. 16, 1056-1065.

Fraichard, A., Chassande, O., Bilbaut, G., Dehay, C., Savatier, P. and Samarut, J. (1995). In vitro differentiation of embryonic stem cells into glial cells and functional neurons. **J. Cell Sci.** 108, 3181-3188 (1995).

Francis, P. Palmer, A. M. Snape, M. and Wilcock, G. K. (1999). The cholinergic hypothesis of Alzheimer's disease: a review of progress. **J. Neurol. Neurosur. Ps.** 66, 137-147.

Gauthier, S. (2002). Advances in the pharmacotherapy of Alzheimer's disease. **Can. Med. Assoc. J.** 166, 616-623.

Gauthier, S., M. D., F. R. C. P. (1997). Treatment strategies for Alzheimer's disease. **McGill Journal of Medicine** 3, 149-152.

Glozak, M. A., and Rogers, M. B. (1996). Specific induction of apoptosis in P19 embryonic carcinoma cells by retinoic acid and BMP2 or BMP4. **Dev. Biol**. 179, 458-470.

Glozak, M. A., and Rogers, M. B. (1998). BMP4 and RA-induced apoptosis is mediated through the activation of retinoic acid receptor α and γ in P19 embryonal carcinoma cells. **Exp. Cell. Res**. 242, 165-173.

Glozak, M. A., and Rogers, M. B. (2001). Retinoic acid and bone morphogenetic protein 4-induced apoptosis in P19 embryonal carcinoma cells required p27. **Exp. Cell. Res**. 268, 128-138.

Grant, E. R., Errico, M. A., Emanuel, S. L. et. al. (2000). Protection against glutamate toxicity through inhibition of the p44/42 mitogen-activated protein kinase pathway in neuronally differentiated P19 cells. **Biochem. Pharmacol**. 62, 283-296.

Grisaru, D., Sternfeld, M., Eldor, A., Glick, D. and Soreq, H. (1999). Structural roles of acetylcholinesterase variants in biology and pathology. **Eur. J. Biochem**. 264, 672-686.

Hakansson, L. (1993). Mechanism of action of cholinesterase inhibitors in Alzheimer's disease. **Acta Neurol. Scand. Suppl**. 149, 7-9.

Holmes, C. and Wilkinson, D. (2000). Molecular biology of Alzheimer's disease. **Advan. Psychiatr. Treat.** 6, 193-200.

Jantarayota, P. (1988). Effects of barakol extracted from leaves of *Cassia siamea* on the rat central nervous system. **A Thesis submitted for the degree of Master of Sciences in Pharmacy**, Chulalongkorn University, Bangkok, Thailand, 1988.

Jho, E-H., Davis, R. J., Malbon, C. C. (1997). c-Jun amino-terminal kinase is regulated by G12/G13 and obligate for differentiation of P19 embryonic carcinoma cells by retinoic acid. **J. Biol. Chem**. 272, 24468-24474.

Jones-Villeneuve, E. M. V., McBurney, M. W., Rogers, K. A. and Vitauts, I. K. (1982). Retinoic acid induces embryonal carcinoma cells to differentiate into neurons and glial cells. **J. Cell. Biol**. 94, 253-262.

Jones-Villeneuve, Rudnicki, M. A., Harris, J. F., and McBurney, M. W. (1983). Retinoic acid-induced neural differentiation of embryonic carcinoma cells. **Mol. Cell. Biol**. 3, 2271-2279.

Jonk, L. J. C., Jonge, M. E. J., Kruyt, F. A. E., Mummery, C. L. et. al. (1992). Aggregation and cell cycle dependent retinoic acid receptor mRNA expression in P19 embryonic carcinoma cells. **Mech. Dev**. 36, 165-172.

Karnovsky, M. J., and Roots, L. A. (1964). A "direct coloring" thiocholine method for cholinesterase. **J. Histochem. Cytochem**. 12, 219-224.

Kroemer, G., Dallaporta, B. and Resche-Rigon, M. (1998). The mitochondrial death/life regulator in apoptosis and necrosis. **Annu. Rev. Physiol**. 60, 619-642.

Krupka, R. M. (1964). Acetylcholinesterase. **Indian J. Biochem**. 42, 677-693.

Lawanprasert, S., Chaichantipyuth, C., Unchern, S., Lawanprasert, Y. and Clair, D. St. (2001). *In vitro* hepatotoxicity study of barakol using human hepatoma cell line HepG2. **Thai. J. Pharm. Sci**. 25, 149-152.

Legay, C., Mankal, F. A., Massoulie, J. and Jasmin, B. J. et. al. (1999). Stability and secretion of acetylcholinesterase forms in skeletal muscle cells. **J. Neurosci**. 19, 8252-8259.

Lin, J. H., Lu, A. H. (1997). Role of pharmacokinetics and metabolism in drug discovery and development. **Pharmacol. Rev**. 49,403-449.

Lin, P., Kusano, K., Zhang, Q., et. al. (1996). $GABA_A$ receptors modulate early spontaneous excitatory activity in differentiating P19 neurons. **J. Neurochem**. 66, 233-242.

MacPherson, P. A., Jones, S., Pawson, P. A. *et. al*. (1997). P19 cells differentiate into glutamatergic and glutamate-responsive neurons *in vitro*. **Neuroscience** 80, 487-499.

Magnuson, D. S. K., Morassutti, D. J., McBurney, M. W. and Marshall, K. C. (1995). Neurons derived from P19 embryonal carcinoma cells develop responses to excitatory and inhibitory neurotransmitters. **Dev. Brain. Res**. 90, 141-150.

Maltby, N., Broe, G. A., Creasey, H. et. al. (1994). Efficacy of tacrine and lecithin in mild to moderate Alzheimer's disease:double blind trial. **BMJ**. 308, 879-883.

Mansergh, F. C., Wride, M. A., Rancourt, D. E. (2000). Neurons from stem cells: Implications for understanding nervous system development and repair. **Biochem. Cell. Biol**. 78, 613-628.

Massoulie, J., Anselmet, A. Bon, S., etl al. (1998). Acetylcholinesterase:C-terminal domains, molecular forms and functional localization. **J. Physiology** 92, 183-190.

Mayeux, R. and Sano, M. (1999) Treatment of Alzheimer's disease. **N. Engl. J. Med**. 341, 1670-1679.

McBurney, M. W. and Roger, B. J. (1982). Isolation of male embryonal carcinoma cells and their chromosome replication patterns. **Dev. Biol**. 89, 503-508.

Meisami, E. (1984). Is butyrylcholinesterase of the rat CNS a membrane-bound enzyme?. **J. Neurochem**. 42, 883-886.

Morley, P., MacPherson, P., Whitfield, J. F., Harris, E. W., and McBurney, M. W. (1995). Glutamate receptor-mediated calcium surges in neurons derived from P19 cells. **J. Neurochem**. 65, 1093-1099.

Mosmann, T. (1983). Rapid colorimetric assay for cellular growth and survival: Application to proliferation and cytotoxicity assays. **J. Immunol. Med**. 65, 55-63.

Muangman, V., Charoenboon, S., and Chanthepthewan, W. (2000). A clinical trial on a herbal medicine, Khi-Lek (Cassia siamea) syrup and tablet for insomnia. **Thai. J. Phytopharm**. 7, 18-22.

Mummery, C. L., Brink, C. E. V. D., Laat, S. W. D. (1987). Commitment to differentiation induced by retinoic acid in P19 embryonic carcinoma cells is cell cycle dependent. **Dev. Biol**. 121, 10-19.

Munoz, D. G., and Feldman, H. (2000). Causes of Alzheimer's disease. **Can. Med. Assoc. J.** 162(1), 65-72.

Newall, D. R., and Beedles, K. E. (1996). The stem-cell test: an in vitro assay for teratogenic potential. Results of a blind trial with 25 compounds. **Toxicol. in Vitro** 10, 229-240.

Ninomiya, Y., Adams, R. Morriss-Kay, G. M. and Eto, K. (1997). Apoptotic cell death in neuronal differentiation of P19 EC cells: Cell death follows reentry into S phase. **J. Cell. Physio**. 172, 25-35.

Okazawa, H., Shimizu, J., Kamei, M. et. al. (1996). Bcl-2 inhibits retinoic acid-induced apoptosis during the neural differentiation of embryonic stem cells. **J. Cell. Biol**. 132, 955-968.

Parnas, D. and Linial, M. (1995). Cholinergic properties of neurons differentiated from an embryonal carcinoma cell-line (P19). **Int. J. Dev. Neuroscience** 13, 767-781.

Patricia, J. M., Hasdai, D. Sangiorgi, G. et. al. (1998). Apoptosis: Basic concepts and implications in coronary artery disease. **Arterioscler. Thromb. Vasc. Biol**. 19, 14-22.

Peter, M. C., Heufelder, A. E. and Hengartner, M. O. (1997). Advances in apoptosis research. **Proc. Natl. Acad. Sci**. 94, 12736-12737.

Pevny, L. H., Sockanathan, S., Placzek, M. and Lovell-Badge, R. (1998). A role for SOX1 in neural determination. **Development** 125, 1967-1978.

Philipp, J., Mitchell, P. J., Malipiero, U. and Fontana, A. (1994). Cell type-specific regulation of expression of transcription factor AP-2 in neuroectodermal cells. **Dev. Biol**. 165, 602-614.

Pooviboonsuk, P., Tappayuthijarn, P., Hincheeranund, T. (2000). Hypnotic effect of modified herbal extract from *Cassia siamea* in human subjects. **J. Psychiatr Assoc. Thailand** 45, 251-158.

Raff, M. C., Barres, B. A., Burne, H. S. Et. Al. (1993). Programmed cell death and the control of cell survival: Lessons from the nervous system. **Science** 262, 695-700.

Raju, T., Bignami, A., Dahl, D. (1981). *In vivo* and *in vitro* differentiation of neurons and astrocytes in the rat embryo. **Development** 85, 344-357.

Ray, W. J. and Gottlieb, D. I. (1993). Expression of ionotropic glutamate receptor genes by P19 embryonic carcinoma cells. **Biochem. Biophys. Res. Comm.** 197, 1475-1482.

Riddell, R. J. Clothier, R. H. and Balls, M. (1986). An evaluation of three *in vitro* cytotoxicity assays. **Fd. Chem. Toxic**. 24, 469-471.

Robersno, M. R. and Harrell, L. E. (1997). Cholinergic activity and amyloid precursor protein metabolism. **Brain. Res. Rev**. 25, 50-69.

Rochm, N. W., Rodgers, G. H., Hatfield, S. M., and Glasebrook, A. L. (1991). An improved colorimetric assay for cell proliferation and viability utilizing the tetrazolium salt XTT. **J. Immunol. Methods** 142, 257-265.

Rohwedel, J., Guan, K. and Wobus, A. M. (2001). Embryonic stem cells as an in vitro model for mutagenicity, cytotoxicity and embryotoxicity studies: present state and future prospects. **Toxicol. in Vitro** 15, 741-753.

Rosenberry, T. L., Rabl, C-R. and Neumann, E. (1996). Binding of the neurotoxin fasciculin 2 to the acetylcholinesterase peripheral site drastically reduces the association and dissociation rate constant for *N*-methylacridinium binding to the active site. **Biochemistry** 35, 685-690.

Rossant, R. (2001). Stem cells from the mammalian blastocyst. **Stem Cells** 19, 477-482.

Rotundo, R. L., Thomas, K. Jordan, K. P. et. al. (1989). Intracellular transport, sorting and turnover of acetylcholinesterase. **J. Biol. Chem**. 264, 3146-3152.

Rudolf, E., Peychl, J. and Cervinka, M. (2000). The dynamics of the hexavalent chromium induced apoptotic patterns in vitro. **Acta Med**. 43, 83-89.

Sahara, Y., Kobayashi, T., Onodera, H., et. al. (1996). Okadaic acid suppresses neural differentiation-dependent expression of the neurofilament-L gene in P19 embryonic carcinoma cells by post-transcriptional modification. **J. Biol. Chem**. 271, 25950-25957.

Saraste, A., and Pulkki, K. (2000). Morphologic and biochemical hallmarks of apoptosis. **Cardio. Res**. 45, 528-537.

Sastry, P. S. And Rao, K. S. (2000). Apoptosis and the nervous system. **J. Neurochem**. 74, 1-20.

Sawyer, T. W. (1999). Toxicity of sulfur mustard in primary neuron culture. **Toxicol. In Vitro** 13, 249-258.

Schegg, K. M., Harrington, L., Neilsen, S. et. al. (1992). Soluble and membrane-bound forms of brain acetylcholinesterase in Alzheimer's disease. **Neurobiol. Aging** 13, 697-704.

Schlett, K., Czirok, A., Tarnok, K., Vicsek, T., and Madarasz, E. (2000). Dynamics of cell aggregation during in vitro neurogenesis by immortalized neuroectodermal progenitors. **J. Neurosci. Res**. 60, 184-194.

Seeley, M. R. and Faustman, E. M. (1998). Evaluation of P19 cells for studying mechanisms of developmental toxicity: application to four direct-acting alklylating agents. **Toxicology**. 127, 49-58.

Sehlmeyer, U., Rohwedel, J. and Wobus, A. M. (1996). Primodial germ cell-derived embryonic germ cells of the mouse- in vitro model for cytotoxicity studies with chemical mutagens. **Toxicol. in Vitro** 10, 755-763.

Slack, R. S., Skerjanc, I. S., Lach, B. and et. al. (1995). Cells differentiating into neuroectoderm undergo apoptosis in the absence of functional retinoblastoma family proteins. **J. Cell. Biol**. 129:779-788.

Staines, W. A., Morassutti, D. J., Reuhl, K. R., Ally, A. I. And McBurney, M. W. (1994). Neurons derived from P19 embryonal carcinoma cells have varied morphologies and neurotransmitters. **Neuroscience** 58, 735-751.

Sukma, Monrudee., Chaichantipyuth, C., Murakami, Y. et. al. (2002). CNS inhibitory effects of barakol, a constituent of *Cassia siamea* Lamk. **J. Ethnopharmacol**. 83, 87-94.

Sunderland, T. (1998). Alzheimer's disease: Cholinergic therapy and beyond. **Am. J. Geriat. Psychiat** 6, S56-S63.

Szegletes, T., Mallender, W. D., and Rosenberry, T. L. (1998). Nonequilibrium analysis alters the mechanistic interpretation of inhibition of acetylcholinesterase by peripheral site ligands. **Biochemistry** 37, 4206-4216.

Thongsaard, W. (1998). Physiological and pharmacological properties of *Cassia siamea* and its active constituent, barakol. **Thai. J. Physiol. Sci**. 11, 1-26.

Thongsaard, W. Chainakul, S. Bennett, G. W. and Marsden, C. A. (2001). Determination of barakol extracted from *Cassia siamea* by HPLC with electrochemical detection. **J. Pharm. Biomed. Anal**. 25, 853-859.

Thongsaard, W. Deachapunya, C., Pongsakorn, S. and et. al. (1996). Barakol: A potential anxiolytic extracted from *Cassia siamea*. **Pharmacol. Biochem. Behav**. 53, 753-758.

Thongsaard, W., Pongsakorn, S., Sudsuang, R., and et. al. (1997). Barakol, a natural anxiolytic, inhibits striatal dopamine release but not uptake in vitro. **Eur. J. Pharmacol**. 319, 157-164.

Tran, P. B. and Miller, R. J. (1999). Apoptosis: death and transfiguration. **Science & Medicine** May/June, 18-27.

Valero, J. S., Sberna, G. Catriona, A., McLean, C. A. and Small, D. H. (1999). Molecular isoform distribution and glycosylation of acetylcholinesterase are altered in brain and cerebrospinal fluid of patients with Alzheimer's disease. **J. Neurochem**. 72, 1600-1608.

Vellom, D. C. Radic, Z., Li, Y., et. al. (1993). Amino acid residues controlling acetylcholinesterase and butyrylcholinesterase specificity. **Biochemistry** 32,12-17.

Wang, H., Ikeda, S., Kanno, S., Guang, M., Ohnishi, M. et. al. (2001). Activation of c-Jum amino-terminal kinase is required for retinoic acid-induced neural differentiation of P19 embryonal carcinoma cells. **FEBS Lett.** 503, 91-96.

Wilson, B. W., Nieberg, P. S., Walker, C. R., et. al. (1973). Production and release of acetylcholinesterase by cultured chick embryo muscle**. Dev. Biol**. 33, 285-299.

Yao, M., Bain, G. and Gottlieb, D. I. (1995). Neuronal differentiation of P19 embryonic carcinoma cells in defined media. **J. Neurochem. Res**. 41, 792-804.

Yokote, H., terada, T., Matsumoto, H. et. al. (2000). Dephosphorylation-induced decrease of anti-apoptotic function of Bcl-2 in neuronally differentiated P19 cells following ischemic insults. **Brain Research** 857, 78-86.

APPENDICES

Table. 2 Concentration-dependent study of barakol on P19 cells assessed by XTT assay. The absorbance of the vehicle control was assigned a value of 100 % viability and any decrease/increase was calculated as a percentage of this value. Statistical significance was evaluated by one-way analysis of variance. In the Tukey multiple comparison test determined the concentration of barakol at which the percentage of cell viability was significantly different. * denote $P<0.05$, ** denote $P<0.01$ versus vehicle control group. n = 11.

	% Cell viability	
Barakol conc. (mM)	mean	S.D.
0.05	98.81	6.75
0.1	94.30	8.28
0.2	95.56	8.40
0.4	91.89	9.82
0.8	86.76*	7.04
1	77.72**	7.68

Table. 3 Concentration-dependent study of barakol on P19 cells assessed by trypan blue dye exclusion assay. P19 cells were treated with barakol at the indicated concentrations. Following 24 h of exposure, cells were triturated to detach cells and stained with 0.4 % trypan blue. After staining, P19 cells were counted under microscope using hemocytometer. Data are investigated at least triplicate and presente as mean ± S.D. n = 6.

	Cell number x 10^4 (cells/ml)	
Barakol conc. (mM)	mean	S.D.
Control	24.13	2.77
0.05	24.13	1.47
0.1	22.8	1.89
0.2	22.27	1.49
0.4	22.73	0.99
0.8	21.67	1.14
1.0	21.53	1.17

Table. 4 Time-course study of barakol on P19 cells assessed by XTT assay. The absorbance of the vehicle control was assigned a value of 100 % cell viability and any decrease/increase was calculated as a percentage of this value. Statistical analysis was performed by ANOVA. In the Tukey multiple comparison test determined the concentration of barakol at which the percentage of cell viability was significantly different. Data are presented as mean ± S.D. n = 9. ** denote $P<0.01$ versus control. Barakol showed the cytotoxic effect at the IC_{50} values of 0.62, 0.63, 0.54 and 0.50 mM for 36, 48, 60 and 72 h of exposure time, respectively.

		Barakol conc. (mM)					
Time (h)	% Cell viability	0.05	0.1	0.2	0.4	0.8	1.0
24	Mean	97.83	95.02	94.67	95.00	77.28**	76.51**
	S.D.	6.13	13.35	10.52	11.69	5.90	6.61
36	Mean	96.88	94.73	93.07	86.58**	24.88**	16.03**
	S.D.	3.50	5.83	4.79	4.47	7.70	6.38
48	Mean	105.99	105.93	104.05	90.75**	23.92**	16.27**
	S.D.	2.59	1.90	8.95	1.82	0.56	2.30
60	Mean	103.05	101.61	87.79	75.90**	3.42**	0.65**
	S.D.	7.02	4.86	6.95	5.06	5.92	1.13
72	Mean	94.87	93.12	93.27	66.53**	5.70**	1.60**
	S.D.	6.30	4.96	3.91	7.59	5.35	2.98

Table. 5 Time-course study of barakol on P19 cells assessed by trypan blue dye exclusion assay. Each barakol concentration was tested in triplicate in a randomized manner. Statistical analysis was performed by ANOVA. In the Tukey multiple comparison test determined the concentration of barakol at which the percentage of cell viability was significantly different. Data are presented as mean ± S.D. n = 3.
* denote $P<0.05$, ** denote $P<0.01$ versus control.

Time (h)	Cell number x 10^4 (cells/ml)	Barakol conc. (mM)						
		control	0.05	0.1	0.2	0.4	0.8	1.0
24	Mean	8.4	7.96	8.27	8.53	7.56	6.8	6.18
	S.D.	1.64	0.66	1.60	1.87	1.30	1.06	1.28
36	Mean	11.47	11.2	12.09	10.58	10.71	6.00**	5.29**
	S.D.	1.51	1.09	1.61	1.47	2.90	0.13	0.91
48	Mean	17.2	17.74	17.51	17.55	14.62*	6.44**	5.15**
	S.D.	0.70	0.23	0.66	1.19	0.68	0.66	0.89
60	Mean	22.45	23.51	23.42	20.62	13.06**	6.22**	5.33**
	S.D.	2.02	4.56	4.34	2.06	0.46	0.28	0.48
72	Mean	23.2	23.38	23.82	22.89	12.31**	6.35**	5.55**
	S.D.	1.97	3.51	2.74	1.56	2.47	0.2	0.56

Table. 6 Recovery study of P19 cells after exposure with barakol. P19 cells were incubated with barakol at the concentrations of 0.4, 0.8 and 1.0 mM for 72 h. Then the medium was changed with barakol-free medium. After the following of 48 and 96 h, cells were stained with trypan blue and counted under microscope. Data are presented as mean ± S.D. n = 3. ** denote $P<0.01$ versus control.

Time (h)	Cell number x 10^4 (cells/ml)	Barakol conc. (mM)		
		0.4	0.8	1.0
control	mean	12.31	2.44	2.04
	S.D.	2.47	0.78	0.43
48	mean	43.73**	13.91**	1.87
	S.D.	2.54	1.21	0.88
96	Mean	50.93**	32.71**	2.98
	S.D.	2.82	3.66	0.41

Fig. 7 Concentration-dependent study of barakol on P19 neurons assessed by XTT assay. On day 7 after plating, P19 neurons were incubated with barakol at the concentrations ranging from 0.05-1.0 mM. Following 24 h, cell viability was determined by XTT assay. Results were given as a percentage of the cell viability of treated compared with untreated groups. Each barakol concentration was tested in triplicate in a randomized manner. Data are represented as mean ± S.D. n = 3.

	% Cell viability	
Barakol conc. (mM)	mean	S.D.
0.05	102.06	9.25
0.1	97.69	18.28
0.2	96.63	6.16
0.4	91.91	3.99
0.8	91.81	4.42
1.0	85.33	7.79

Fig. 8 Concentration-dependent study of barakol on P19 neurons assessed by trypan blue dye exclusion assay. P19 neurons were exposed to barakol at the concentrations ranging from 0.05-1.0 mM for 24 h. At the end of incubation, cells were detached from surface by triturated 20-30 times and incubated for 1-2 min with 0.4 % trypan blue at room temperature and counted under microscope. Each barakol concentration was tested in triplicate in a randomized manner. Each value is represented as mean ± S.D. of triplicate determinations. n = 3.

	Cell number x 10^4 (cells/ml)	
Barakol conc. (mM)	mean	S.D.
Control	2.94	0.23
0.05	2.76	0.28
0.1	2.62	0.28
0.2	3.11	0.55
0.4	2.58	0.20
0.8	2.49	0.28
1	3.02	0.43

Table. 9 Time-course study of barakol on P19 neurons assessed by XTT assay. The absorbance of the vehicle control was assigned a value of 100 % viability and any decrease/increase was calculated as a percentage of this value. Each barakol concentration was tested in triplicate in a randomized manner. Statistical analysis was performed by ANOVA. In the Tukey multiple comparison test determined the concentration of barakol at which the percentage of cell viability was significantly different. Data are presented as mean ± S.D. ** denote $P<0.01$. n = 4.

		Barakol conc. (mM)					
Time (h)	% Cell viability	0.05	0.1	0.2	0.4	0.8	1.0
24	mean	102.06	97.69	96.63	91.61	91.81	85.33
	S.D.	9.25	18.28	6.16	4.00	4.43	7.79
36	mean	99.32	96.85	94.19	92.09	85.06**	90.37**
	S.D.	3.44	5.49	9.45	9.12	13.66	7.21
48	mean	97.67	94.62	93.01	89.48	82.09**	78.63**
	S.D.	4.03	6.25	4.10	7.21	9.77	11.05
60	mean	95.05	95.09	92.95	90.9	84.89**	74.56**
	S.D.	7.10	3.78	2.66	5.60	6.32	9.27
72	mean	99.62	98.27	97.7	94.82	84.98**	83.18**
	S.D.	3.43	4.95	5.61	7.99	8.08	8.89

Table. 10 Time-course study of barakol on P19 neurons assessed by trypan blue dye exclusion assay. After P19 neurons were treated with barakol at the concentrations ranging from 0.05-1.0 mM for 24-72 h, the cells were stained with trypan blue and were counted under microscope. Each barakol concentration was tested in triplicate in a randomized manner. Data are presented as mean ± S.D. n = 3.

Time (h)	Cell number x 10^4 (cells/ml)	Barakol conc. (mM)						
		control	0.05	0.1	0.2	0.4	0.8	1.0
24	mean	3.91	4.13	3.91	3.91	3.87	3.87	3.96
	S.D.	0.08	0.27	0.08	0.28	0.14	0.14	0.15
36	mean	3.87	3.96	4.09	3.91	3.96	3.82	3.64
	S.D.	0.36	0.08	0.31	0.43	0.28	0.31	0.34
48	mean	3.73	3.69	3.78	3.82	3.69	3.42	3.69
	S.D.	0.14	0.28	0.33	0.33	0.54	0.67	0.94
60	mean	3.73	3.51	3.65	3.69	3.24	3.24	3.24
	S.D.	0.14	0.20	0.20	0.28	0.28	0.28	0.43
72	mean	2.89	2.71	2.71	2.98	2.98	3.07	2.89
	S.D.	0.16	0.41	0.28	0.08	1.01	0.40	0.43

Table. 11 The effect of barakol on intracellular soluble AChE in P19 neurons. On day 7 after plating, P19 neurons were incubated with barakol at the concentrations ranging from 0.05-1.0 mM. The AChE activity was performed by Ellman's method in a reaction mixture containing; 0.75 mM acetylthiocholine iodide, 0.3 mM DTNB and 20 μM iso-OMPA. Absorbance was read at 415 nm at 30 sec intervals for 30 min. Protein was determined by Lowry method. Each barakol concentration was tested in triplicate in a randomized manner. Data are represented as mean ± S.D. n = 3.

	Barakol conc. (mM)						
Time (h)	control	0.05	0.1	0.2	0.4	0.8	1
	Specific activity (nmol/min/mg protein)						
24	0.33	0.31	0.43		0.24	0.21	0.20
	0.12	0.13	0.06	0.10	0.05	0.04	0.00
48	0.32	0.32	0.37	0.37	0.26	0.21	0.21
	0.15	0.01	0.15	0.16	0.02	0.00	0.01
72	0.25	0.27	0.27	0.27	0.24	0.21	0.25
	0.08	0.15	0.10	0.04	0.02	0.06	0.03

Table. 12 Comparison of the kinetic parameters of acetylthiocholine hydrolysis and effects of the inhibitors on AChE from crude rat brain and commercial electric eel AChE. n = 6.

Parameters	**Wistar rat brain AChE**	**Electric eel AChE**
Kinetic parameters		
Km (mM)	0.12 ± 0.01	0.133 ± 0.01
Vmax (uM/min)	3.29 ± 0.08	3.31 ± 0.06
IC_{50} values		
Physostigmine (μM)	0.77 ± 0.02	0.39 ± 0.02
BW284C51 (nM)	10.51 ± 0.41	9.59 ± 0.84
Barakol (mM)	0.40 ± 0.03	0.21 ± 0.01
Aqueous extract of *C. siamea* (mg/ml)	1.31 ± 0.04	1.31 ± 0.01
Inhibition coefficient (Ki)		
Barakol (mM)	0.08 ± 0.01	0.084 ± 0.01

Fig. 32 Lineweaver-Burk plot of AChE inhibition by barakol on Wistar rat brain AChE (A) and Electric eel AChE. (B) 0.3mM Barakol (■), 0.1 mM Barakol (♦) and no inhibition, control (▪).

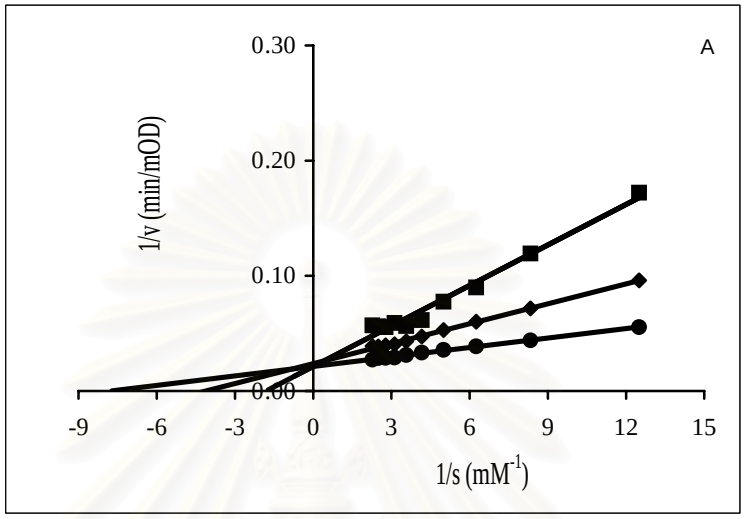

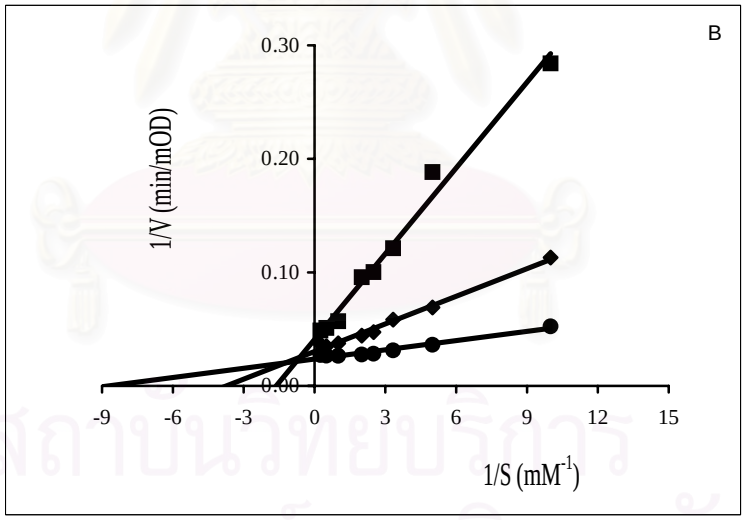

VITA

Mr. Chalermsin Permtermsin was born on February 3, 1974, in Khon-Kaen, Thailand. He received his Bachelor of Science in Pharmacy in 1998 from the Faculty of Pharmaceutical Sciences, Khon-Kaen University, Thailand. He received the Royal Thai Government Scholarship in 2000. Now he is a staff of Research and Development, Office of Atoms for Peace, Bangkok, Thailand.